


Summer 8-19-2016

EHD1 As a Positive Regulator of Macrophage Colony-Stimulating Factor-1 Receptor

Luke R. Cypher
University of Nebraska Medical Center

Tell us how you used this information in this [short survey](#).

Follow this and additional works at: <https://digitalcommons.unmc.edu/etd>

 Part of the [Allergy and Immunology Commons](#), [Infectious Disease Commons](#), [Medical Biochemistry Commons](#), and the [Medical Cell Biology Commons](#)

Recommended Citation

Cypher, Luke R., "EHD1 As a Positive Regulator of Macrophage Colony-Stimulating Factor-1 Receptor" (2016). *Theses & Dissertations*. 119.
<https://digitalcommons.unmc.edu/etd/119>

This Dissertation is brought to you for free and open access by the Graduate Studies at DigitalCommons@UNMC. It has been accepted for inclusion in Theses & Dissertations by an authorized administrator of DigitalCommons@UNMC. For more information, please contact digitalcommons@unmc.edu.

EHD1 AS A POSITIVE REGULATOR OF MACROPHAGE COLONY-STIMULATING FACTOR-1 RECEPTOR

By
Luke Cypher

A DISSERTATION

Presented to the Faculty of
The University of Nebraska Graduate College
In Partial Fulfillment of the Requirements
for the Degree of Doctor of Philosophy

Cancer Research
Graduate Program

Under the supervision of Professor Hamid Band
University of Nebraska Medical Center
Omaha, Nebraska
June 23rd, 2016

Supervisory Committee Members

Tammy Kielian, Ph.D.
Joyce Solheim, Ph.D.
Jing Wang, Ph.D.

I would like to dedicate this dissertation to my mother,

Kimberly A. Cypher, Ph.D.

EHD1 AS A POSITIVE REGULATOR OF MACROPHAGE COLONY-STIMULATING FACTOR-1 RECEPTOR

Luke R. Cypher, Ph.D.

University of Nebraska, 2016

Supervisor: Hamid Band, M.D., Ph.D.

The master regulator of the macrophage development, differentiation, proliferation, survival, phagocytosis, cytokine secretion, motility, adhesion, migration, and spreading is the receptor tyrosine kinase (RTK) colony stimulating factor-1 receptor (CSF-1R). Aberrant CSF-1R signaling is present amongst a variety of highly prevalent and devastating human diseases in the United States such as atherosclerosis, cancer, inflammatory bowel disease, arthritis, and neuro-demyelination/neuro-degeneration. A better understanding of basic mechanisms that govern macrophage development and function is of vital importance in treating patients afflicted with these conditions/diseases. CSF-1R presentation on the macrophage cell surface is a required precursor for CSF1-induced RTK dimerization (activation) and downstream CSF-1R signaling cascades. Mechanisms which regulate CSF-1R trafficking are unstudied and mechanisms of RTK trafficking regulation are poorly understood. The evolutionarily conserved C-terminal Eps15 Homology Domain (EHD) protein family consists of vesicular trafficking regulating proteins. However, the role of EHD proteins in CSF-1R trafficking and signaling has not been studied. I have utilized primary (non-immortalized) murine/mammalian macrophages under

inducible Ehd1 gene deletion/knockout (EHD1-KO) to explore the role of EHD1 in CSF-1R trafficking in macrophages. I have discovered an entirely novel function for EHD1 in anterograde transport and presentation of CSF-1R on the macrophage cell surface. EHD1-KO macrophages have significantly depleted total and surface CSF-1R expression (i.e. receptor available for ligand-binding and subsequently CSF-1R activation/signaling) when compared with control macrophages. In EHD1-KO macrophages, newly synthesized CSF-1R *en route* to the cell surface is essentially shunted to the lysosome and degraded. These findings reveal an entirely novel and essential role for EHD1 in anterograde transport/presentation of CSF-1R to the macrophage cell surface.

ACKNOWLEDGEMENTS

I sincerely thank Dr. Hamid Band for his foresight, guidance, understanding, and patience throughout the course of my training to become a physician scientist. Thank you for believing me and providing me with all the tools and resources needed for my thesis project.

I thank my graduate committee members: Jenny Wang Ph.D. and Tammy Kielian Ph.D. for all of their advice and evaluation during my time as a Ph.D. student and Joyce Solheim Ph.D. whose door was always open.

To Richard Stanley, my Ph.D. would have been impossible without your detailed and transparent protocols. Your method's sections taught me macrophage cell culture. Thank You

To Adam Hoppe's laboratory from South Dakota State University (SDSU). It has been a joy to work with your lab. I greatly appreciate your flexibility and willingness to work with me on macrophage/CSF-1R imaging. The insight, knowledge, and technical savvy your lab brought to my project was invaluable, and I thank you for it.

To all the current and former members of the Hamid Band laboratory. I will always remember the times we shared and friendships formed—Cheers!

TABLE OF CONTENTS

ACKNOWLEDGEMENTS.....	I
TABLE OF CONTENTS	II
LIST OF FIGURES	V
LIST OF TABLES	VIII
LIST OF ABBREVIATIONS	IX
CHAPTER 1: INTRODUCTION.....	1
The monocyte/macrophage cell lineage	2
CSF-1R as the master regulator of macrophages	4
C-terminal Eps15 Homology Domain (EHD) containing proteins.....	6
Mouse models to study EHD proteins.....	7
Hypothesis	9
CHAPTER 2: MATERIALS & METHODS.....	28
Materials	29
Mouse Models	30
Bone Marrow-Derived Macrophages (BMDMs)	31
Fluorescence Activated Cell Sorting (FACS)	31
Quantitative Real-Time-PCR (qRT-PCR).....	32
Immunoblotting (IB)	32
Immunofluorescence (IF)	33
³ H-thymidine incorporation assay of cellular proliferation	34
CFSE dye dilution assays to access macrophage proliferation	34

Macrophage CSF1-induced spreading assay	35
Macrophage CSF1-induced migration assay	35
[³⁵ S]-methionine/cysteine metabolic labeling of CSF-1R	35
Immunoprecipitation (IP)	36
Statistics	36
CHAPTER 3: RESULTS	52
Expression of EHD proteins in Ehd1-WT and Ehd1-null BMDMs	53
Deletion of EHD1 in BMDMs leads to reduced CSF1-induced responses	53
Deletion of EHD1 in BMDMs leads to reduced CSF-1R signaling	54
Reduced surface CSF-1R expression in EHD1-KO BMDMs	55
EHD1 inducible deletion in BMDMs	55
Inducible deletion of EHD1 in BMDMs from <i>Ehd1^{fl/fl}; Cre^{ERT2}</i> mice	56
Tamoxifen is not toxic to BMDMs <i>in vitro</i>	57
Inducible EHD1-KO results in reduced CSF1-induced macrophage functions	58
EHD1-KO BMDMs have reduced CSF-1R signaling	59
CSF-1R internalization and degradation are similar in EHD1-KO BMDMs	60
Reduced surface CSF-1R expression in EHD1-KO BMDMs	60
EHD1 deletion results in depletion of CSF-1R protein in BMDMs	61
EHD1 functions to transport newly synthesized CSF-1R to the cell surface	61
CSF-1R was found localizes to this EHD1 ⁺ /GM130 ⁺ compartment	63

Newly synthesized CSF-1R transits to lysosomes for degradation in EHD1-KO BMDMs	64
CHAPTER 4: DISCUSSION & CONCLUSION	125
Discussion	126
Conclusion	133
BIBLIOGRAPHY	138

LIST OF FIGURES

Figure 1.1. Macrophages in human disease.	16
Figure 1.2. The origins of tissue macrophages.	18
Figure 1.3. Model of how CSF-1R controls macrophage tissue density.	20
Figure 1.4. CSF-1R signaling governs macrophage biology.	22
Figure 1.5. C-terminal Eps15 homology domain (EHD) proteins.	24
Figure 1.6. Regulation of endocytic transport by EHD proteins.	26
Figure 2.1. Genotyping analysis.	42
Figure 2.2. BMDMs from freshly isolated bone marrow.	44
Figure 2.3. BMDMs with inducible EHD1 deletion.	46
Figure 2.4. ³ H-thymidine incorporation assays for cell proliferation.	48
Figure 2.5. CFSE dye dilution assays to assess macrophage proliferation.	50
Figure 3.1. BMDMs defined by F4/80 ⁺ flow cytometry staining.	67
Figure 3.2. EHD family expression in Ehd1-WT and Ehd1-null BMDMs.	69
Figure 3.3. ³ H-thymidine proliferation assay using BMDMs.	71
Figure 3.4. CFSE assays using Ehd1-WT and Ehd1-null BMDMs.	73
Figure 3.5. CFSE population differences in Ehd1-WT and Ehd1-null BMDMs.	75
Figure 3.6. Ehd1-null BMDMs have reduced CSF1-induced cellular spreading.	77
Figure 3.7. CSF-1 stimulation induces CSF-1R signaling.	79
Figure 3.8. Ehd1-null BMDMs have decreased surface CSF-1R expression upon CSF-1 deprivation.	81
Figure 3.9. F4/80 ⁺ Control and EHD1-KO BMDMs.	83

Figure 3.10. EHD family expression in control and inducible EHD1-KO BMDMs.	85
Figure 3.11. Lack of CSF-1 response alteration due to TAM treatment.	87
Figure 3.12. Lack of apoptosis toxicity of TAM in BMDMs.	89
Figure 3.13. EHD1 deletion results in reduced proliferation.	91
Figure 3.14. EHD1-KO BMDMs have reduced CSF1-induced proliferation.	93
Figure 3.15. CFSE population model in BMDMs.	95
Figure 3.16. EHD1 deletion results in reduced spreading.	97
Figure 3.17. EHD1-KO BMDMs have reduced migration.	99
Figure 3.18. EHD1-KO BMDMs have decreased pERK downstream CSF-1R signaling.	101
Figure 3.19. EHD1 deletion has no significant effect on activated CSF-1R internalization.	103
Figure 3.20. EHD1 deletion has no significant effect on activated CSF-1R degradation.	105
Figure 3.21. EHD1-KO BMDMs have reduced surface CSF-1R expression.	107
Figure 3.22. EHD1 deletion in BMDMs results in reduced surface CSF-1R expression.	109
Figure 3.23. EHD1 deletion in BMDMs leads to a reduction in total CSF-1R, demonstrated by immunoblotting.	111
Figure 3.24. EHD1-KO BMDMs have reduced total CSF-1R using IF.	113
Figure 3.25. EHD1 deletion does not affect CSF-1R synthesis.	115

Figure 3.26. EHD1-KO deletion reduces transport of newly synthesized CSF-1R to the cell surface.	117
Figure 3.27. CSF-1R co-localizes to a EHD1 ⁺ /GM130 ⁺ compartment.	119
Figure 3.28. EHD1-KO BMDMs have increased CSF-1R lysosomal degradation.	121
Figure 3.29. EHD1-KO BMDMs shunt CSF-1R to the lysosome.	123
Figure 4.1. Working model of the novel EHD1 function in CSF-1R delivery and display on the macrophage cell surface.	136

LIST OF TABLES

Table 1.1. Modulation of the protein expression by CSF-1.	11
Table 1.2. Relationship of EHD proteins to human disease.	13
Table 2.1. Genotypes of mice used in this study.	38
Table 2.2. Genotyping PCR primer sequences.	39
Table 2.3. Real-time PCR primer sequences.	40

LIST OF ABBREVIATIONS

BACE1	Beta-Secretase 1
Baf-A1	Bafilomycin A1
BMDMs	Bone Marrow Derived Macrophages
BSA	Bovine Serum Albumin
CCR	Chemokine CC Receptor;
CSF-1	Colony-Stimulating Factor-1
CSF-1R	Colony-Stimulating Factor-1 Receptor
CNS	Central Nervous System
EE	Early Endosome
EGF	Epidermal Growth Factor
EGFR	Epidermal Growth Factor Receptor
EHD1	Eps-15 Homology Domain-containing protein 1
EHD1-KO	EHD1-Knockout
EHD2	Eps-15 Homology Domain-containing protein 2
EHD3	Eps-15 Homology Domain-containing protein 3
EHD4	Eps-15 Homology Domain-containing protein 4
FACS	Fluorescence Activated Cell Sorting
GM130	Golgi Matrix Protein, 130kDa

GM-CSF	Granulocyte/Macrophage Colony-Stimulating Factor
HSC	Hemopoietic Stem Cell
IB	Immunoblotting
IF	Immunofluorescence
IP	Immunoprecipitation
IL	Interleukin
iNKT	invariant Natural Killer T
LAMP1	Lysosomal associated membrane protein 1
LC	Langerhans Cell
LCMV	Lymphocytic Choriomeningitis Virus
LE	Late Endosome
LPS	Lipopolysaccharide
M-CSF	Macrophage-Colony-Stimulating Factor
MF	Macrophage
mG	Microglia
MICAL-L1	Microtubule associated monooxygenase, Calpain & LIM domain containing protein 1
OC	Osteoclast
PBS	Phosphate Buffered Saline

PFA	Paraformaldehyde
PI	Propidium Iodide
qRT-PCR	Quantitative Real-Time-PCR
RT	Room Temperature
RTK	Receptor Tyrosine Kinase
SC	Synoviocytes
SE	Sorting Endosome
TAM	4-Hydroxytamoxifen
TAM Φ	Tumor Associated Macrophage
VEGF	Vascular Endothelial Growth Factor
VEGFR	Vascular Endothelial Growth Factor Receptor
VSV	Vesicular Stomatitis Virus
WASH	Wiskott-Aldrich syndrome protein & Scar Homologue

CHAPTER 1: INTRODUCTION

The material covered in the following chapter is the topic of the following published article:

Luke R. Cypher, Timothy Alan Bielecki, Oluwadamilola Adepegba, Lu Huang, An Wei, Fany Iseka, Haitao Luan, Eric Tom, Matthew D. Storck, Adam D. Hoppe, Vimla Band, Hamid Band. CSF-1 receptor signalling is governed by pre-requisite EHD1 mediated receptor display on the macrophage cell surface.

(Accepted for Publication: *Cellular Signalling*, Available online 17 May 2016)

The monocyte/macrophage cell lineage

Cells of the monocyte/macrophage lineage play fundamental roles in integrating the two major arms (innate and adaptive) immune system. Colony-stimulating factor-1 receptor (CSF-1R) signaling is essential for the development of the cells of the monocyte-macrophage lineage by mediating the proliferation and differentiation of myeloid progenitors into mature, fully functional macrophages (1). CSF-1R signaling has been demonstrated to instruct hematopoietic stem cells (HSCs) to differentiate into macrophages via myeloid-lineage transcription factor PU.1, providing a mechanism for the immune system to increase macrophage numbers during infection/inflammation (2). Abnormalities in the development of this cell lineage are incompatible with an efficient and healthy immune system (3–5).

Macrophages also play pivotal roles in wound repair and the removal of apoptotic cells. Phagocytosis and subsequent removal of necrotic tissues by macrophages is an important part of normal human physiology. In wound repair, macrophages function in the production of the new extracellular matrix. The mechanism by which macrophages help produce this extracellular matrix is via macrophage arginase which allows the conversion of arginine to ornithine. This conversion is necessary to make collagen—an essential building block for reconstruction of damaged tissues (6).

Of clinical relevance, macrophages are also known to be present in

common in human diseases (Figure 1.1). More specifically, macrophages are known to be involved in immunological diseases (7–9) such as rheumatoid arthritis, inflammatory bowel disease, and demyelinating neurological diseases (10–12). Additionally, macrophages also play key homeostatic roles in non-immune diseases such as atherosclerosis and cancer (13–15).

In the context of cancer, macrophages are key players in regulating/maintaining the tumor microenvironment and are known as Tumor-Associated Macrophages (TAM Φ). TAM Φ s take part in a positive feedback loop involving tumor cells. Briefly, the tumor cells secrete CSF-1, which attracts and maintains TAM Φ s along with a combination of other growth factors. TAM Φ s in return secrete Epidermal Growth Factor (EGF) and Vascular Endothelial Growth Factor (VEGF) which promotes survival of the tumor cells. Specifically, EGF promotes the growth of the tumor directly, and VEGF promotes vascularization of the neoplastic tissue (16).

Given their relatively short life span yet relatively constant numbers in circulation and tissues under homeostasis, and a rapid and sometimes marked increase in numbers in the face of infection or inflammation, macrophages need to be continuously produced to match the body's needs. CSF-1R signaling is essential for this process to occur (17). It is also known that critical proliferative signals generated by CSF-1R occur when the receptor has been internalized and is in the endocytic recycling compartment (18). However, mechanisms which regulate CSF-1R trafficking have not been studied. A better understanding of basic mechanisms that govern macrophage biology/CSF-1R signaling is of vital

importance regarding treatment of patients afflicted with these conditions.

CSF-1R as the master regulator of macrophages

CSF-1R signaling that is essential for appropriate macrophage development and population maintenance (Figures 1.2 and 1.3) is controlled by binding and subsequent activation of the receptor by CSF-1. CSF1-induced CSF-1R signaling has also been shown directly to regulate the physiological functions of macrophages such as proliferation, differentiation, spreading, migration, phagocytosis, and cytokine secretion (Figure 1.4). Furthermore, CSF-1R signaling also controls universal transcription of the macrophage genome and subsequent protein expression (19). Hence, if CSF-1R does not directly regulate macrophage function, the receptor indirectly regulates macrophage biology due regulation of cellular protein expression (Table 1.1).

CSF-1R, like all receptor tyrosine kinases (RTKs), is synthesized in the endoplasmic reticulum, glycosylated/matured in the Golgi apparatus, and then transported to the cell surface where it can become activated via binding of ligand (CSF-1). Transport of newly synthesized receptor is a prerequisite step in RTK/CSF-1R activation and signaling (20). Furthermore, if CSF-1R does not make it to the cell surface or is not oriented on the plasma membrane correctly, it cannot bind ligand and become activated (signal).

Similarly, to other RTKs, ligand binding of CSF-1 (M-CSF) or IL-34 activates CSF-1R by inducing conformational changes, dimerization, and trans-phosphorylation, leading to the association of key cytoplasmic signaling

intermediates. Signal transduction cascades are activated, including the PI3-kinase/AKT, Ras/Erk, and Rho/Rac pathways (21, 22). Transcription occurs downstream of these signaling pathways dictating changes in macrophage biology.

When CSF-1 binding of CSF-1R occurs at the macrophage's surface (RTK activation) endocytic internalization of CSF-1R occurs (18, 23).

Endocytosed RTKs are targeted to the lysosome, which our laboratory and others have demonstrated to be dependent on CBL-family proteins and ESCRT complexes (20, 24–26). Also, ligand-stimulated and internalized RTKs can transit through an endocytic recycling pathway (27). These alternate fates of internalized RTKs are of a high biological interest as their balance determines the magnitude and duration of signaling in response to ligand-induced stimulation (28). Furthermore, activated RTKs continue to signal in endosomes and indeed may require endocytosis to transduce specific signals (20). CSF-1R signaling at the cell surface is known to induce phosphorylation of the STAT3 pathway specifically and not the Erk and Akt pathways. However, once internalized, CSF-1R signaling from the endosome results in phosphorylation of the Erk and Akt pathways (18).

After newly synthesized receptor has been transported to the cell surface, it will undergo constitutive recycling if CSF-1 activation does not occur. CSF-1R is known to undergo constitutive recycling at a rate of 4 molecules/cell/s at steady state (29). The combinatory effects of the rate of receptor internalization, constitutive recycling, and degradation determine the half-life ($t_{1/2}$) of an RTK.

CSF-1R has one of the fastest turnover rates ($t_{1/2} < 1$ hour) of any known RTK (25). Trafficking of CSF-1R happens extremely fast. In contrast, EGFR has one of the slowest turnover rates ($t_{1/2} > 24$ hours). The rapid turnover rate of CSF-1R, as compared to other RTKS, is an important caveat which must be taken into account when trying to understand the biology of the receptor.

C-terminal Eps15 Homology Domain (EHD) containing proteins

The four members of C-terminal Eps15-homology domain-containing (EHD) protein family have recently emerged as regulators of endocytic traffic of cell surface receptors (30). EHD proteins are characterized by highly related primary amino acid sequences amongst family members and similar domain structure. The domains are composed of a nucleotide-binding G-domain, coiled-coiled regions that form a membrane lipid-binding domain, an EH domain (67-86% homology, Figure 1.5A), and a C-terminus that mediates interactions with partner proteins by binding to asparagine-proline-phenylalanine (NPF)-containing motifs (Figure 1.5B). *In vitro* studies have suggested EHD proteins function in a manner similar to the protein dynamin—as scission proteins to promote vesicular budding and membrane tubulation (Figure 1.5C). Furthermore, EHD1 has been linked to the cellular endocytic recycling compartment (Figure 1.6). These studies have shown EHD proteins to be involved in the recycling of immune-relevant receptors such as MHC class I, MHC class II, $\beta 1$ integrins (30). Furthermore, EHD proteins have been correlated with various human diseases (Table 1.2). However, the role of EHD proteins in CSF-1R trafficking and

signaling has not been studied.

Mouse models to study EHD proteins

Our laboratory has previously used individual and combined gene deletion approaches in mice to discover physiological roles of EHD proteins *in vivo*. EHD1 deletion on a mixed C57BL/6 and 129Sv background is partially embryonic lethal and associated with defective spermatogenesis and lens developmental defects. EHD1 deletion is fully embryonic lethal on a predominantly C57BL/6 background and related to defective neural tube closure due to lack of ciliogenesis and altered Hedgehog signaling (31–33). EHD1-null mice also exhibit a skeletal myopathy (34, 35). EHD4-null mice exhibit reduced testes size and male fertility while EHD3-null mice are normal (36); however, EHD3/EHD4-null mice show high early neonatal lethality and develop rapidly progressive renal thrombotic microangiopathy (37). Further analyses of EHD3-null mice have revealed a pivotal role of EHD3 in regulating cardiac membrane excitability and rhythm (38). Consistent with these physiological functions, EHD proteins have been found to regulate trafficking to the cell surface of non-RTK receptors, such as Sodium/Calcium (Ca^{2+}) exchanger L-type Ca^{2+} channel type 1.2 (39) and voltage-gated T-type Ca^{2+} channels $\text{CaV}3.1$, and $\text{CaV}3.2$ (40) in cardiomyocytes, and feeling protein Fer1L1 in skeletal muscle cells (34, 35). Currently, little is known about the physiological roles of EHD proteins. EHD-regulated endocytic traffic of other receptors characterized in cellular models, including transferrin receptor (41), MHC class I (42), $\beta 1$ integrin (43), cadherin 23 (44), L1/Ng-CAM

(45), and surface protease BACE1 (46). Similarly, the functional importance of EHD1 and EHD4 localization to the neuromuscular junction (47) remains unclear.

In contrast to non-RTK receptors, less is known about the roles of EHD proteins in RTK traffic. EHD4 expression was found to be upregulated by neurotrophin stimulation of neuronal cultures, and knockdown studies showed that EHD4 was required for the post-stimulation retrograde traffic of neurotrophin receptor TrkA (48). We have observed an increased cytoplasmic and reduced surface localization of vascular growth factor receptor 2 (VEGF2) in glomerular endothelial cells of EHD3/EHD4 double knockout mice with a glomerular disease, suggesting a potential role of EHD proteins in facilitating the surface mobilization of RTKs. At present, no role of EHD proteins in CSF-1R traffic or monocyte-macrophage function is known.

To establish a biological system in which the functions of endocytic recycling can be examined *in vivo* as well as *ex vivo*, our laboratory has focused on four highly conserved proteins of the Eps15-homology domain-containing (EHD) protein family. By creating constitutive as well as inducible mouse knockout (KO) models, our laboratory aims to uncover previously unanticipated roles of these proteins in physiological processes. To elucidate the roles of EHD protein-dependent endocytic recycling in the macrophages, I initiated studies using mouse macrophages, given the critical duties of the endocytic machinery in basic macrophage biology, including phagocytosis, endocytic internalization of foreign antigens or antigen/antibody complexes, antigen processing and display on the surface, and other roles (49, 50). Mutations of endocytic regulatory

proteins in genetic immune disorders, such as Chediak-Higashi Syndrome (51) and familial lymphohistiocytosis (52) significantly affect macrophage function.

Hypothesis

I hypothesize that EHD1 orchestrates optimal CSF-1R expression and signaling in macrophages. Furthermore, EHD1 regulates macrophage CSF-1R surface expression via control of CSF-1R transport to the cell surface, thus permitting stabilization of the dimerized form of the receptor by CSF-1 (activation). This hypothesis will be explored using primary murine bone marrow-derived macrophages (BMDMs) from constitutive and inducible EHD knockout mice. Using an array of biochemistry, immunofluorescence, and Fluorescence Activated Cell Sorting (FACS) analysis, I will characterize the physiological functions of EHD1 in the context of CSF-1R signaling in macrophages responses. Furthermore, I will seek to describe a mechanism behind any differences detected between control and EHD1-KO macrophages.

CHAPTER 1: TABLES

Table 1.1. Modulation of the protein expression by CSF-1.

Antigen	Function	Effect of CSF-1	References
CD markers			
CD11b	Leukocyte integrin α subunit	↑	[18]
CD14	LPS receptor	↑	[18]
CD16	Fc γ receptor III	↑	[18,28,29]
CD23	Fc ϵ receptor II	↑	[18]
CD64	Fc γ receptor I	↑ ^a	[18]
MHC antigens			
HLA-I	Antigen presentation	↑	[18]
HLA-II	Antigen presentation	↑	[18]
Cytokines			
IL-6	Pleiotropic cytokine	↑	[18]
IL-8	Leukocyte chemokine, angiogenic, tumorigenic	↑	[18]
IL-12	Inflammatory cytokine	↓ ^b , ↓↓ ^c	[18]
IL-18	Inflammatory cytokine	↑ ^b	[18]
TNF- α	Inflammatory cytokine	↑	[18]
Toll-like receptors			
TLR1	Tri-acyl lipopeptide receptor (bacteria, mycobacteria)	↓	[17]
TLR2	Receptor for lipoprotein, zymosan (fungi), lipoteichoic acid (Gram+ bacteria), peptidoglycan (Gram+ bacteria) and lipoarabinomannan (mycobacteria)	↓	[17]
TLR4	LPS receptor (Gram-)	NA	[17]
TLR6	Di-acyl lipopeptide receptor (mycobacteria)	↓	[17]
TLR9	Bacterial and viral CpG DNA receptor	↓↓↓	[17]
Other receptors			
P2X7	Extracellular ATP receptor, regulating inflammatory responses	↑	[19]

Abbreviations: ↑, increased; ↓, decreased; ↓ ↓, markedly decreased; ↓ ↓ ↓, dramatically decreased; HLA, human leukocyte antigen; NA, not affected.

^a CSF-1 in combination with IL-10.

^b CSF-1 in combination with LPS.

^c CSF-1 in combination with IL-10 and LPS.

Table 1.1. Modulation of protein expression by CSF-1. CSF-1 up-regulates human monocyte expression of the P2X7 extracellular ATP receptor that regulates DCs and macrophage inflammatory functions, including intracellular bacterial killing, and favors the generation of cytokines that stimulate T helper 2 responses. Independently of LPS, CSF-1 induces monocytes to express a variety of cytokines and immunologically relevant cell surface molecules.

Used with permission (7)

Table 1.2. Relationship of EHD proteins to human disease.

EHD Protein	Disease or condition	Aberrancy phenotype	Transcript or protein	Fold increase or decrease
EHD1	Pseudoexfoliation glaucoma	Enhanced levels of serum antibodies	N.a. ^a	N.a.
EHD1	<i>Apergillus fumigatus</i> infection	Enhanced EHD1 expression in monocytes	Transcript	1.5–2-fold increase
EHD1	Metastatic ability of well-differentiated pancreatic endocrine neoplasms	Decreased expression	Transcript	3.1-fold decrease
EHD1	Sickle-cell disease	Decreased expression	Protein	Not given
EHD1	<i>Aeromonas hydrophila</i> cytotoxic enterotoxin induced-genes	Increased expression in macrophages	transcript	3–4-fold increase
EHD1	<i>Plasmodium falciparum</i> infected erythrocytes	Increased expression in erythrocytes	Transcript	4.9-fold increase
EHD1	Prostate cancer	Secreted from exosomes of prostate cancer cells	Protein	N.a.
EHD1	Cutaneous T cell lymphoma	Increased expression in lesion	Transcript	1.5-fold increase
EHD1–4	Glioma	Gene loss proposed	N.a.	N.a.
EHD2	Diabetes mellitus-associated bladder dysfunction	Decreased EHD2 expression	Protein	1.5-fold decrease
EHD2	Primary pigmented nodular adrenocortical disease	Increased EHD2 expression	Transcript	0.19% expression compared to 0% in control
EHD3	Oral squamous cell carcinoma	Decreased EHD3 expression	Transcript	11.9-fold decrease
EHD3	Small-cell lung cancer	Increased EHD3 expression	Transcript	Abundant increase (value not given)
EHD3	Acute myeloid leukemias	Gene methylation	N.a.	N.a.
EHD4	Systemic onset juvenile idiopathic arthritis	Increased EHD4 expression	Transcript	0.8-fold increase

Table 1.2. Relationship of EHD proteins to human disease. The table highlights known correlation between EHD proteins and human diseases using fold increase or decrease of the corresponding EHD protein to a given human disease.

Used with permission (30)

CHAPTER 1: FIGURES

Figure 1.1. Macrophages in human disease.

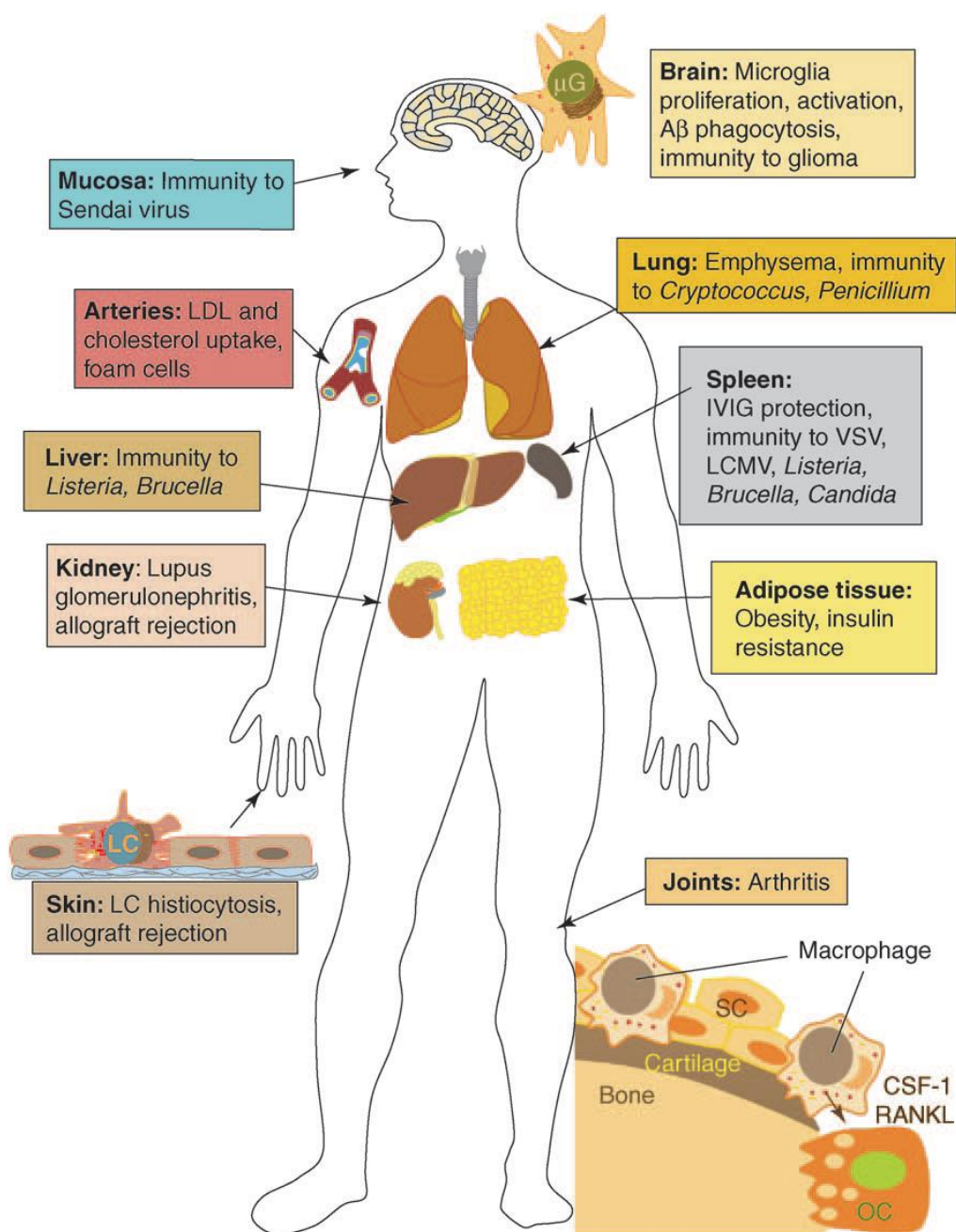


Figure 1.1. Macrophages in human disease. Involvement of CSF1-regulated mononuclear phagocytes in immunity and inflammation. By regulating the development and activation of mononuclear phagocytes, CSF-1 contributes to immunity to viral, bacterial and fungal infections and increases the efficiency of vaccination (e.g. Sendai virus and glioma vaccines). The involvement of specific macrophage populations is shown. CSF-1 is also involved in promoting and sustaining inflammation in several diseases (e.g. Alzheimer's disease, systemic lupus erythematosus, arthritis and obesity) and in the regulation of TAMΦs in enhancing tumor progression and metastasis (not shown). Although most studies have been performed in rodents, for illustrative purposes this information is depicted on a human body.

Used with permission (7)

Figure 1.2. The origins of tissue macrophages.

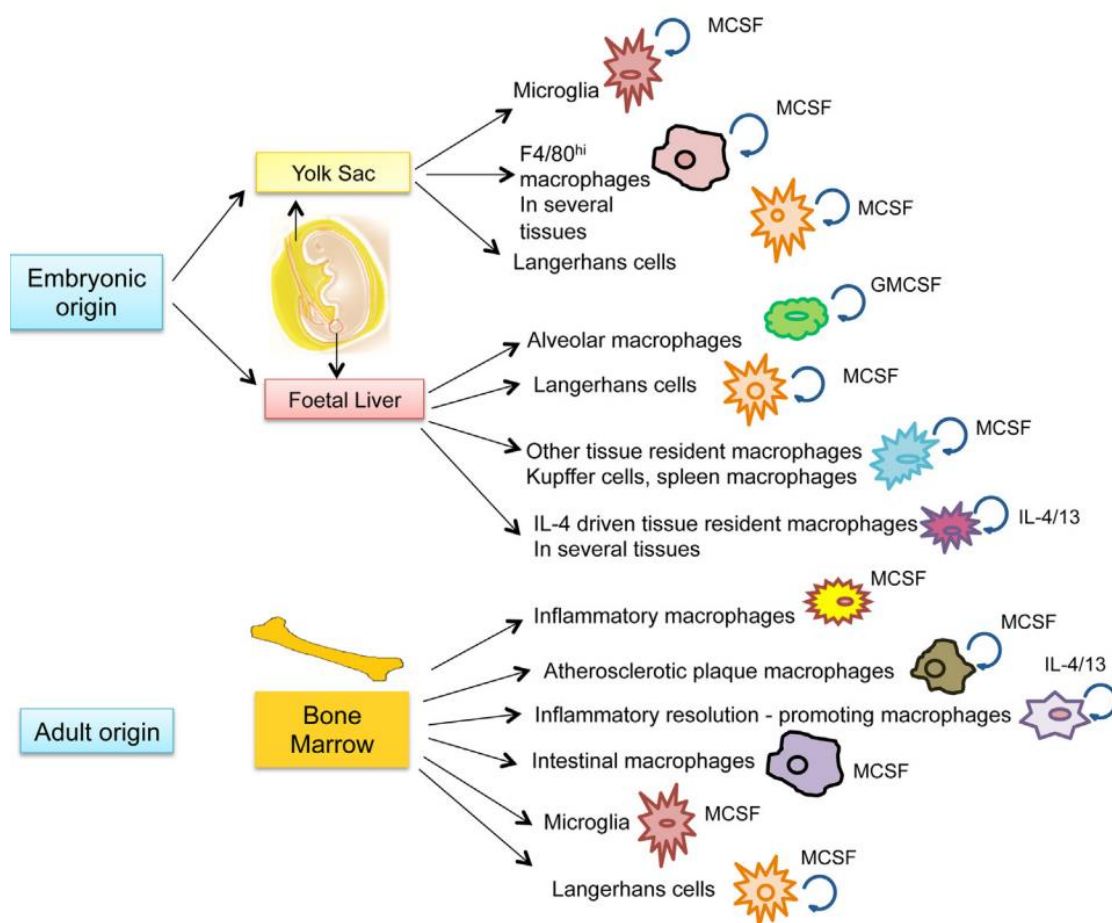


Figure 1.2. The origins of tissue macrophages. Developmental origin of tissue macrophages in the mononuclear phagocyte system. Embryonic macrophages from the yolk sac and fetal liver self-renew in homeostatic conditions and are driven by M-CSF (CSF-1) or GM-CSF. Inflammatory macrophages of embryonic origin also self-renew.

Used with permission (53)

Figure 1.3. Model of how CSF-1R controls macrophage tissue density.

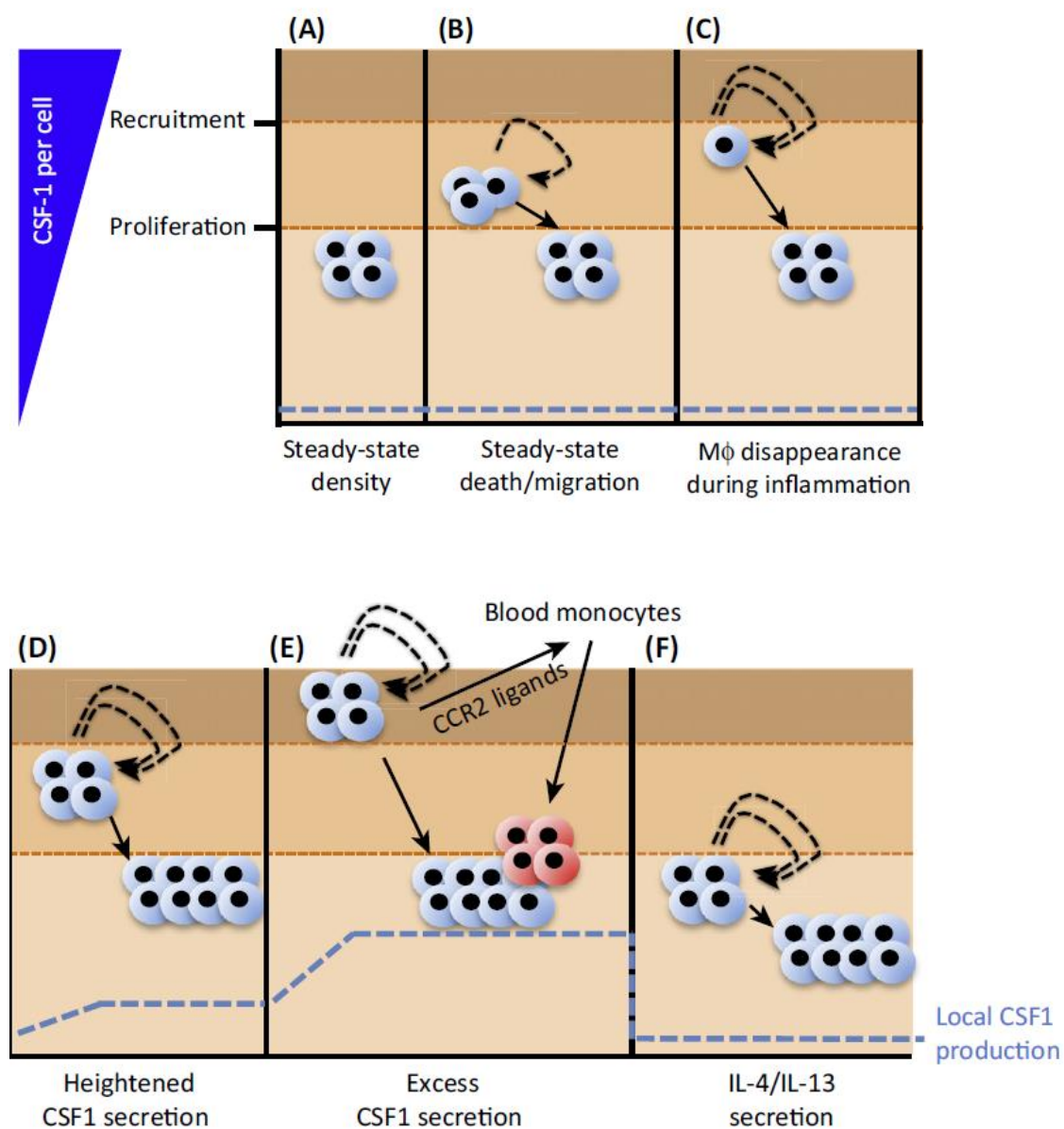


Figure 1.3. Model of how CSF-1R controls macrophage tissue density. CSF-1R signaling controls the proliferation of tissue macrophages. Constant secretion of CSF-1 by tissue stroma and consumption by macrophages maintains population density just below the CSF-1R signaling threshold required for proliferation (A). Steady state death/ migration (B) or disappearance during inflammation (C) increases available CSF-1 without necessarily changing production of CSF-1, thereby allowing proliferation to restore normal density. Elevated CSF-1 secretion stimulates cells to proliferate to higher tissue density than normal (D), but can also stimulate monocyte recruitment via macrophage chemokine production (E). Recruitment likely requires a higher threshold of CSF-1R signaling than proliferation, but this remains to be established. Other factors, such as IL-4, can allow macrophages to proliferate independently of CSF-1 thereby increasing macrophage numbers when CSF-1 is limiting and without a concurrent increase in monocyte recruitment (F).

Used with permission (54)

Figure 1.4. CSF-1R signaling governs macrophage biology.

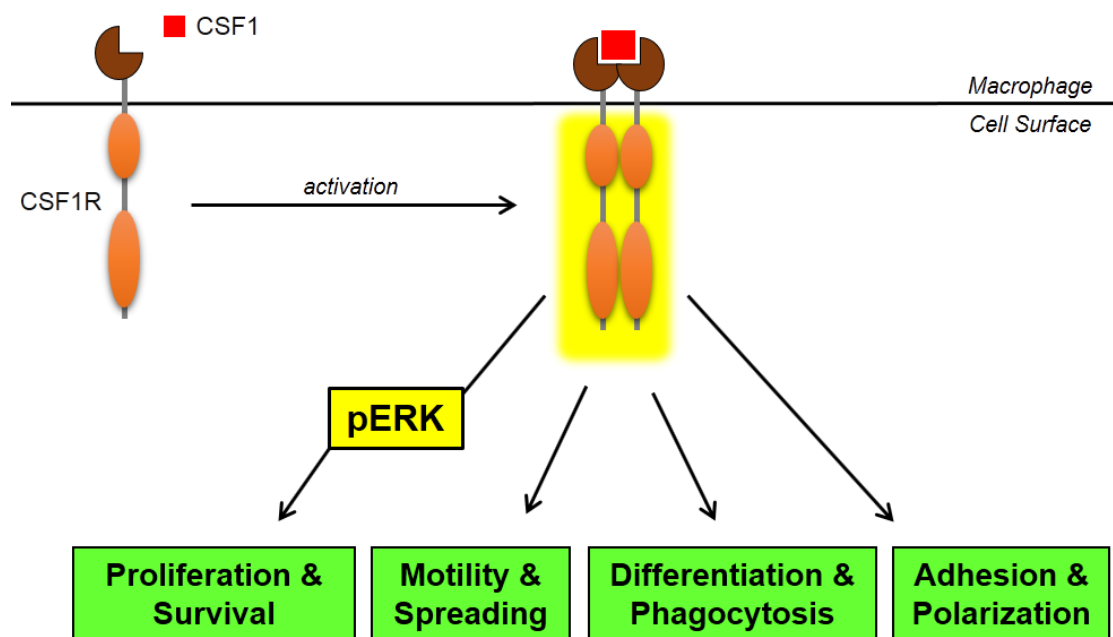


Figure 1.4. CSF-1R signaling governs macrophage biology. Signaling pathways regulated by colony-stimulating factor-1 receptor (CSF-1R) in myeloid cells. Binding of Colony-stimulating factor-1 (CSF-1) stabilizes a dimeric form of the CSF-1R and leads to activation of the CSF-1R kinase, its tyrosine phosphorylation, and the direct association of signaling molecules with the receptor through their phosphotyrosine-binding domains. The precise involvement of the Ras–MEK–MAPK pathway in the CSF1-regulated proliferation and differentiation of myeloid cells is not clear, but Raf-1 seems to signal independently of this pathway. Differences in signaling pathways are also expected to exist between macrophage progenitor cells and macrophages.

Used with permission and modified (17)

Figure 1.5. C-terminal Eps15 homology domain (EHD) proteins.

A

		Sequence Identity
EHD1	EHD2	70.3%
EHD1	EHD3	86.5%
EHD1	EHD4	74.1%
EHD2	EHD3	70.5%
EHD2	EHD4	67.9%
EHD3	EHD4	74.3%

B



C

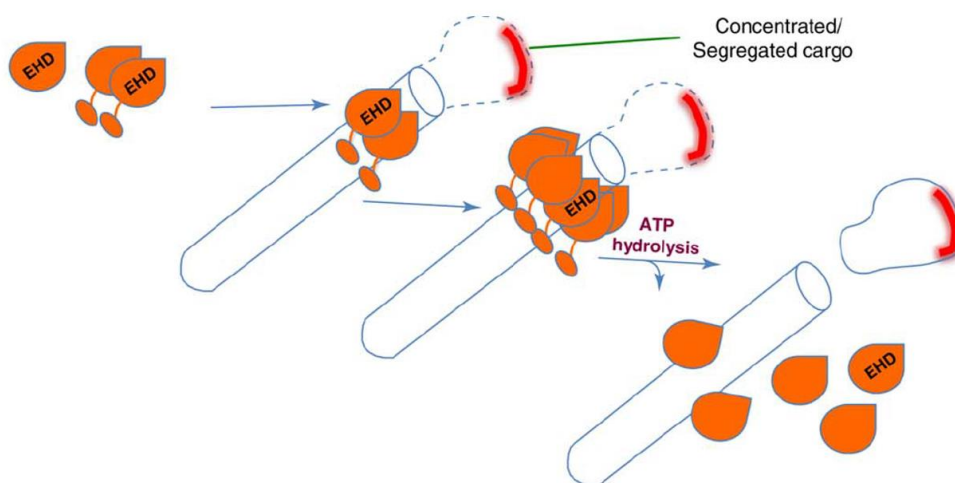


Figure 1.5. Domain architecture, conservation, and function of C-terminal Eps15 homology domain (EHD) proteins. (A) The EHD proteins, comprised of 534–543 amino acids, each contain two helical regions, a conserved ATP-binding domain, a linker region and an EH domain localized to the C-terminus of the protein. (B) Comparison of the amino acid sequence identity of full-length EHD proteins. (C) Proposed model of EHD protein function. Cytoplasmic localized EHD proteins bind ATP and dimerize. EHD dimerization causes the formation of a membrane binding site and the EHD proteins associate with tubular membranes, where they undergo further oligomerization. Upon ATP hydrolysis, the membranes are destabilized, leading to scission of vesicles containing concentrated cargo/receptors, thus facilitating vesicular transport.

Used with permission (30)

Figure 1.6. Regulation of endocytic transport by EHD proteins.

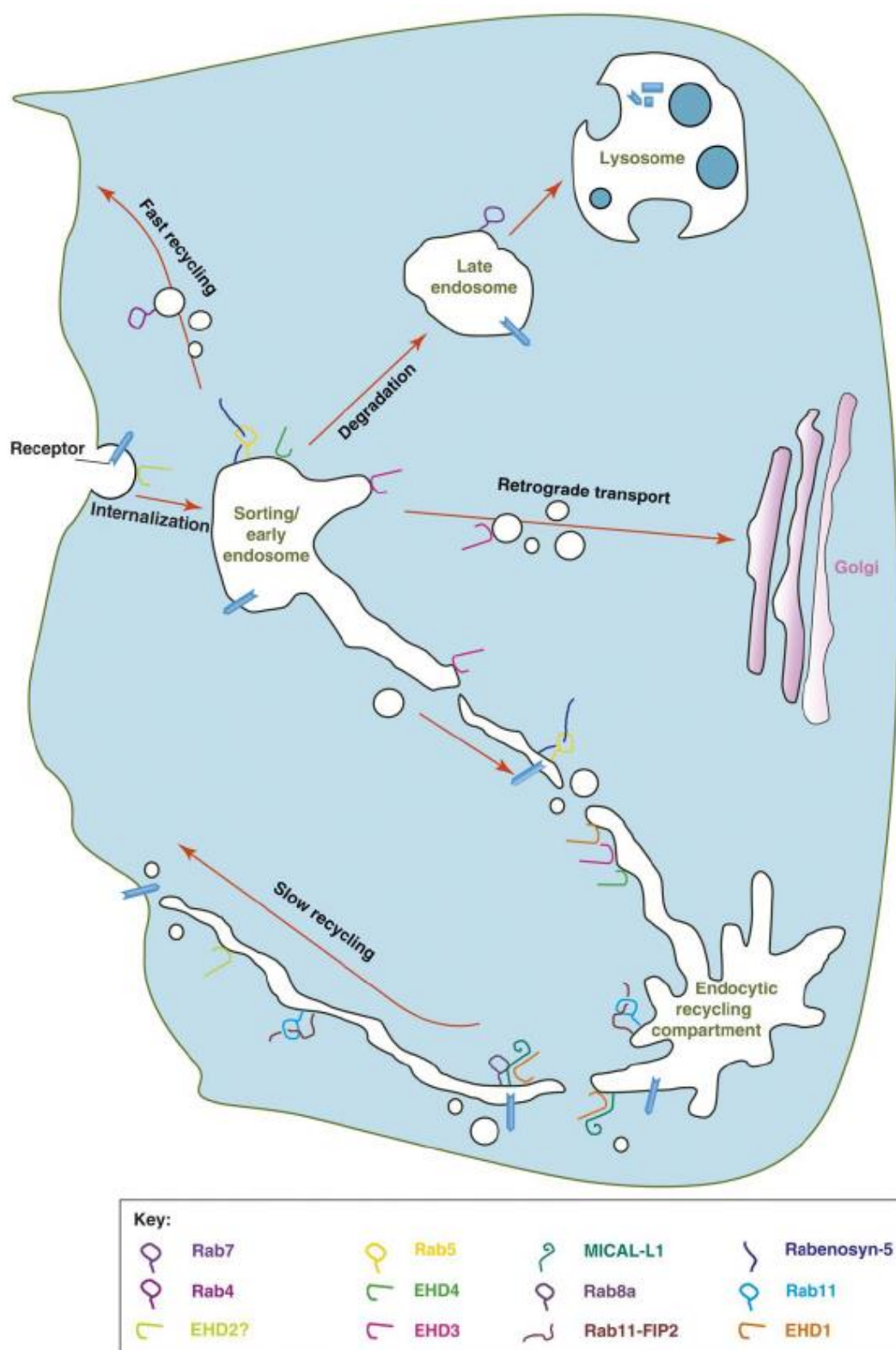


Figure 1.6. Regulation of endocytic transport by EHD proteins. Internalized receptors reach the sorting or early endosome (EE) and are trafficked through one of at least four pathways. Receptors slated for degradation are sorted to EE microdomains containing EHD4, Rab5, and Rabenosyn-5 and transported to late endosomes and lysosomes. Other internalized proteins, such as the Shiga toxin, are carried from EE to the Golgi via an EHD3 and/or EHD1-dependent retrograde pathway. Receptors that recycle back to the plasma membrane can do so directly from EE in a poorly defined manner that requires the function of Rab4 (fast recycling). Alternatively, many receptors are first directed to the perinuclear endocytic recycling compartment and then shuttled to the plasma membrane (slow recycling). Slow recycling requires the following function of multiple regulators including Rab5, Rab11, Rab8a, their effectors (Rabenosyn-5, Rab11-FIP2, and MICAL-L1, respectively), and EHD proteins.

Used with permission (30)

CHAPTER 2: MATERIALS & METHODS

The material covered in the following chapter is the topic of the following published article:

Luke R. Cypher, Timothy Alan Bielecki, Oluwadamilola Adepegba, Lu Huang, An Wei, Fany Iseka, Haitao Luan, Eric Tom, Matthew D. Storck, Adam D. Hoppe, Vimla Band, Hamid Band. CSF-1 receptor signalling is governed by pre-requisite EHD1 mediated receptor display on the macrophage cell surface.

(Accepted for Publication: *Cellular Signalling*, Available online 17 May 2016)

Materials

Bovine Serum Albumin (cat. # A7906-100G), Paraformaldehyde (cat. # 158127-500G), Triton X-100 (cat. # 93418), and 4-hydroxytamoxifen (cat. # T176-10MG) were from Sigma-Aldrich (St. Louis, MO). Propidium Iodide staining solution (cat. # 00-6990-42) was from eBiosciences. Hema staining solutions (cat. # 23-123919) were from Fisher. 3H-thymidine (cat. # 2407001, 2.0Ci/mmol) was from MP Biomedical and [35S] (cat. # NEG772007MC, 1175 Ci/mmol) was from Perkin Elmer. Bafilomycin A1 (cat. # 196000) was from Millipore. EDTA-free protease inhibitor cocktail (cat. # 4693159001) was from Roche, ECL development reagent (cat. # 32106) was from Thermo-Scientific. Recombinant CSF-1 (catalog # 315-02) was from Peprotech (Rocky Hill, NJ). CFSE (cat. # C34554) and RPMI-1640 (cat. # SH30027.02) were from ThermoFisher Scientific. Penicillin/streptomycin (cat. # 15140-122) and Fetal Bovine Serum (cat. # 10427-028; lot # 1662765A120-01) were from Life Technologies.

Antibodies: Brilliant Violet 711 conjugated anti-CSF-1R and anti-CSF-1R, AFS98 (cat. # 135515) were from Biolegend; anti-CSF-1R C-20 (cat. # sc-692), anti-CSF-1R G-17 (cat. # sc-31638) anti-HSC70 (cat. #sc-7298), and anti-LAMP1 1D4B (cat. # sc-19992) were from Santa Cruz Biotechnology; anti-EHD1 (cat. # ab109311) was from Abcam; anti- β -Actin (cat. # A5316) was from Sigma-Aldrich; anti-pErk42/44 (cat. # 9101) was from Cell Signaling Technology; F4/80-APC, BM8 (cat. # 17-4801-82) and anti-GM130 (cat. # 610822) were from BD Biosciences; CD16/32 (cat. # 14-0161), and APC-conjugated anti-Annexin V (cat. # 17-8007-72) were from eBiosciences; a polyclonal rabbit antibody recognizing

EHD1 and EHD4 was generated in-house was described previously (45).
Secondary fluorochrome-conjugated antibodies were from Life Technologies.

Mouse Models

Ehd1-null mice were maintained on mixed 129; B6 background (36).
Single nucleotide polymorphism (SNP) analysis (DartMouse, Lebanon, NH) revealed these to have ~70% contribution from the C57Bl/6 genome (Figure 2.1). *Ehd1*-WT (wild type), *Ehd1*-het (heterozygous), and *Ehd1*-null (homozygous null) mice were generated by mating *Ehd1*-het mice. Mice used in this study are named according to Table 2.1. Breeders were maintained on high-fat chow (#2019, Harlan Laboratories Inc., Madison, WI). Genomic DNA was extracted from embryonic yolk sacs or adult tail tips with proteinase K digestion, isopropanol precipitation and used for genotyping as described previously (Rainey et al., 2010).

To conditionally delete *Ehd1*, *Ehd1*^{flox/flox} (*Ehd1*^{fl/fl}) mice in a predominantly C57BL/6 background (33, 36) were crossed with tamoxifen-inducible CreERT2 expressing mice from Jackson Laboratories (*Gt(ROSA)26Sor^{tm1}(cre/ERT2)Tyj*; strain 008463) to generate *Ehd1*^{fl/fl}; *Cre*^{ERT2} mice. Genotypes were confirmed by subjecting tail clip DNA to qRT-PCR analysis using the KAPA Mouse Genotyping kit (KAPA Biosystems) and primer pairs described in Table 2.2. Mice were treated humanely according to the National Institutes of Health (NIH) and The University of Nebraska Medical Center guidelines. Animal studies were pre-approved by the Institutional Animal Care

and Use Committee (#07-061-FC12).

Bone Marrow-Derived Macrophages (BMDMs)

Bone marrow was harvested from 8-12 week old mice by removing the femur bones, cutting the ends, and flushing with ice-cold PBS. Red blood cells were lysed with solute-free H₂O, and the bone marrow was plated on tissue culture coated dishes for 16 hours to allow mature/non-progenitor cells to attach. The non-adherent progenitor population was collected by pipetting and re-plated in 15-cm Petri dishes (non-tissue culture treated). Cells were then incubated for 6 days in BMDM media (RPMI w/ 15% FBS, 10% L929 supernatant and 1% penicillin/streptomycin) at 37°C and 5% CO₂ to produce differentiated bone marrow-derived macrophages (BMDMs). Culture media was changed every 2 days and cells were cultured for longer than 30 days. To assess the impact of EHD1 deletion, *Ehd1^{fl/fl}*; *Cre^{ERT2}* BMDMs were either cultured in regular medium (wildtype EHD1 expression) or medium containing 200 nM 4-hydroxytamoxifen (TAM) for 4 days to induce EHD1 deletion. This protocol was based on the initial time course and titration studies to determine optimal culture conditions. An illustration of BMDM preparation is displayed in Figure 2.2 and for inducible gene deletion in Figure 2.3.

Fluorescence Activated Cell Sorting (FACS)

BMDMs were washed with ice-cold PBS and blocked for 10 minutes for non-specific binding with CD16/32 (Fc Blocker) and then incubated with

appropriate antibodies at a dilution of 1:400 and put in the dark and on ice for 30min. Cells were then pelleted, washed with PBS twice, and suspended in 400 μ L of 0.1% BSA/PBS, put on ice, and protected from light.

Quantitative Real-Time-PCR (qRT-PCR)

RNA was isolated from BMDMs cultured on 10-cm tissue culture plates using the Trizol reagent, and 1 μ g of total RNA was reverse transcribed using the QuantiTect Reverse Transcription Kit (QIAGEN). 10% volume of the reaction of the ensuing cDNA was used with QuantiTect SYBR Green qRT-PCR Kit (QIAGEN) for qRT-PCR of mouse CSF-1R, using the primer sequences in Table 2.3. GAPDH was used as a control, and changes in CSF-1R were calculated using the threshold cycle method (55). Each reaction was performed in triplicate in a volume of 50 μ L with primers at a final concentration of 250 nM.

Immunoblotting (IB)

Immunoblotting/Western blotting was performed as described (36). Briefly, BMDMs were washed with ice-cold PBS and lysed in ice-cold Triton X-100 lysis buffer (0.5% Triton X-100, 50 mM Tris pH 7.5, 150 mM sodium chloride, and EDTA-free protease inhibitor cocktail). The lysates were vortexed, centrifuged at 13,000 rpm for 30 minutes at 4° C, and supernatants collected. Protein quantification was done by using a Thermo Scientific-Pierce Bicinchoninic acid (BCA) assay (cat. # 23225). 40 μ g of lysate protein per sample was resolved by SDS/PAGE and transferred to a PVDF membrane (Millipore, cat. # IPVH00010).

The membranes were blocked in TBS/1% Bovine Serum Albumin (BSA), incubated with the appropriate primary antibodies diluted in TBS-0.1% Tween 20 (BIO-RAD, cat. # 161-0781) overnight at 4°C. Next, membranes were washed in TBS-0.1% Tween (3 times for 10 minutes) followed by a 1-hour incubation with HRP-conjugated secondary antibody at room temperature. The membrane was washed in TBS-0.1% Tween (3 times for 10 minutes) each and ECL-based detection performed.

Immunofluorescence (IF)

Imaging using immunofluorescence was performed as previously described (56) with minor modifications. BMDMs were cultured on glass coverslips and fixed with 2% PFA/PBS for 5 min to assess the cell surface CSF-1R signals (57). Cells were fixed and permeabilized in methanol for 10 minutes at -20°C to evaluate total CSF-1R. The cells were then blocked with 1% BSA/PBS for 30 minutes and incubated with primary antibodies in 1% BSA/PBS overnight. Cells were then washed with PBS (three times), BMDMs incubated with the appropriate fluorochrome-conjugated secondary antibody for 45 minutes at room temperature (RT), washed and mounted using Fluoromount-G (Southern Biotech, Cat. # 0100-01) or VECTASHEILD mounting medium (Vector Laboratories, Cat. # H-1400 and H-1500). Images were acquired using a LeicaCTR4000 inverted microscope equipped with a QICAM 12-bit color camera, 12V 100 W halogen lamp, QCapture software and 60x oil lens (For CSF-1R) and a Zeiss 710 Meta Confocal Laser Scanning microscope (Carl Zeiss) using a 63x

objective with a numerical aperture of 1.0 and appropriate filters. Merged fluorescence pictures were generated and analyzed using ZEN® 2012 software from Carl Zeiss.

³H-thymidine incorporation assay of cellular proliferation

BMDMs were deprived of CSF-1 for 16 hours and plated in 48-well plates at 10,000 cells/well and allowed to attach overnight at 37°C, 5% CO₂. Cells were then treated with 30 ng/mL CSF-1 and allowed to proliferate for 2, 4 or 6 days. Cells were pulsed with 4 µCi/well of ³H-Thymidine for the last 6 hours of the assay. Radioactivity incorporated into DNA was collected by washing the cells with 10% TCA per well followed by 300 µl per well 0.2 N NaOH at room temperature to dissolve DNA. Each sample was transferred into vials with 5 mL of scintillation fluid and counts per minute (c.p.m.) were recorded with a scintillation counter. The protocol for ³H-thymidine incorporation assay of cellular proliferation is summarized in Figure 2.4.

CFSE dye dilution assays to access macrophage proliferation

Macrophages were cultured with recombinant CSF-1 (30 ng/mL) for 2, 4, or 6 days post initial CFSE population staining (Day 0) according to the manufacturer's protocol. Dilution of CFSE fluorescence as an indicator of cell division was assessed via flow cytometry, and the geometric means of the histograms were used to evaluate the degree of cell division in response to CSF-1. The protocol for CFSE dye dilution assay to access macrophage proliferation

is summarized in Figure 2.5.

Macrophage CSF1-induced spreading assay

BMDMs without (Control) or with (EHD1-KO) TAM were plated on coverslips and allowed to attach for 2 days. The BMDMs were then deprived of CSF-1 for 16 hours and then stimulated with 100 ng/mL CSF-1 for 10 minutes. Cells were fixed for 10 minutes with 4% PFA, washed with PBS (3 times for 10 minutes), and stained using phalloidin-488 (ThermoFisher Scientific, cat. # A12381). ImageJ software was used to quantify the surface area of macrophages.

Macrophage CSF1-induced migration assay

BMDMs were deprived of CSF-1 for 4 hours and placed in the upper chambers of 5 μ m pore inserts (Corning, cat. # 3421) at 1×10^5 cells per chamber in 100 μ l RPMI without CSF-1. Cells were then allowed to migrate towards CSF-1 (30 ng/mL) for 3 hours at 37°C. Cells on the bottom surface of membranes were fixed with 100% methanol and stained with HEMA for 5 minutes. Cells were visualized under a bright field microscope at 20x. Migrated cells were counted in 10 fields per insert, and the total number of migrated cells was calculated for control and EHD1-KO BMDMs.

[³⁵S]-methionine/cysteine metabolic labeling of CSF-1R

BMDMs were seeded at 5×10^6 cells/10-cm plate in CSF1-containing

medium and cultured for 16 hours. The cells were washed and incubated in methionine/cysteine-free RMPI-1640 medium supplemented with 15% FBS and 30 ng/mL recombinant CSF-1 for 30 minutes at 37°C and pulsed with 0.1 mCi of [³⁵S] for 15 minutes at 37°C. Cells were then washed and incubated with regular culture medium containing a 20-fold excess of unlabeled methionine/cysteine for 0, 15, 30, and 60 minutes of chase.

Immunoprecipitation (IP)

Cells were rinsed with ice-cold PBS and immediately lysed in ice-cold Triton X-100 lysis buffer with EDTA-free protease inhibitor cocktail. Anti-CSF-1R immunoprecipitations were carried out using 500 µg samples of cleared lysate protein and anti-CSF-1R (C-20) antibody followed by exposure to Protein-A Sepharose beads. Samples were resolved by SDS/PAGE (8%). Gels were fixed, dried, and incubated with Auto-Fluor (National Diagnostics, cat. # LS-315) to amplify [³⁵S] signals. Radiography was performed after films were exposed to the dried gels at -80°C in metal cassettes with intensifying screens.

Statistics

P-values were calculated by using an unpaired Student's *t*-test and the threshold of significance is *p*<0.05. Data are shown graphically as means ± SEM (error bars).

Chapter 2: Tables

Table 2.1. Genotypes of mice used in this study.

Strain Designation	Genotype
Ehd1-WT	<i>Ehd1</i> ^{+/+}
Ehd1-null	<i>Ehd1</i> ^{-/-}
Control	<i>Ehd1</i> ^{fl/fl} ; Cre ^{ERT2}
EHD1-KO	<i>Ehd1</i> ^{fl/fl} ; Cre ^{ERT2} (+TAM)

Table 2.2. Genotyping PCR primer sequences.

Target	Forward primer 5 - 3'	Reverse primer 5 - 3'
Ehd1-WT	AAGTCAGAAGACAACTTTC TGGAGTTCCT	TCCAGGGCCCACATGGTAG AAGGAGAGAGT
Ehd1-null	AAGTCAGAAGACAACTTTC TGGAGTTCCT	GCTCCGGTCTTGGACTTCA CCAGCATTTAG
Ehd1 ^{fl/fl}	AAGTCAGAAGACAACTTTC TGGAGTTCCT	TCCAGGGCCCACATGGTAG AAGGAGAGAGT
Cre ^{ERT2}	GCGGTCTGGCAGTAAAAAC TATC	GTGAAACAGCATTGCTGTC ACTT

Table 2.3. Real-time PCR primer sequences.

Target	Forward 5' - 3'	Reverse 5' - 3'
CSF-1R	GCAGTACCACCATCCACTTGTA	GTGAGACACTGTCCTTCAGTG C
EHD1	AGGACAGCCGCAAAGTCATA	ACTGGACAGCATCAGCATCA
EHD2	CTTGTTTTCTTCCCGAACA	CAACGACCTAGTGAAACGGG
EHD3	TCATGCCTGGAAAATCCTGT	GATTCGACAACAAGCCCAT
EHD4	CGGCAAACCACTGTAAGACC	GCATCAGCATCATCGACAGT
GAPDH	TTGATGGCAACAATCTCCAC	CGTCCCGTAGACAAAATGGT

CHAPTER 2: FIGURES

Figure 2.1. Genotyping analysis.

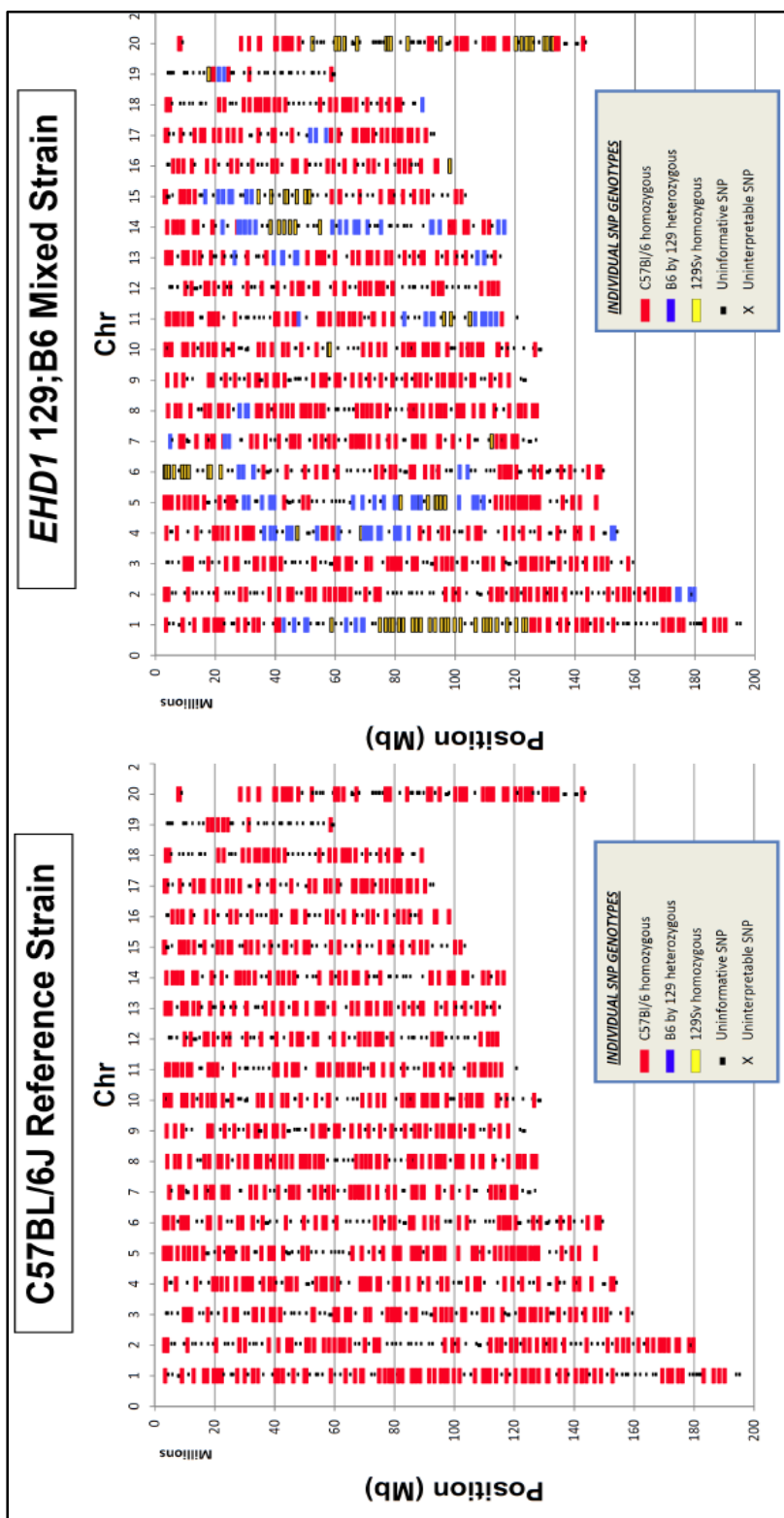


Figure 2.1. Genotyping analysis. Genotyping analysis of Ehd1-WT and Ehd1-null mice in comparison to the Jackson Laboratory C57BL/6J reference strain was carried out by DartMouse, Lebanon, NH using 1449 SNP Illumina Bead Chip. Each SNP output is color coded. Red represents C57Bl/6, blue represents heterozygous (B6 x 129), and yellow represents 129Sv. All analyzed mice (Ehd1-WT and Ehd1-null) correspond to approximately mid-70% C57BL/6 background.

Figure 2.2. BMDMs from freshly isolated bone marrow.

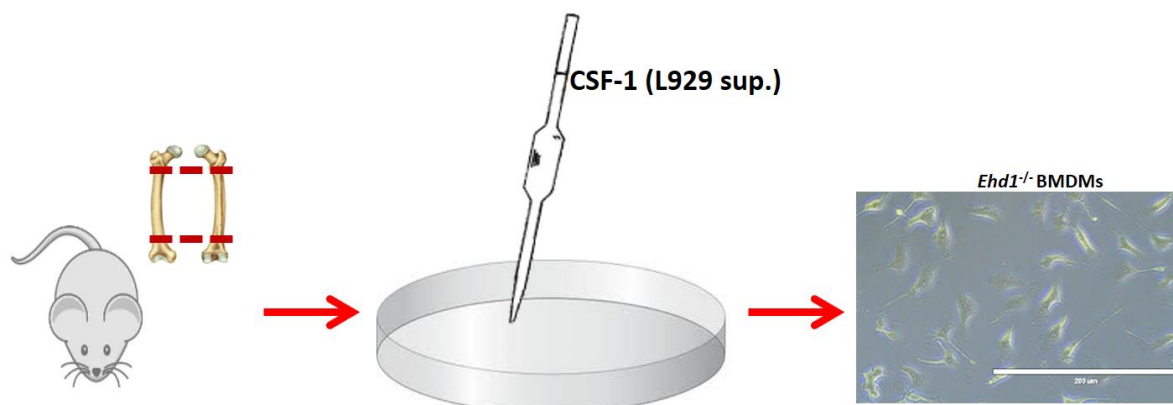


Figure 2.2. BMDMs from Freshly Isolated bone marrow. Bone marrow was harvested from 8-12 week old mice by removing the femur bones, cutting the ends, and flushing with ice-cold PBS. Cells were then incubated for 6 days in BMDM media [RPMI w/ 15% FBS, 10% L929 supernatant (58) 1% penicillin/streptomycin] to produce bone marrow-derived macrophages (BMDMs). If inducible deletion was needed when using *Ehd1^{fl/fl}*; *Cre^{ERT2}* BMDMs, cells were cultured in regular medium (wildtype EHD1 expression) or medium containing 200 nM 4-hydroxytamoxifen (TAM) for an additional 4 days to induce EHD1 deletion (EHD1-KO).

Figure 2.3. BMDMs with inducible EHD1 deletion.

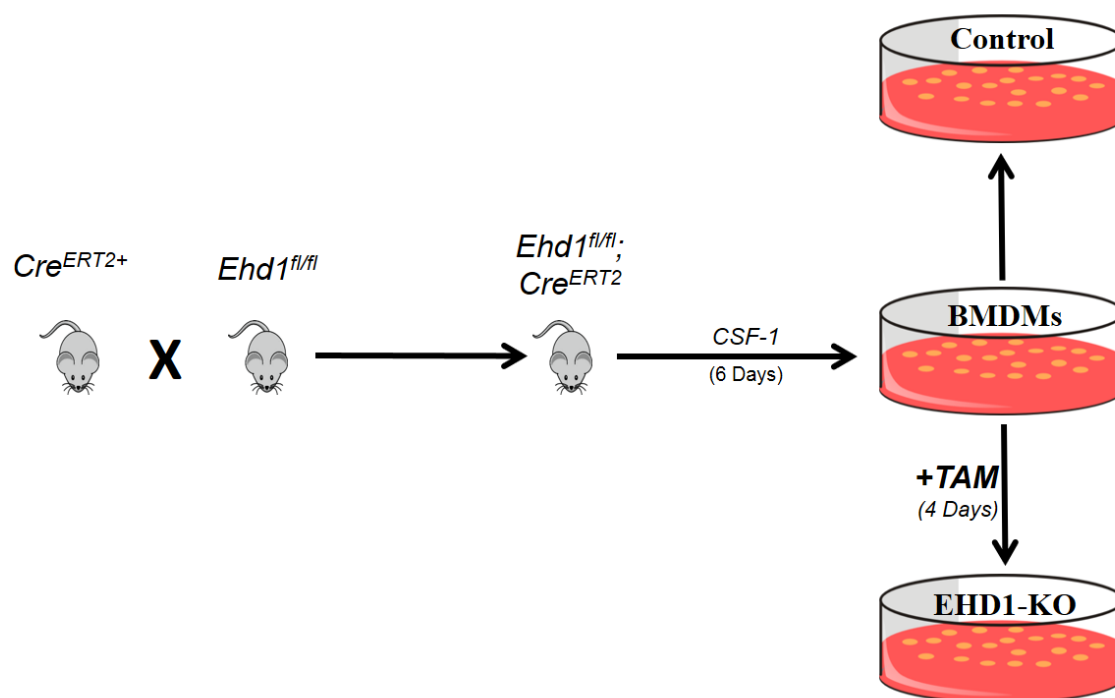


Figure 2.3. BMDMs with inducible EHD1 deletion. *Ehd1^{fl/fl}* mice on a predominantly C57BL/6 background (33, 36) were crossed with tamoxifen-inducible *Cre^{ERT2}* expressing mice from Jackson Laboratories (*Gt(ROSA)26Sor^{tm1(cre/ERT2)Tyj}*; strain 008463) to generate *Ehd1^{fl/fl}; Cre^{ERT2}* mice. Bone marrow was harvested from 8-12 week old mice by removing the femur bones, cutting the ends, and flushing with ice-cold PBS. Cells were then incubated for 6 days in BMDM media [RPMI w/ 15% FBS, 10% L929 supernatant (58) 1% penicillin/streptomycin] to produce bone marrow-derived macrophages (BMDMs). If inducible deletion was needed when using *Ehd1^{fl/fl}; Cre^{ERT2}* BMDMs, cells are further cultured in regular medium (wildtype EHD1 expression) or medium containing 200 nM 4-hydroxytamoxifen (TAM) for an additional 4 days to induce EHD1 deletion (EHD1-KO).

Figure 2.4. ^3H -thymidine incorporation assays for cell proliferation.

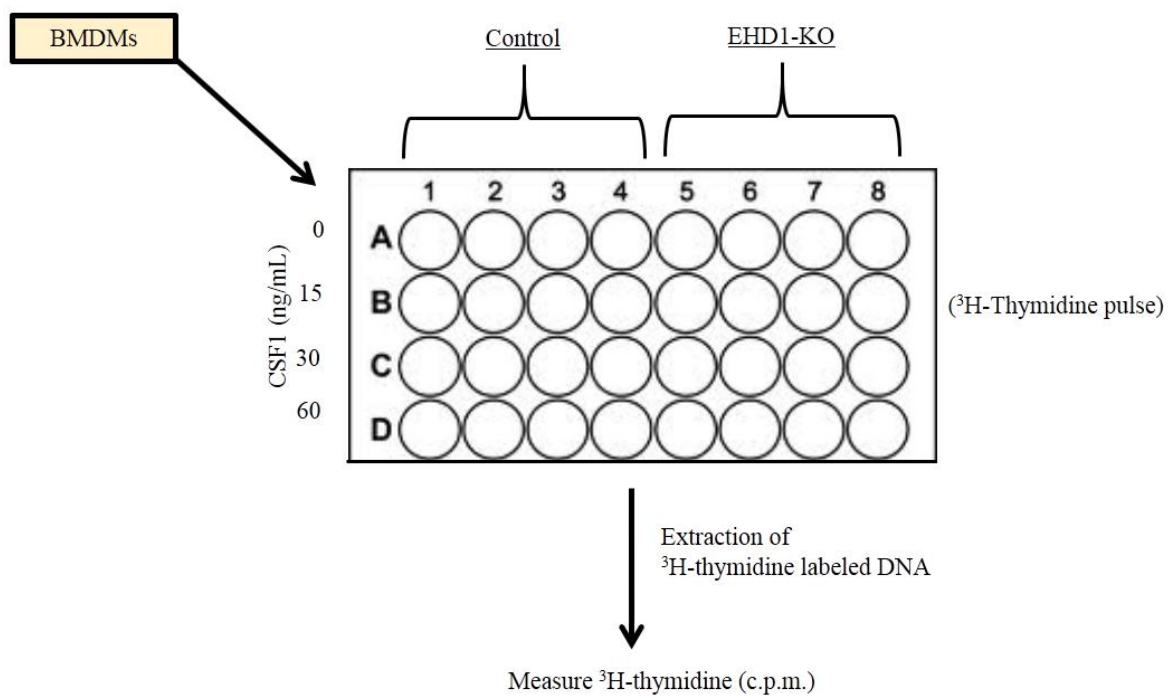


Figure 2.4. ^3H -thymidine incorporation assays for cell proliferation. BMDMs were deprived of CSF-1 for 16 hours and plated in 48-well tissue culture plates at 10,000 cells per well and allowed to attach overnight at 37 °C, 5% CO₂. Cells were then treated with 30 ng/mL CSF-1 and allowed to proliferate for 2, 4 or 6 days. Cells were pulsed with 4 µCi/well of ^3H -thymidine for the last 6 hours of the assay. Radioactivity incorporated into DNA was collected by washing the cells with 10% TCA per well followed by 300 µl per well 0.2 N NaOH at room temperature to dissolve DNA. Each sample was transferred into vials with 5 mL of scintillation fluid and counts per minute (c.p.m.) were recorded with a scintillation counter. Macrophages were cultured with recombinant CSF-1 (30 ng/mL) for 2, 4 or 6 days post initial CFSE population staining (Day 0) according to manufacturer's protocol. Dilution of CFSE fluorescence as an indicator of cell division was assessed via flow cytometry, and the geometric means of the histograms were used to evaluate the degree of cell division in response to CSF-1.

Figure 2.5. CFSE dye dilution assays to assess macrophage proliferation.

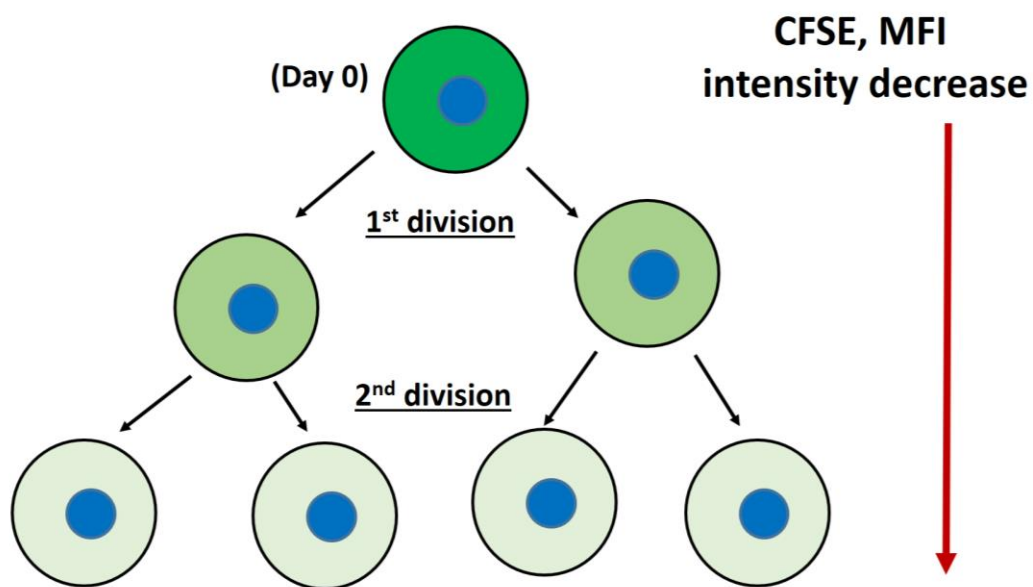


Figure 2.5 CFSE dye dilution assays to access macrophage proliferation.

After initial homogeneous labeling of the cell population at day 0 with the CFSE dye, cells were stimulated (30ng/mL CSF-1) to proliferate. Upon cell division, decreasing fluorescence (theoretically half) of the parent cell's fluorescence is retained by each daughter population. Equal dye distribution dilution upon cell subsequent cellular divisions created different subpopulations, and when analyzed by flow cytometry the relative percentages of the original population in each subpopulation were determined. Note: lower MFI = more cellular proliferation.

CHAPTER 3: RESULTS

The material covered in the following chapter is the topic of the following published article:

Luke R. Cypher, Timothy Alan Bielecki, Oluwadamilola Adepegba, Lu Huang, An Wei, Fany Iseka, Haitao Luan, Eric Tom, Matthew D. Storck, Adam D. Hoppe, Vimla Band, Hamid Band. CSF-1 receptor signalling is governed by pre-requisite EHD1 mediated receptor display on the macrophage cell surface.

(Accepted for Publication: *Cellular Signalling*, Available online 17 May 2016)

Expression of EHD proteins in Ehd1-WT and Ehd1-null BMDMs

To assess the potential role of EHD proteins in the context of CSF-1R, I chose to use primary BMDMs as these cells recapitulate *in vitro* the requirement of CSF1R-mediated signals for appropriate development and function (59). Flow cytometry analysis of mature macrophage marker F4/80 (58) confirmed the expected homogeneous differentiation of bone marrow progenitors into BMDMs when cultured in CSF1-containing medium (Figure 3.1).

To assess EHD levels in BMDMs and to assure Ehd1-deletion, qRT-PCR and immunoblotting were performed for EHD family members. qRT-PCR revealed that Ehd1-WT BMDMs express EHD1 and EHD4 mRNA but not significant levels of EHD2 or EHD3 (Figure 3.2). Ehd1-null BMDMs had the same profile as Ehd1-WT BMDMs with the exception that Ehd1-null BMDMs had undetectable EHD1 mRNA expression (Figure 3.2). Western blot analysis of EHD1 and EHD4 expression confirmed the qRT-PCR results (Figure 3.2). Neither qRT-PCR nor Western blot analyses revealed a significant compensatory increase in the expression of EHD family members when EHD1 was deleted (Figure 3.2). These initial analyses provided a basis to explore a potential role of EHD1 in regulating CSF-1R signaling and traffic.

Deletion of EHD1 in BMDMs leads to reduced CSF1-induced responses

To assess implications of inducible EHD1 deletion on CSF1-induced

cellular responses, I first compared the CSF1-induced proliferation of BMDMs using two separate methods: ^3H -thymidine incorporation and CFSE dye dilution assays. Both of these assays have previously been used to assess macrophage proliferation in response to CSF-1 [54, 55]. Both ^3H -thymidine incorporation and CFSE dye dilution proliferation assays showed a significant deficit in CSF1-induced macrophage proliferation in the Ehd1-null population of BMDMs (Figures 3.3-3.5).

As stimulation through CSF-1R is known to correlate with rapid macrophage spreading (62), I next conducted a spreading assay to examine the impact of EHD1 deletion on macrophage cellular spreading. Ehd1-WT and Ehd1-null BMDMs were deprived of CSF-1 for 16 hours and then stimulated with CSF-1 for 10 minutes. The cells were then fixed and stained (Phalloidin-488) to assess the extent of cell spreading by quantifying the surface area of individual macrophages in both Ehd1-WT and Ehd1-null BMDMs. Ehd1-null BMDMs exhibited reduced spreading in response to CSF-1 stimulation (Figure 3.6). Collectively, these results indicate that Ehd1-deletion in BMDMs impairs the CSF1-induced macrophage phenotype.

Deletion of EHD1 in BMDMs leads to reduced CSF-1R signaling

I next sought to determine the effect of EHD1 deficiency on CSF-1R signaling activation of the ERK pathway since macrophage proliferation is known to be mediated by this pathway (17). The levels of pERK upon CSF-1 stimulation were significantly lower in Ehd1-null as compared to Ehd1-WT BMDMs (Figure

3.7). Thus, Ehd1-deletion results in decreased CSF1-induced CSF-1R signaling in macrophages.

Reduced surface CSF-1R expression in EHD1-KO BMDMs

CSF-1R display at the cell surface is essential for CSF-1R activation/signaling by CSF-1 (17). Given the results above and the known role of EHD1 in the endocytic trafficking of cellular surface receptors (41–47), I next sought to determine if absence of EHD1 alters cell surface CSF-1R expression in BMDMs.

Since BMDMs require CSF-1 for *in vitro* culture, surface levels of CSF-1R are low under steady state conditions due to continuous activation and lysosomal degradation of ligand-activated CSF-1R (25, 29). Therefore, I assessed the cell surface CSF-1R levels at 16 hours following the removal of CSF-1 from the culture medium (CSF-1 deprivation) in order to allow the newly synthesized CSF-1R to accumulate at the cell surface. As expected, Ehd1-WT surface CSF-1R levels increased to a high level. In contrast, accumulation of cell surface CSF-1R on Ehd1-null BMDMs was significantly less after 16 hours CSF-1 deprivation (Figure 3.8). Thus, EHD1 deletion in BMDMs results in decreased surface CSF-1R expression.

EHD1 inducible deletion in BMDMs

Our initial analysis thus far of BMDMs derived from whole-body Ehd1-null mice showed that EHD1 and EHD4 are expressed in BMDMs and that loss of

EHD1 led to reduced CSF-1R signaling, CSF-1R surface levels, cell proliferation, and cellular spreading (Figures 3.1-3.8). Thus, EHD1 functions as a positive regulator of CSF-1R signaling in macrophages.

While our existing *Ehd1*-null mice provide a reasonable approach, I sought to eliminate any macrophage developmental bias in the whole body *Ehd1*-null mice. Moreover, I used BMDMs isolated from *Ehd1^{fl/fl}; Cre^{ERT2}* mice without (Control) and with (EHD1-KO) tamoxifen (TAM) treatment to confirm my findings that *Ehd1* is a positive regulator of CSF-1R signaling in macrophages.

Inducible deletion of EHD1 in BMDMs from *Ehd1^{fl/fl}; Cre^{ERT2}* mice.

To determine if deletion of inducible EHD1 deletion had a functional impact in BMDMs, I first assessed whether or not EHD1-KO bone marrow progenitors could be differentiated into BMDMs and subsequently have EHD1 deletion induced by TAM treatment *in vitro*. *Ehd1^{fl/fl}; Cre^{ERT2}* BMDMs cultured in the absence or presence of TAM were stained with F4/80 antibody and analyzed via Facilitated Analysis Cell Sorting (FACS). Greater than 99% of BMDMs without (Control) and with (EHD1-KO) TAM treatment stained positive for F4/80⁺ (Figure 3.9). Thus, these results demonstrate the ability of bone marrow from *Ehd1^{fl/fl}; Cre^{ERT2}* mice to differentiate into mature macrophages.

Next, to confirm EHD family expression in BMDMs from *Ehd1^{fl/fl}; Cre^{ERT2}* mice without (Control) and with (EHD1-KO), qRT-PCR was carried out. BMDMs from *Ehd1^{fl/fl}; Cre^{ERT2}* mice without (Control) and with (EHD1-KO) expressed

EHD1 and EHD4 mRNA but did not express significant levels of EHD2 or EHD3 (Figure 3.10A). Furthermore, BMDMs cultured in the presence (EHD1-KO) of TAM showed undetectable EHD1 mRNA expression (Figure 3.10A). Thus, these data confirmed an efficient and effective knockout of EHD1 (EHD1-KO) with TAM treatment. Western blot analysis of EHD1 and EHD4 expression confirmed the qRT-PCR results of a successful EHD1-KO (Figure 3.10B). Neither qRT-PCR nor Western blot analyses revealed a significant compensatory increase in the expression of other EHD family members when EHD1 is deleted (Figure 3.10). These findings solidified our initial findings of EHD family protein expression in BMDMs using whole-body *Ehd1*-null mice.

Tamoxifen is not toxic to BMDMs *in vitro*

I next performed control experiments to verify that any phenotypic effects I observed using EHD1-KO BMDMs were *bona fide* effects of EHD1 deletion and not effects of tamoxifen treatment. To exclude the possibility that reduced CSF-1 elicited biological responses in tamoxifen-induced EHD1-KO BMDMs were not due to incidental toxicity of tamoxifen, as observed in previously reported systems (63), I cultured BMDMs from *Ehd1^{fl/fl}* mice (lacking *Cre^{ERT2}*), with or without TAM, and assessed their CSF1-induced proliferation using the CFSE dye dilution assay. Untreated vs. TAM-treated *Ehd1^{fl/fl}* BMDMs exhibited comparable proliferative responses to CSF-1 (Figure 3.11), indicating TAM treatment did not alter *in vitro* BMDM CSF-1R signaling.

To further control for possible toxic side-effects of TAM treatment, I

assessed apoptosis with Annexin V and propidium iodide (PI) staining using *Ehd1^{fl/fl}* BMDMs cultured with or without TAM. The double staining with Annexin V and PI was analyzed by flow cytometry and did not reveal any significant differences in the percentage of apoptotic cells in *Ehd1^{fl/fl}* BMDMs cultured with or without TAM (Figure 3.12). These assays showed a lack of TAM treatment toxicity or attenuation of CSF1-induced CSF-1R signaling responses in BMDMs.

Inducible EHD1-KO results in reduced CSF1-induced macrophage functions

To assess the role of EHD1 in macrophage CSF1-induced cellular responses, I assayed the effects of CSF1-induced proliferation on BMDMs derived from *Ehd1^{fl/fl}; Cre^{ERT2}* mice without (Control) and with (EHD1-KO) TAM treatment. I used two independent methods to assess macrophage proliferation as with my initial studies using BMDMs from *Ehd1*-null mice: ³H-thymidine incorporation and CFSE dye dilution assays. Both assays showed EHD1-KO macrophages had significantly reduced proliferative responses when stimulated with CSF-1 (Figures 3.13-3.15). These findings confirmed my initial findings using BMDMS from *Ehd1*-WT and *Ehd1*-null mice.

Next, I sought to examine the impact of EHD1 deletion on CSF1-induced macrophage functional response. BMDMs cultured without (Control) or with (EHD1-KO) TAM were subjected to a spreading assay. EHD1-KO BMDMs exhibited reduced spreading in response to CSF-1 stimulation (Figure 3.16). These findings confirmed my initial findings using BMDMS from *Ehd1*-WT and

Ehd1-null mice.

To further assess the impact of EHD1 deletion on CSF1-induced macrophage functional responses, I conducted a trans-well migration. This migration assay is a well-established way to assess macrophages response to CSF-1 stimulation (64). Compared to the control group, EHD1-KO BMDMs showed a significant reduction in migration (Figure 3.17).

Collectively, these results demonstrated that EHD1-KO in BMDMs leads to a significant deficit in CSF1-induced cellular responses. Furthermore, EHD1 appears to mediate CSF1-induced macrophage function via regulation of CSF-1R signaling. These findings solidified my initial findings using Ehd1-WT and Ehd1-null BMDMS.

EHD1-KO BMDMs have reduced CSF-1R signaling

Next, I assessed the effects of EHD1-KO on CSF-1R signaling downstream activation of the MAPK pathway, which is known to modulate cellular proliferation (65, 66). After 16 hours of CSF-1 deprivation, the total CSF-1R levels were lower in the EHD1-KO compared to Control BMDMs (Figure 3.18; 0-time points). Commensurate with diminished CSF-1R, accumulation of pERK in EHD1-KO BMDMs was significantly lower than in control BMDMs (Figure 3.18). These findings suggest diminished CSF-1R signaling is a consequence of EHD1 absence in macrophages and is likely due to decreased total CSF-1R protein. These findings solidify our findings using Ehd1-WT and Ehd1-null BMDMS.

CSF-1R internalization and degradation are similar in EHD1-KO BMDMs

Since EHD1 has thus far been primarily characterized as a regulator of the recycling back to the cell surface of previously internalized cell surface receptors (30), I wished to determine if the post-endocytic traffic of CSF-1R may also be regulated by EHD1. CSF-1 stimulation of BMDMs is known to induce rapid CSF-1R internalization (~5 minutes), transport to macropinosomes (~5–15 minutes) and lysosomal degradation (~30 minutes) (23, 25, 57). Both Control and EHD1-KO macrophages were deprived of CSF-1 for 16 hours followed by stimulation with CSF-1 and both surface and total CSF-1R expression was assessed by immunofluorescence microscopy. No apparent difference in the kinetics of CSF-1R internalization (Figures 3.19) or degradation (Figure 3.20) was observed between Control and EHD1-KO BMDMs. However, consistent with experiments using Ehd1-WT and Ehd1-null BMDMs, a markedly lower surface and total CSF-1R levels were seen in EHD1-KO BMDMs prior to CSF-1 addition (16 hours after CSF-1 deprivation).

Reduced surface CSF-1R expression in EHD1-KO BMDMs

To further understand the decreased surface CSF-1R expression observed in EHD1-KO BMDMs (Figure 3.19), I assessed the cell surface CSF-1R levels using flow cytometry after 2, 4, 8 or 16 hours of CSF-1 deprivation. Initially, low CSF-1R surface levels increased steadily over time in Control BMDMs; however, surface CSF-1R in EHD1-KO BMDMs accumulated at a significantly

lower rate. Surface expression of CSF-1R was considerably less at all-time points following CSF-1 deprivation in EHD1-KO as compared to Control BMDMs (Figures 3.21 and 3.22). Thus, loss of EHD1 leads to reduced CSF-1R present at the cell surface in BMDMs available for activation by CSF-1. These findings agree with my initial findings using Ehd1-WT and Ehd1-null BMDMs.

EHD1 deletion results in depletion of CSF-1R protein in BMDMs

To investigate the mechanism responsible for reduced cell surface expression of CSF-1R on EHD1-KO BMDMs, I first examined (by western blotting) the accumulation of total cellular CSF-1R protein after CSF-1 was removed from the culture medium. *Ehd1^{fl/fl}; Cre^{ERT2}* BMDMs grown in regular CSF1-containing medium without (Control) or with (EHD1-KO) TAM treatment were deprived of CSF-1 for 2, 4, 8 or 16 hours. At the given time-points, cells were lysed and subsequently analyzed by immunoblotting for total CSF-1R levels. Notably, EHD1-KO BMDMs showed a significant and substantial reduction in the total CSF-1R protein levels at each CSF-1 deprivation time point (Figures 3.23 and 3.24). Thus, EHD1-KO BMDMs are characterized by reduced total CSF-1R.

EHD1 functions to transport newly synthesized CSF-1R to the cell surface

Given the reduction in surface and total CSF1R in EHD1-KO BMDMs, I carried out qRT-PCR analysis to assess the levels of CSF-1R mRNA expression

(synthesis) in Control and EHD1-KO BMDMs. *Ehd1^{fl/fl}; Cre^{ERT2}* BMDMs cultured without (Control) or with (EHD1-KO) TAM were harvested under steady state culture conditions (with CSF-1) or 16 hours after CSF-1 removal from the culture medium. The CSF-1R mRNA levels increased nearly 50% when control BMDMs cultured under steady-state conditions (with CSF-1) were changed to CSF1-free medium for 16 hours. CSF-1R mRNA levels were not significantly different in EHD1-KO compared to those of Control BMDMs (Figure 3.25). Thus, I concluded the reduction in total CSF-1R levels in EHD1-KO BMDMs was not likely due to a defect in CSF-1R synthesis.

To more rigorously assess if EHD1 deletion affects CSF-1R protein synthesis and/or its post-translational maturation and transport to the cell surface, I performed metabolic pulse labeling with [³⁵S]-methionine/cysteine. Under these conditions, newly synthesized and mature CSF-1R that reaches the cell surface will bind CSF-1, undergo immediate activation, be targeted for degradation in the lysosome, and result in a reduction in radioactive signals of mature CSF-1R at later time points of the chase experiment. Equal amounts of lysates collected at various time points were subjected to anti-CSF-1R immunoprecipitation to visualize the immature and mature CSF-1R polypeptides. The signals of immature CSF-1R synthesized during pulse-labeling (time 0) were comparable between control and EHD1-KO BMDMs (Figure 3.26; lower band), thus excluding any alteration in the rate of protein synthesis as a determinant of the observed reduced total CSF-1R levels in EHD1-KO cells previously seen in Figure 3.23.

Analysis at various times during chase showed that the conversion of immature CSF-1R to a higher molecular weight, a fully glycosylated form known to be generated in the Golgi (17) was similar to a majority of immature forms converting to mature forms by 30 min of chase (Figure 3.26). Notably, mature CSF-1R signals in control BMDMs were sharply lower by 60 min of chase, reflecting its arrival at the cell surface and subsequent CSF1-induced internalization and degradation (Figure 3.26) (26). In contrast, the mature CSF-1R signals remained high, and nearly unaltered, at 60 min of the chase in EHD1-KO BMDMs (Figure 3.26), indicative of a block in the surface transport of newly synthesized and mature CSF-1R. These observations support the conclusion that EHD1 is required at a post-Golgi glycosylation step in the surface transport of the newly synthesized and fully glycosylated CSF-1R.

CSF-1R was found localized to this EHD1⁺/GM130⁺ compartment

Given the results of pulse-chase analyses, I sought to determine if EHD1 co-localizes with CSF-1R at the Golgi apparatus. Three-color confocal imaging was performed on fixed and permeabilized BMDMs previously cultured without (Control) or with (EHD1-KO) TAM for 2, 4, 8, and 16 hours after removal of CSF-1 to allow CSF-1R synthesis and accumulation. In control BMDMs, a pool of EHD1 co-localizes with the Golgi marker GM130, and a pool of CSF-1R was found localize to this EHD1⁺/GM130⁺ compartment (Figure 3.27). As expected, no EHD1 staining was detected in BMDMs rendered EHD1-KO by culture in the presence of TAM (Figure 3.27). The EHD1-KO BMDMs also exhibited a pool of

CSF-1R localized to GM130⁺ Golgi compartment, with lower CSF-1R signals near the cell surface (Figure 3.27).

These results, together with those of the metabolic pulse-chase, support the conclusion that EHD1 is involved in directing the Golgi-localized (newly synthesized) CSF-1R to the cell surface.

Newly synthesized CSF-1R transits to lysosomes for degradation in EHD1-KO BMDMs

In view of a block in the post-Golgi transport of CSF-1R to the cell surface in EHD1-KO BMDMs, combined with reduced total CSF-1R levels without any alterations in its initial synthesis and glycosylation, I hypothesized that EHD1 was required for the efficient sorting of Golgi-localized CSF-1R towards the cell surface, and that absence of this mechanism resulted in CSF-1R transit to the lysosome for degradation. BMDMs cultured in the absence (Control), or presence (EHD1-KO) of TAM were switched from regular to CSF1-free medium for 4 hours either in the absence or presence of lysosomal proton pump blocker Bafilomycin A1 (Baf-A1). Western blot analysis demonstrated the expected lower levels of total CSF-1R observed previously in EHD1-KO vs. control BMDMs cultured in the absence of Baf-A1 (Figure 3.28; first and third lanes).

The inclusion of Baf-A1 led to a dramatic and statistically significant increase in CSF-1R levels in EHD1-KO BMDMs compared to the no Baf-A1 control, and nearly approaching the levels in Control BMDMs (Figure 3.28). These results suggest that CSF-1R rapidly transits from the Golgi to the

lysosome in EHD1-KO BMDMs and undergoes degradation.

To further demonstrate this proposed mechanism, I carried out confocal imaging of Control and EHD1-KO BMDMs cultured for 4 hours in Baf-A1. BMDMs from both groups were stained for CSF-1R and LAMP1 (a lysosomal marker). In contrast to a small pool of CSF-1R that localized in LAMP1⁺ lysosomes in control BMDMs, a significantly higher level of co-localization between CSF-1R and LAMP1 was seen in EHD1-KO BMDMs (Figure 3.29).

Overall, these results support the conclusion that EHD1 helps in the transport of CSF-1R from a Golgi sorting compartment to the cell surface. Furthermore, CSF-1R is shunted to the lysosome in EHD1-KO BMDM, resulting in lysosomal degradation of the receptor.

CHAPTER 3: FIGURES

Figure 3.1. BMDMs defined by F4/80⁺ flow cytometry staining.

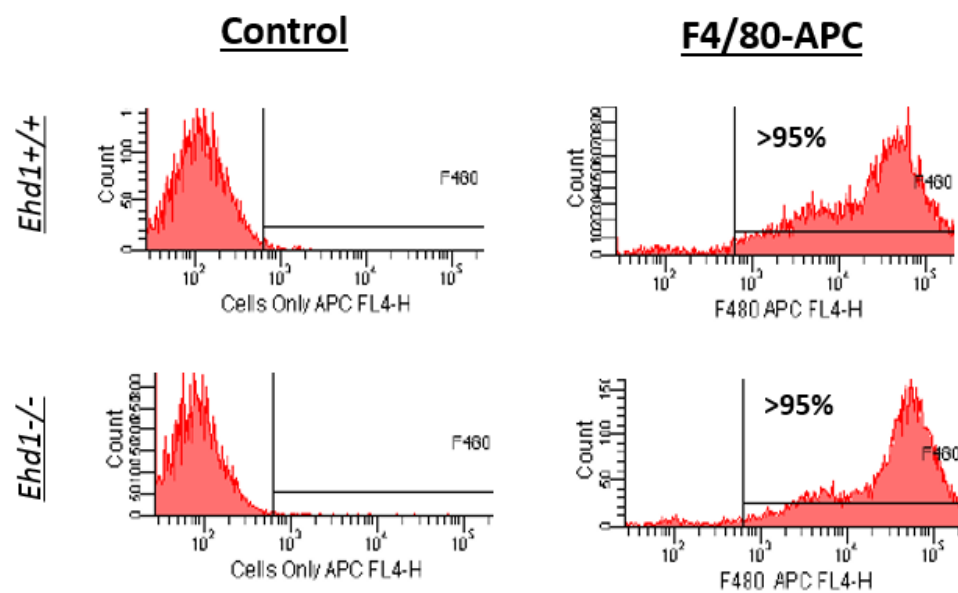


Figure 3.1. BMDMs defined by F4/80⁺ flow cytometry staining. BMDMs were stained on day 6 of bone marrow culture from Ehd1-WT and Ehd1-null mice for mature macrophage marker F4/80.

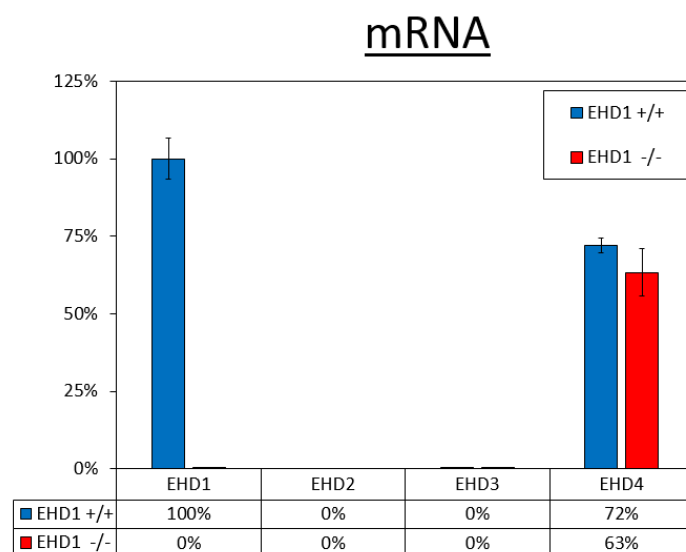
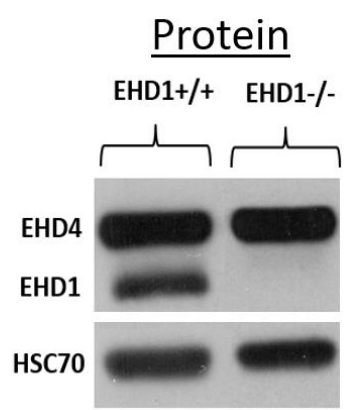
Figure 3.2. EHD family expression in Ehd1-WT and Ehd1-null BMDMs.**A****B**

Figure 3.2. EHD family expression in Ehd1-WT and Ehd1-null BMDMs. (A) Quantitative real-time-PCR analysis of EHD family proteins in BMDMs. Data was normalized to GAPDH and was expressed as a fold change with EHD1 expression in Ehd1-WT BMDMs set to 1. (B) Lysate from Ehd1-WT and Ehd1-null BMDMs. Immunoblotting was for EHD1, EHD4, and HSC70. Note specific deletion of EHD1 protein in BMDMs matured from Ehd1-null mice, but not from Ehd1-WT mice. Representative data from 3 separate biological replicates are shown (mean \pm SEM; * = $p < 0.05$, n.s. = not significant).

Figure 3.3. ^3H -thymidine proliferation assay using BMDMs.

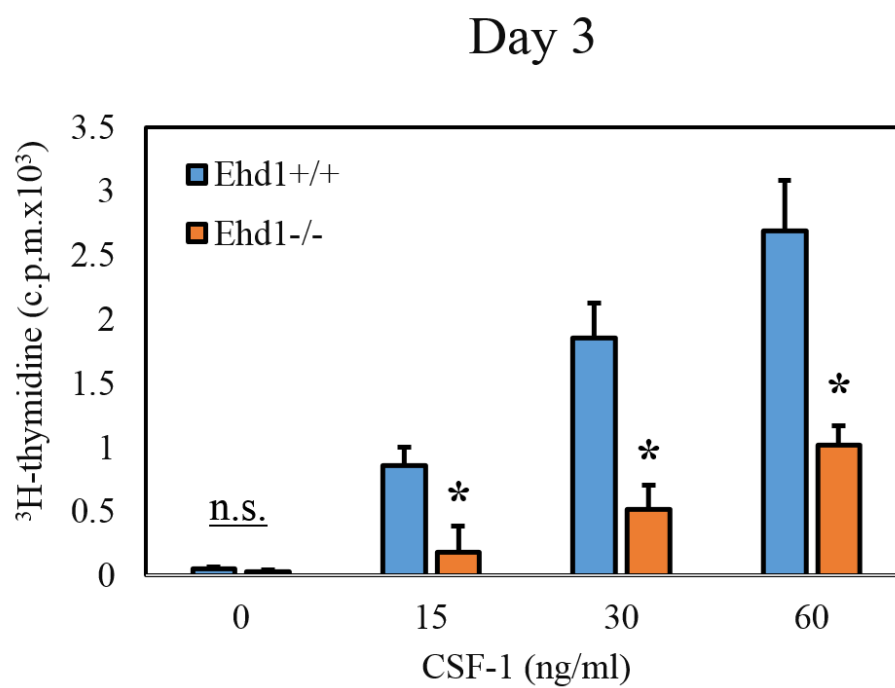


Figure 3.3. ^3H -thymidine proliferation assay using BMDMs. BMDM proliferation as measured by ^3H -thymidine incorporation. Ehd1-WT and Ehd1-null BMDMs were stimulated with CSF-1 at 0, 15, 30 or 60 ng/mL for 3 days. Representative data from 3 separate biological replicates are shown (mean \pm SEM; * = $p < 0.05$, n.s. = not significant).

Figure 3.4. CFSE assays using Ehd1-WT and Ehd1-null BMDMs.

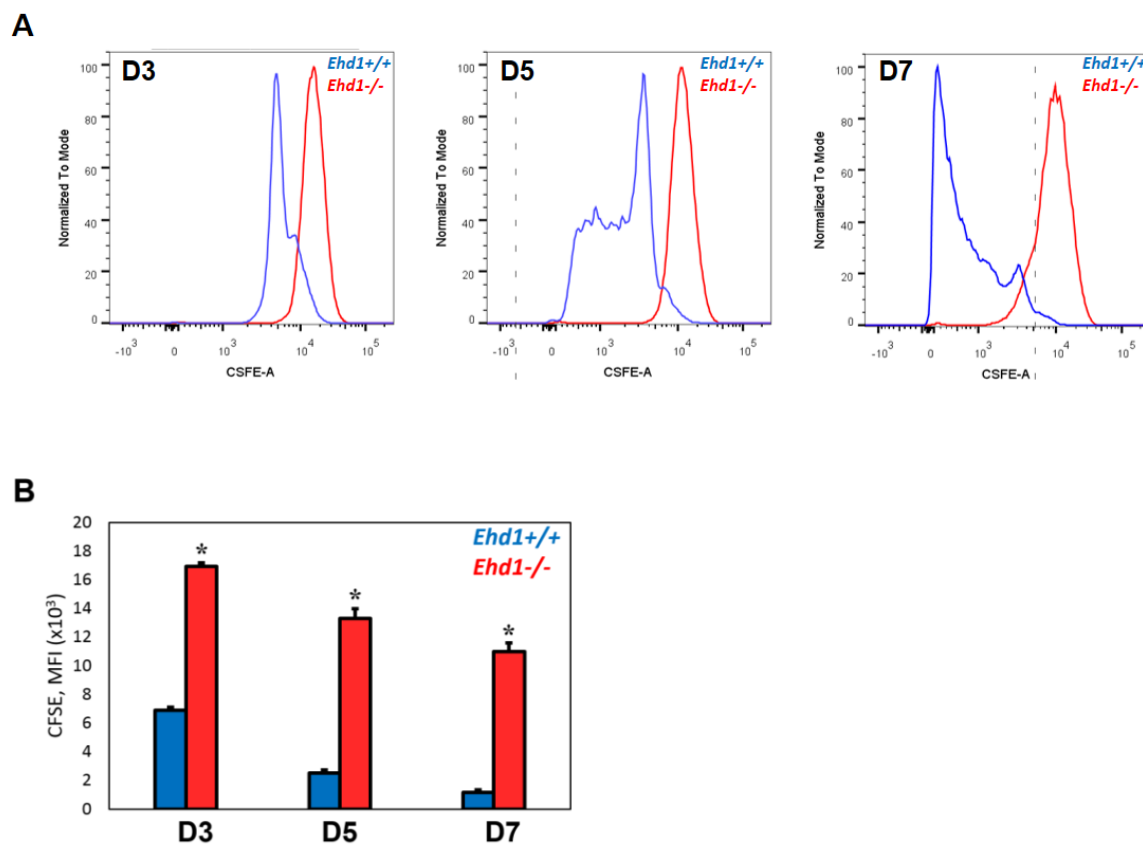


Figure 3.4. CFSE assays using Ehd1-WT and Ehd1-null BMDMs. (A) BMDM proliferation as measured by CFSE dye dilution assay. Ehd1-WT and Ehd1-null BMDMs were stained with CFSE dye (day 0) and subsequently stimulated with 30 ng/mL recombinant CSF-1 for 3, 5, or 7 days. (B) Quantification of Mean Fluorescence Intensity (MFI) CFSE dye dilution assay from Figure 3.4B. MFI fold change was normalized relative to Control BMDMs. Representative data from 3 separate biological replicates are shown (mean \pm SEM; * = $p < 0.05$).

Figure 3.5. CFSE population differences in Ehd1-WT and Ehd1-null BMDMs.

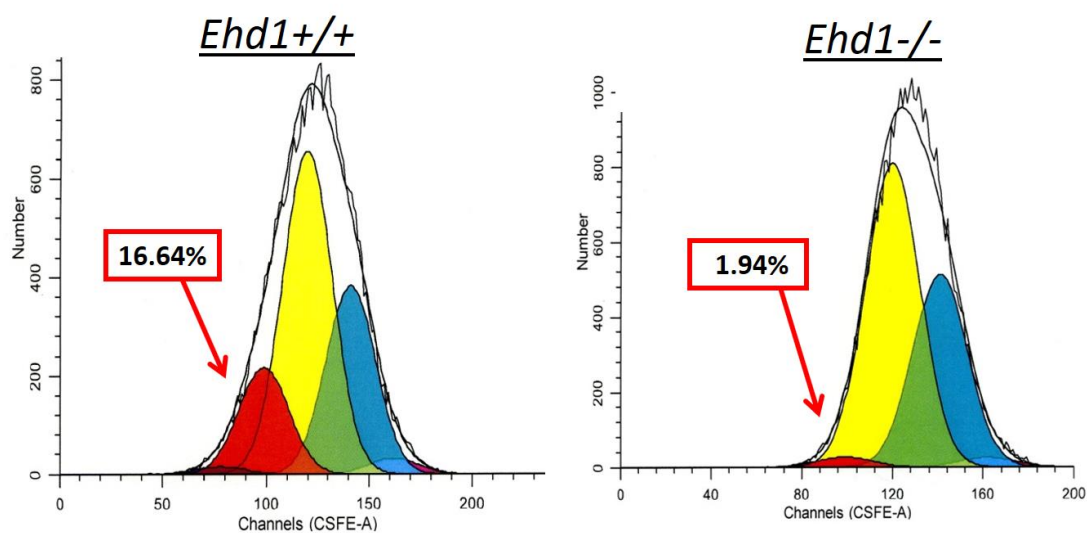


Figure 3.5. CFSE population differences in Ehd1-WT and Ehd1-null BMDMs.

BMDM proliferation as measured by CFSE dye dilution assay. Ehd1-WT and Ehd1-null BMDMs were stained with CFSE dye (day 0) and subsequently stimulated with 30 ng/mL recombinant CSF-1 for 3 days. Then population modeling of cell population divisions was carried out using software available through the Flow Cytometry Core Facility. The percentages in the red boxes indicate the percentage of the population in the highest generation. Representative data from 3 separate biological replicates are shown.

Figure 3.6. Ehd1-null BMDMs have reduced CSF1-induced cellular spreading.

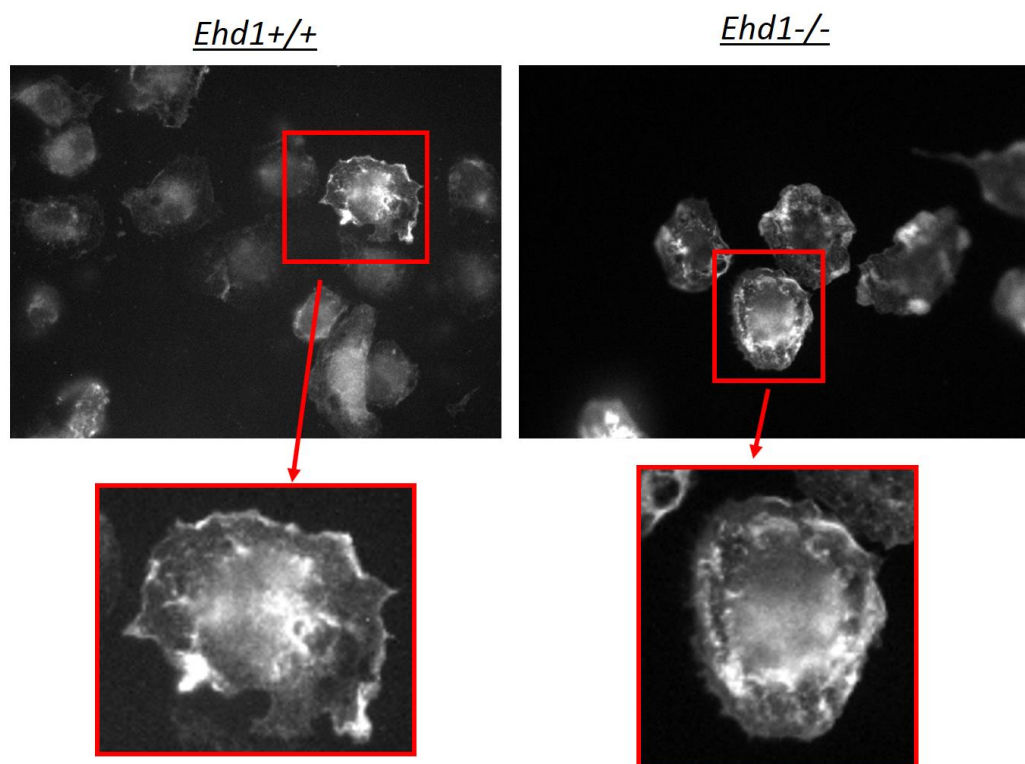
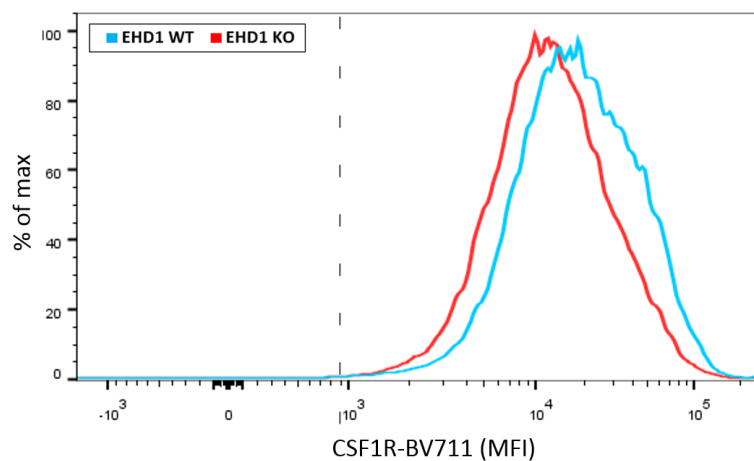


Figure 3.6. Ehd1-null BMDMs have reduced CSF1-induced cellular spreading. Cells were starved of CSF-1 overnight and then stimulated with 100 ng/mL CSF-1 for 10 minutes. Fixation and staining was performed with phalloidin (actin stain). Representative data from 3 separate biological replicates are shown.

Figure 3.7. CSF-1 stimulation induces CSF-1R signaling. Reduced CSF1-induced pERK levels in Ehd1null BMDMs. Ehd1-WT and Ehd1-null BMDMs were CSF1-deprived for 16 hours and subsequently stimulated for 10 minutes with 100 ng/mL CSF-1 for 3, 10, 30, 90, and 270 minutes. 40 µg aliquots of sample protein lysate were immunoblotted with the indicated antibodies. Representative data from 3 separate biological replicates are shown.

Figure 3.8. Ehd1-null BMDMs have decreased surface CSF-1R expression upon CSF-1 deprivation.

A



B

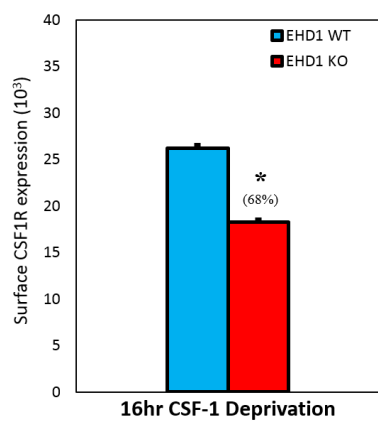


Figure 3.8. Ehd1-null BMDMs have decreased surface CSF-1R expression upon CSF-1 deprivation.

(A) Flow cytometry analysis for CSF-1R surface expression. Ehd1-WT and Ehd1-null BMDMs were deprived of CSF-1 for 16 hours and subsequently stained with anti-CSF-1R antibody and analyzed by flow cytometry. Grey histograms are IgG control. (B) Quantification of CSF-1R surface expression from Figure 3.8A. Data are presented as the fold change of MFIs, with control BMDMs deprived of CSF-1 for 16 hours set to 1 (mean \pm SE; $n = 3$; $*p < 0.05$). Representative data from 3 separate biological replicates are shown (mean \pm SEM; $* = p < 0.05$).

Figure 3.9. F4/80⁺ Control and EHD1-KO BMDMs.

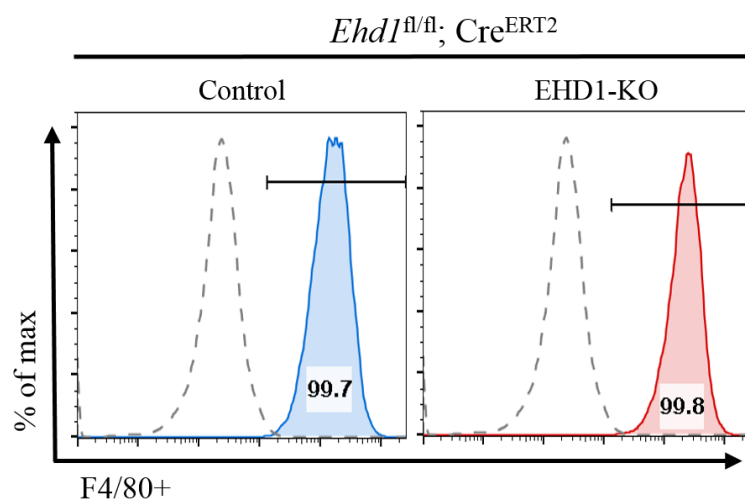
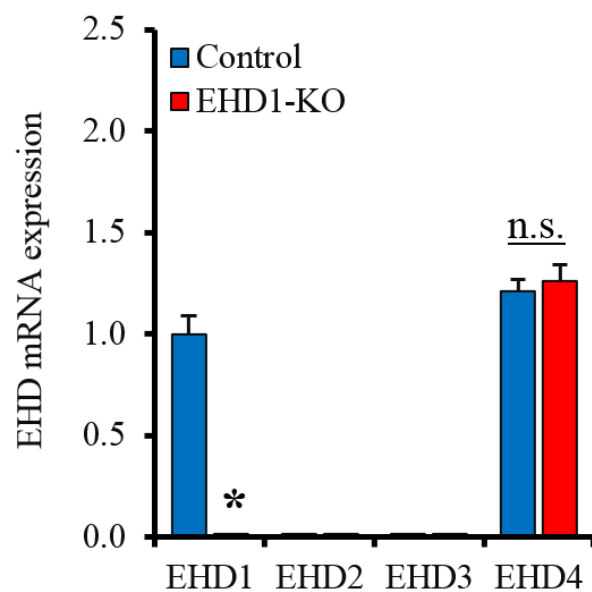


Figure 3.9. F4/80⁺ Control and EHD1-KO BMDMs. BMDMs were stained on day 10 of bone marrow culture from *Ehd1^{fl/fl} Cre^{ERT2}* mice for mature macrophage marker F4/80 and analyzed by flow cytometry.

Figure 3.10. EHD family expression in control and inducible EHD1-KO BMDMs.

A



B

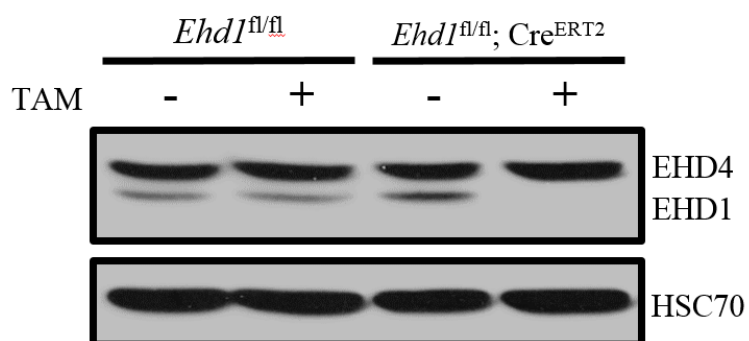
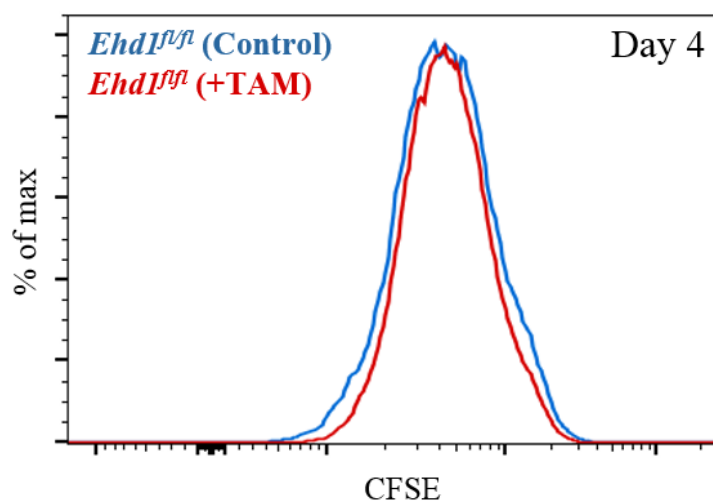


Figure 3.10. EHD family expression in control and inducible EHD1-KO BMDMs. Quantitative real-time-PCR analysis of EHD family proteins in BMDMs. Data was normalized to GAPDH and was expressed as a fold change with EHD1 expression in *Ehd1^{fl/fl}Cre^{ERT2}* BMDMs –TAM set to 1 (n = 3). **(C)** Lysate from *Ehd1^{fl/fl}* and *Ehd1^{fl/fl}Cre^{ERT2}* BMDMs cultured for 4 days -/+TAM. Note specific deletion of EHD1 protein in BMDMs matured from *Ehd1^{fl/fl}Cre^{ERT2}* mice, but not from *Ehd1^{fl/fl}* mice. Representative data from 3 separate biological replicates are shown (mean \pm SEM; * = $p < 0.05$, n.s. = not significant).

Figure 3.11. Lack of CSF-1 response alteration due to TAM treatment.

A



B

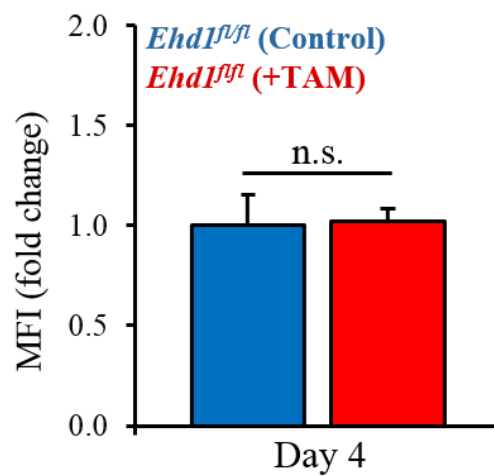


Figure 3.11. Lack of CSF-1 response alteration due to TAM treatment. (A)

BMDMs from *Ehd1^{fl/fl}* mice +/-TAM were labeled with CFSE and allowed to proliferate for 4 days in the presence of 30 ng/mL CSF-1 (B) Quantification of CFSE dye dilution assay from Figure 3.11A; CFSE MFI normalized to *Ehd1^{fl/fl}* BMDMs +TAM. Representative data from 3 separate biological replicates are shown (mean \pm SEM; n.s. = not significant).

Figure 3.12. Lack of apoptosis toxicity of TAM in BMDMs.

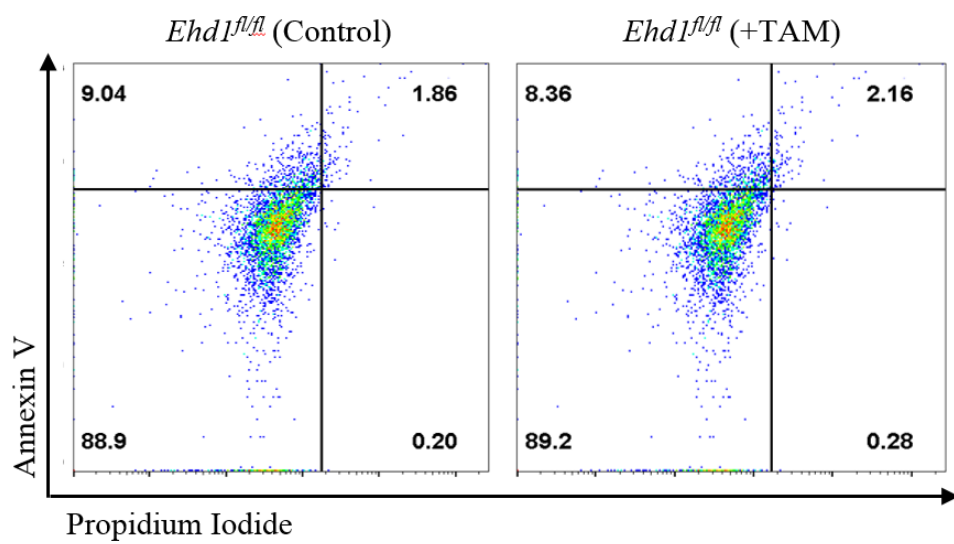


Figure 3.12. Lack of apoptosis toxicity of TAM in BMDMs. *Ehd1^{fl/fl}* BMDMs cultured with or without TAM were stained with anti-Annexin V and propidium iodide followed by flow cytometry analysis to assess the proportion of apoptotic cells. Representative data from 3 separate biological replicates are shown.

Figure 3.13. EHD1 deletion results in reduced proliferation.

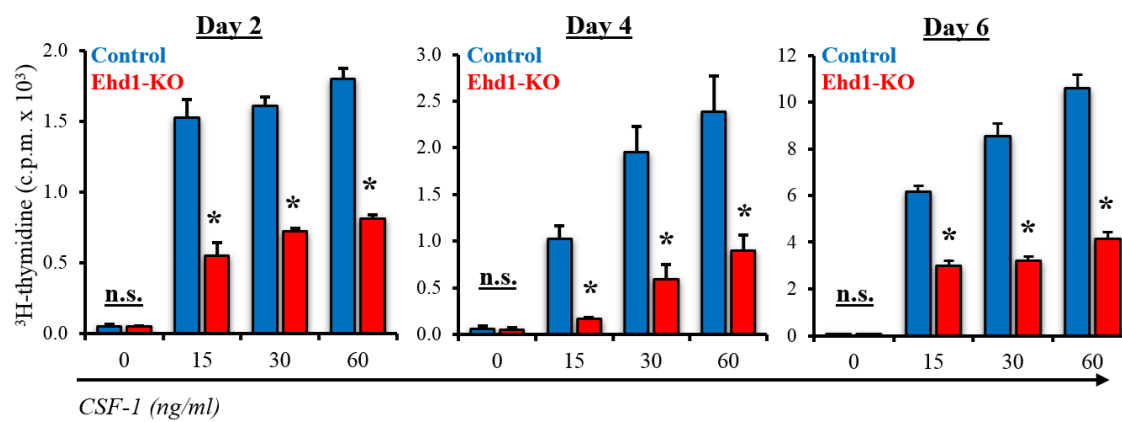


Figure 3.13. EHD1 deletion results in reduced proliferation. (A) BMDM proliferation via ^3H -thymidine incorporation. *Ehd1^{fl/fl}; Cre^{ERT2}* BMDMs cultured without (Control) or with (EHD1-KO) TAM were stimulated with CSF-1 at 0, 15, 30 or 60 ng/mL for 2, 4 or 6 days. Representative data from 3 separate biological replicates are shown (mean \pm SD; * $p < 0.05$, n.s. = not significant).

Figure 3.14. EHD1-KO BMDMs have reduced CSF1-induced proliferation.

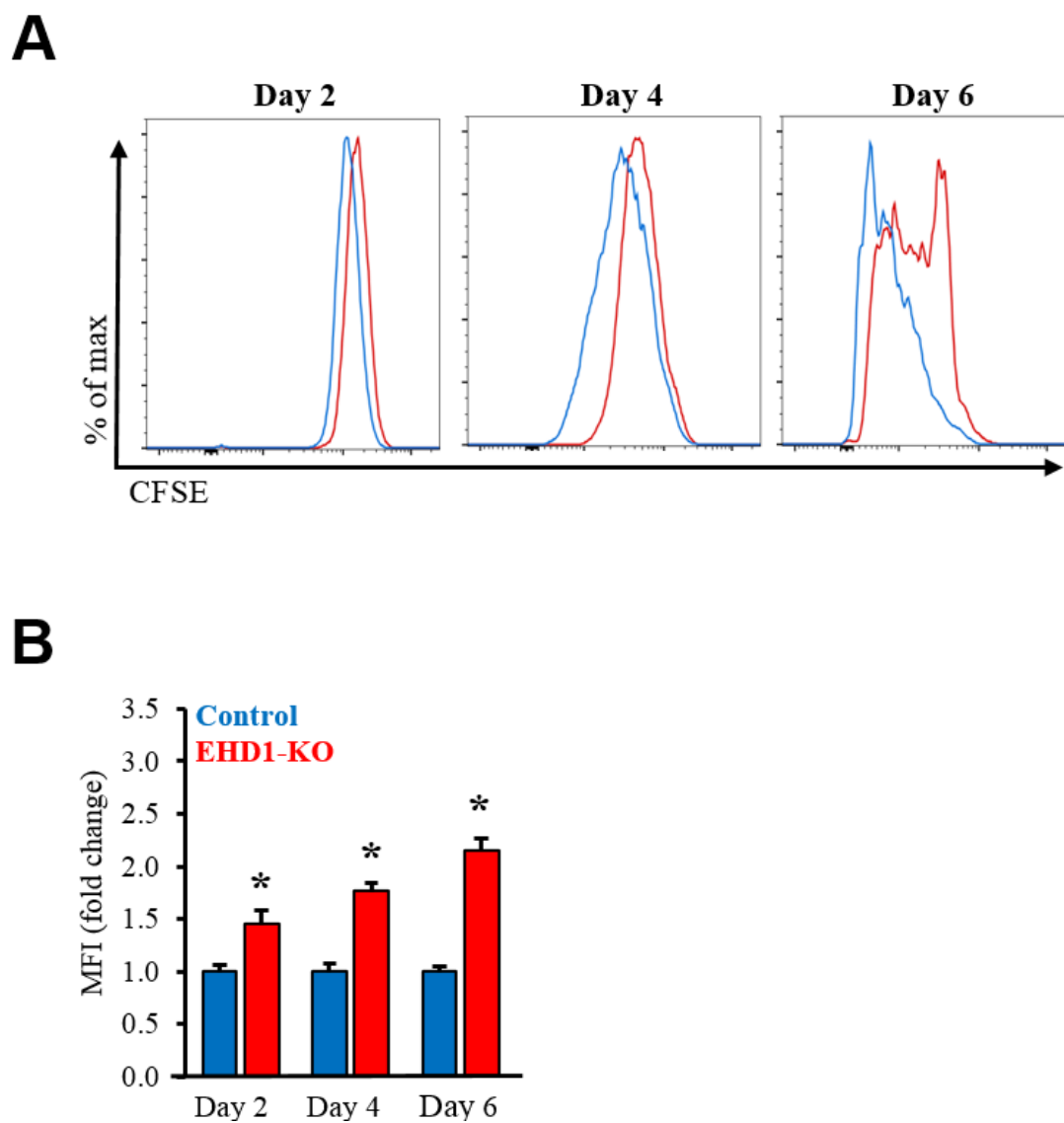


Figure 3.14. EHD1-KO BMDMs have reduced CSF1-induced proliferation.

(A) BMDMs proliferation with CFSE (dye dilution assay). *Ehd1^{fl/fl}; Cre^{ERT2}* BMDMs were previously cultured without (Control) or with (EHD1-KO) TAM were stained with CFSE dye (day 0) and then stimulated with 30 ng/mL recombinant CSF-1 for 2, 4, or 6 days. (B) Quantification of Mean Fluorescence Intensity (MFI) CFSE from Figure 3.15B. MFI fold change was normalized relative to control BMDM population. Representative data from 3 separate biological replicates are shown (mean \pm SEM; * = $p < 0.05$).

Figure 3.15. CFSE population model in BMDMs.

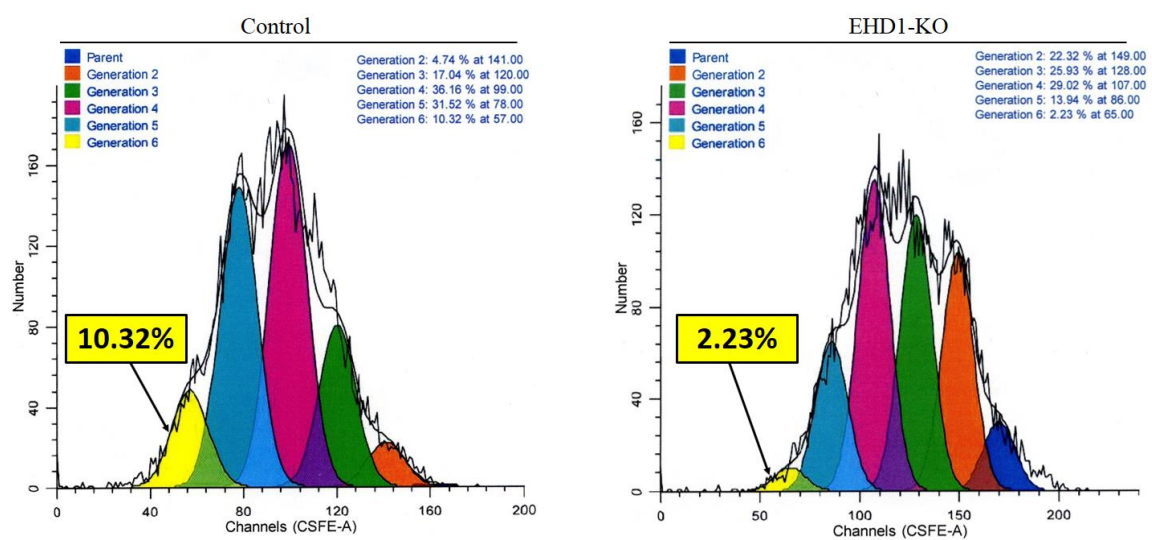


Figure 3.15. CFSE population model in BMDMs. BMDMs proliferation was monitored with the CFSE dye dilution assay. *Ehd1^{fl/fl}; Cre^{ERT2}* Control or EHD1-KO BMDMs were stained with CFSE dye (day 0) and then stimulated with 30 ng/mL recombinant CSF-1 for 5 days. Software available at the UNMC Flow Cytometry facility was used to model the populations according to the number of divisions each BMDM populations had undergone. Representative data from 3 separate biological replicates are shown.

Figure 3.16. EHD1 deletion results in reduced spreading.

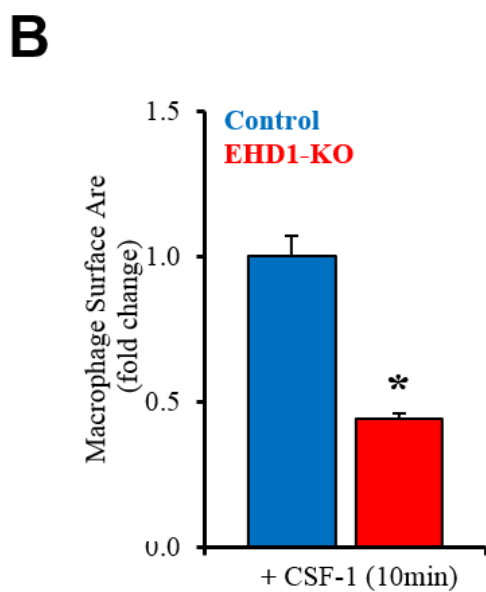
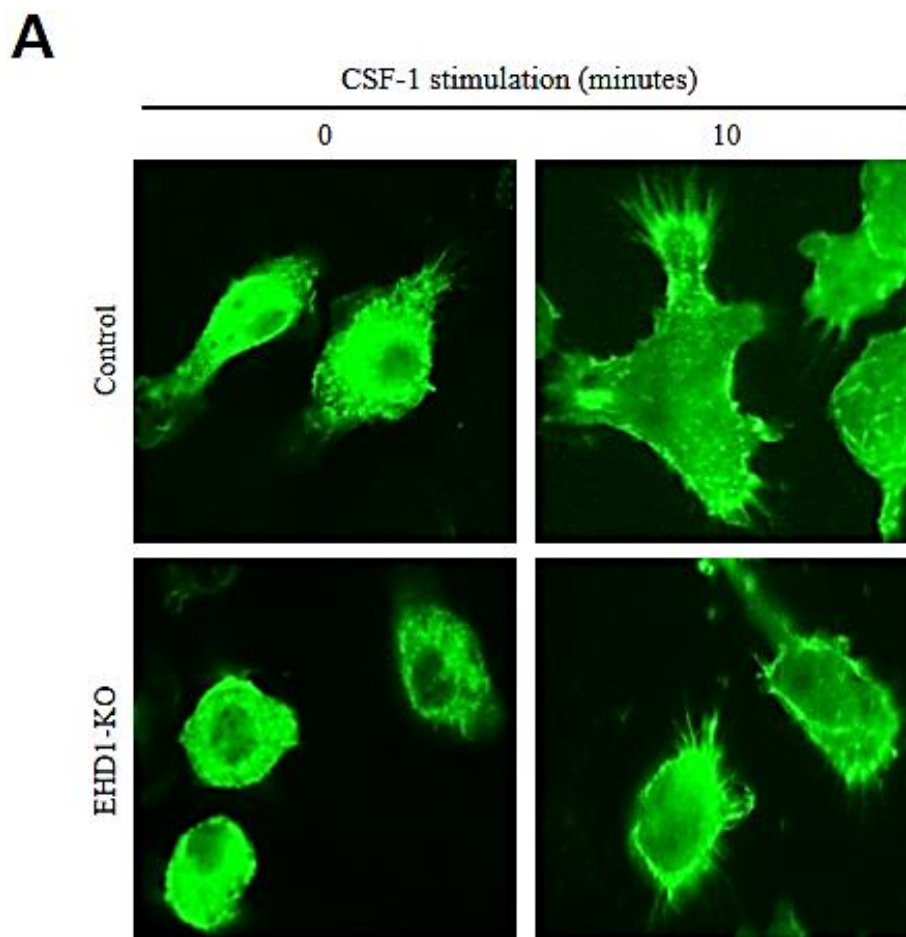
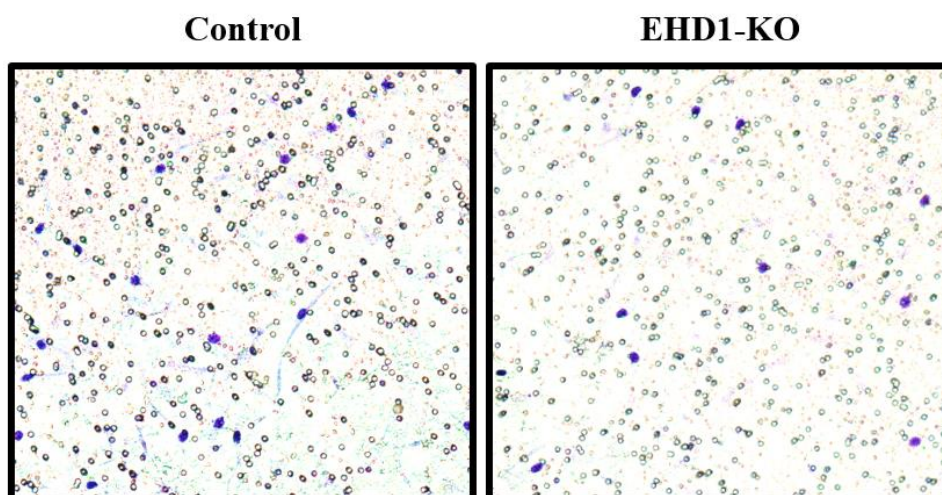


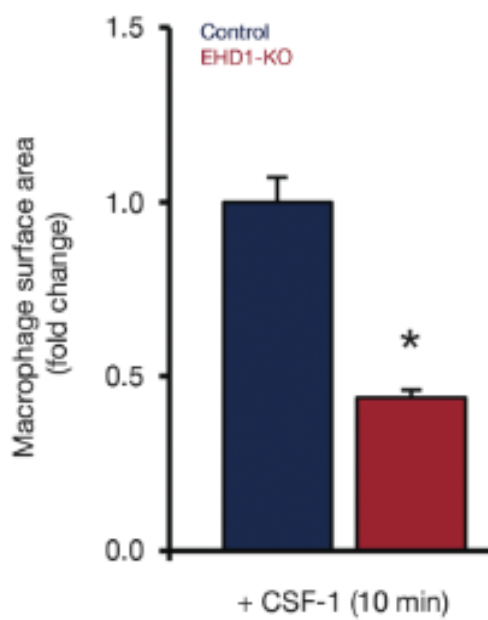
Figure 3.16. EHD1 deletion results in reduced spreading. (A) Microscopy analysis of CSF1-induced macrophage cell spreading. *Ehd1^{fl/fl}; Cre^{ERT2}* BMDMs were cultured without (Control) or with (EHD1-KO) TAM, CSF-1 deprived for 16 hours, and subsequently stimulated with 100 ng/mL CSF-1 for 10 minutes. Cells were then fixed, permeabilized, and stained for polymerized actin using conjugated phalloidin—488 followed by confocal microscopy. (B) Quantification of cellular spreading (Figure 3.16A) via calculating cell surface area (corresponding to phalloidin staining) using ImageJ software. 100 cells were counted for 3 independent experiments. Cell surface area was normalized to control BMDM population. Representative data from 3 separate biological replicates are shown (mean \pm SEM; * $p < 0.05$).

Figure 3.17. EHD1-KO BMDMs have reduced migration.

A

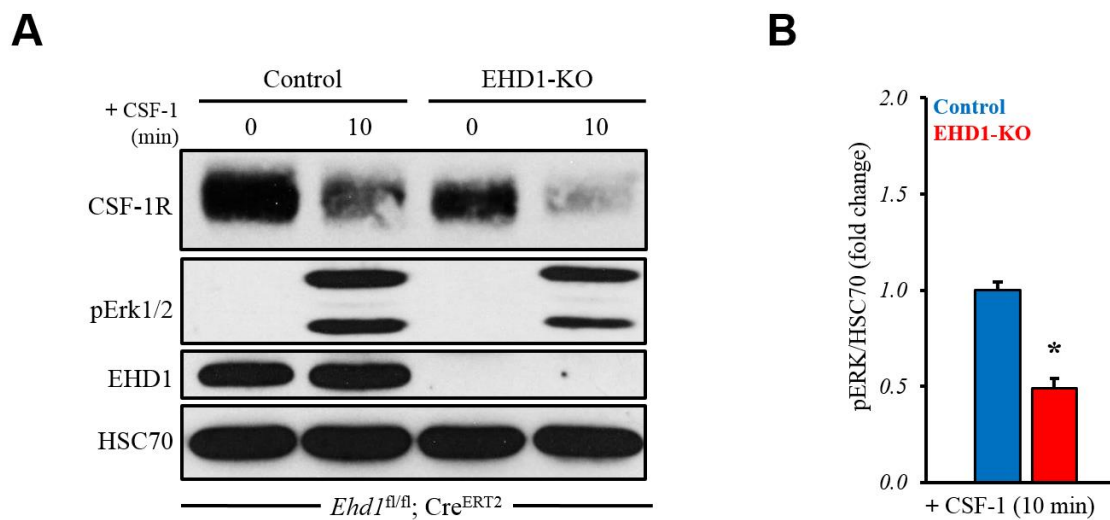


B



3.17. EHD1-KO BMDMs have reduced migration. (A) Transwell migration assay. *Ehd1^{fl/fl}; Cre^{ERT2}* BMDMs cultured without (Control) or with (EHD1-KO) TAM were deprived of CSF-1 for 4 hours and allowed to migrate towards CSF-1 (30 ng/mL) in the lower chamber of Boyden Transwell chambers. Filters were HEMA stained and photographed at 20x. (B) Quantification of migration assays from Figure 3.17A. Total cells migrated were normalized to control BMDM population. Representative data from 3 separate biological replicates are shown (mean \pm SEM; * p <0.05).

Figure 3.18. EHD1-KO BMDMs have decreased pERK downstream CSF-1R signaling.



3.18. EHD1-KO BMDMs have decreased pERK downstream CSF-1R

signaling. (a) Reduced CSF1-induced pERK levels in EHD1-KO BMDMs.

Ehd1^{fl/fl}; Cre^{ERT2} BMDMs were deprived of CSF-1 for 16 hours and then stimulated with 100ng/mL CSF-1 for 10 minutes. 40 µg aliquots of sample protein lysate were immunoblotted with the indicated antibodies. **(b)** The quantification of Figure 3.18A is shown. The relative levels of pERK signals were normalized to HSC70 and expressed as a fold change by setting the control BMDM population stimulated with CSF-1 for 10 minutes at 1. Representative data from 3 separate biological replicates are shown (mean ± SEM; * $p < 0.05$).

Figure 3.19. EHD1 deletion has no significant effect on activated CSF-1R internalization.

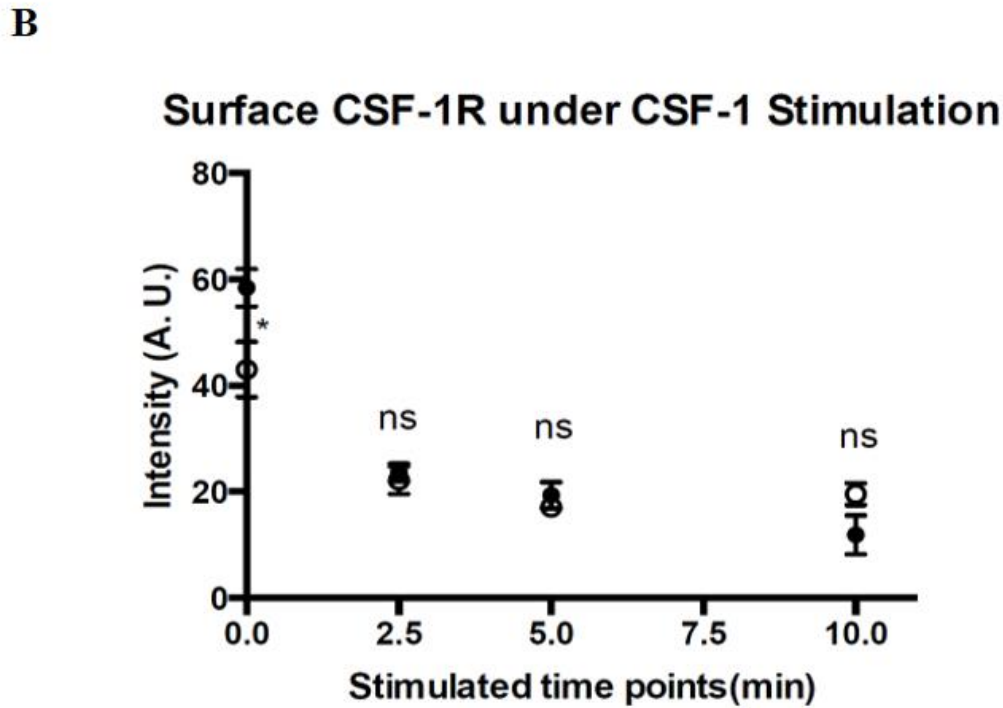
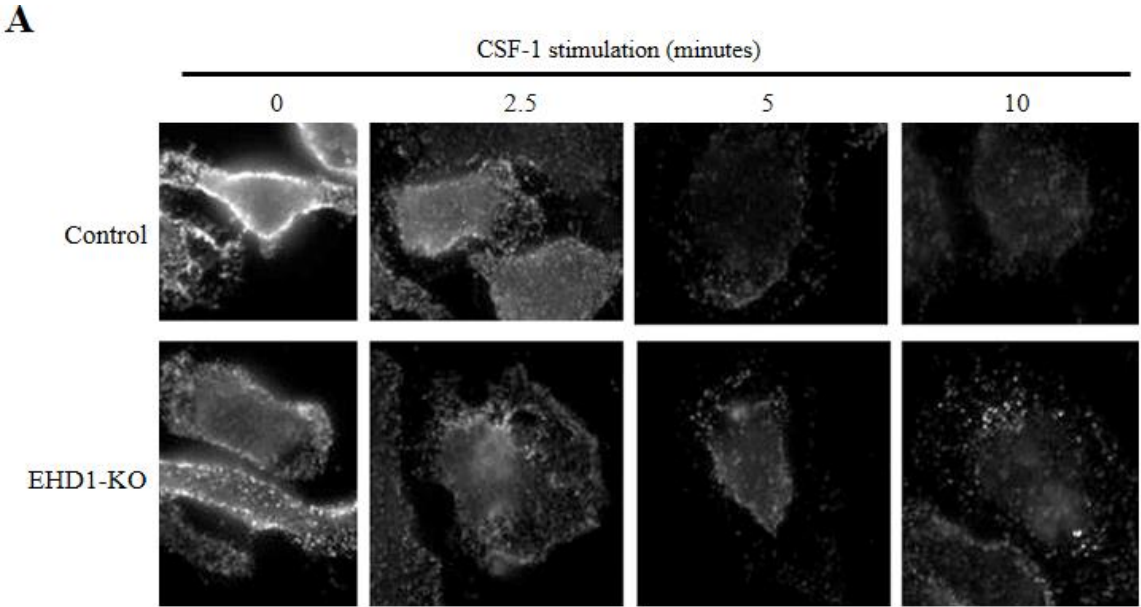
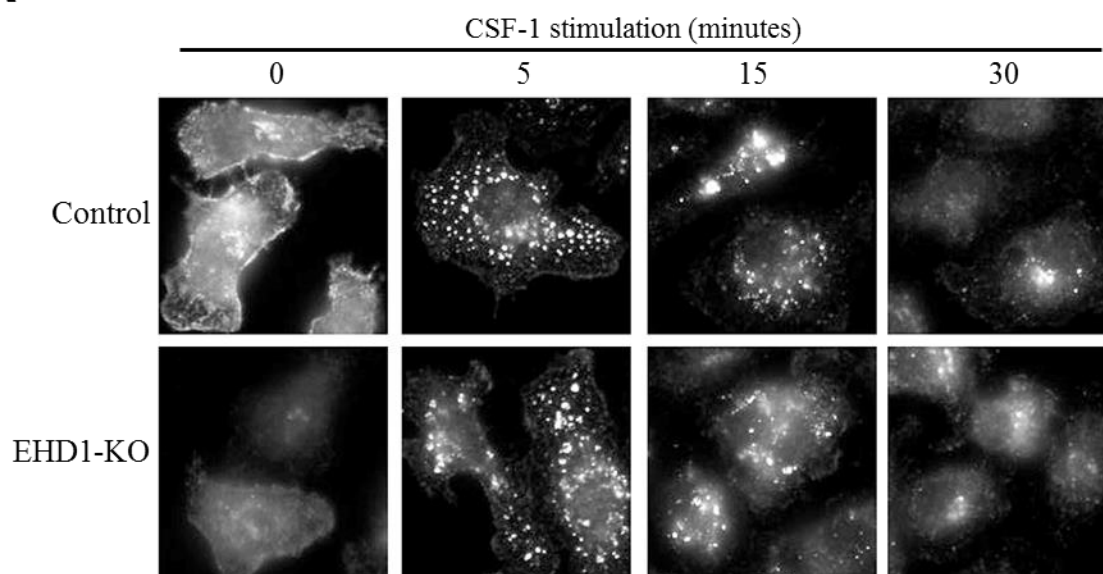


Figure 3.19. EHD1 deletion has no significant effect on activated CSF-1R internalization. (A) No impact of EHD1 deletion on ligand-induced downregulation of surface CSF-1R. *Ehd1^{fl/fl}; Cre^{ERT2}* BMDMs cultured without (Control) or with (EHD1-KO) TAM were deprived of CSF-1 for 16 hours and stimulated with 100 ng/mL CSF-1 for 0, 2.5, 5 or 10 minutes were fixed and stained for surface CSF-1R followed by immunofluorescence microscopy analysis. (B) Quantification of the data in Figure 3.19A is displayed. Representative data from 3 separate biological replicates are shown (mean \pm SD; * p <0.05, n.s. = not significant).

Figure 3.20. EHD1 deletion has no significant effect on activated CSF-1R degradation.

A



B

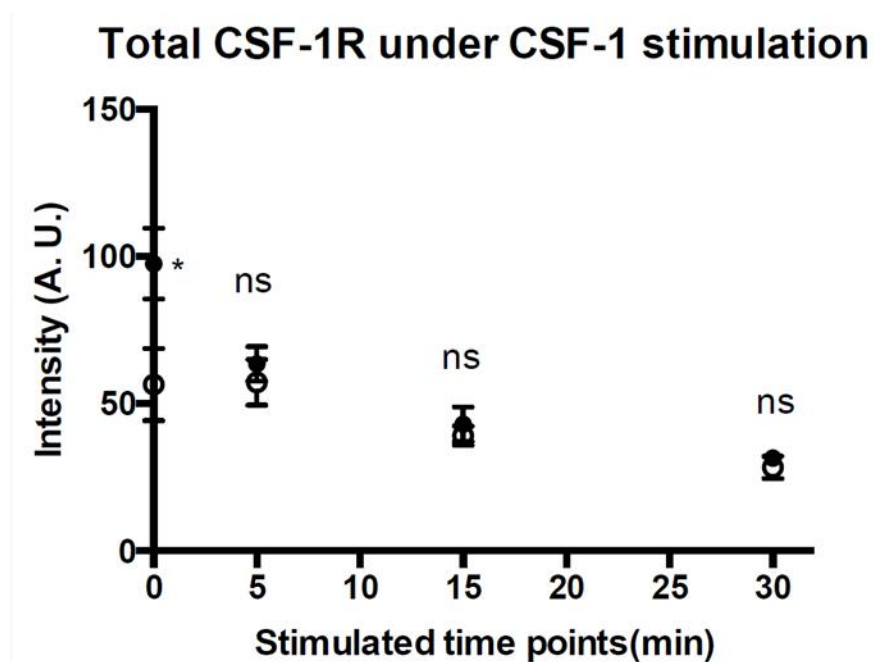
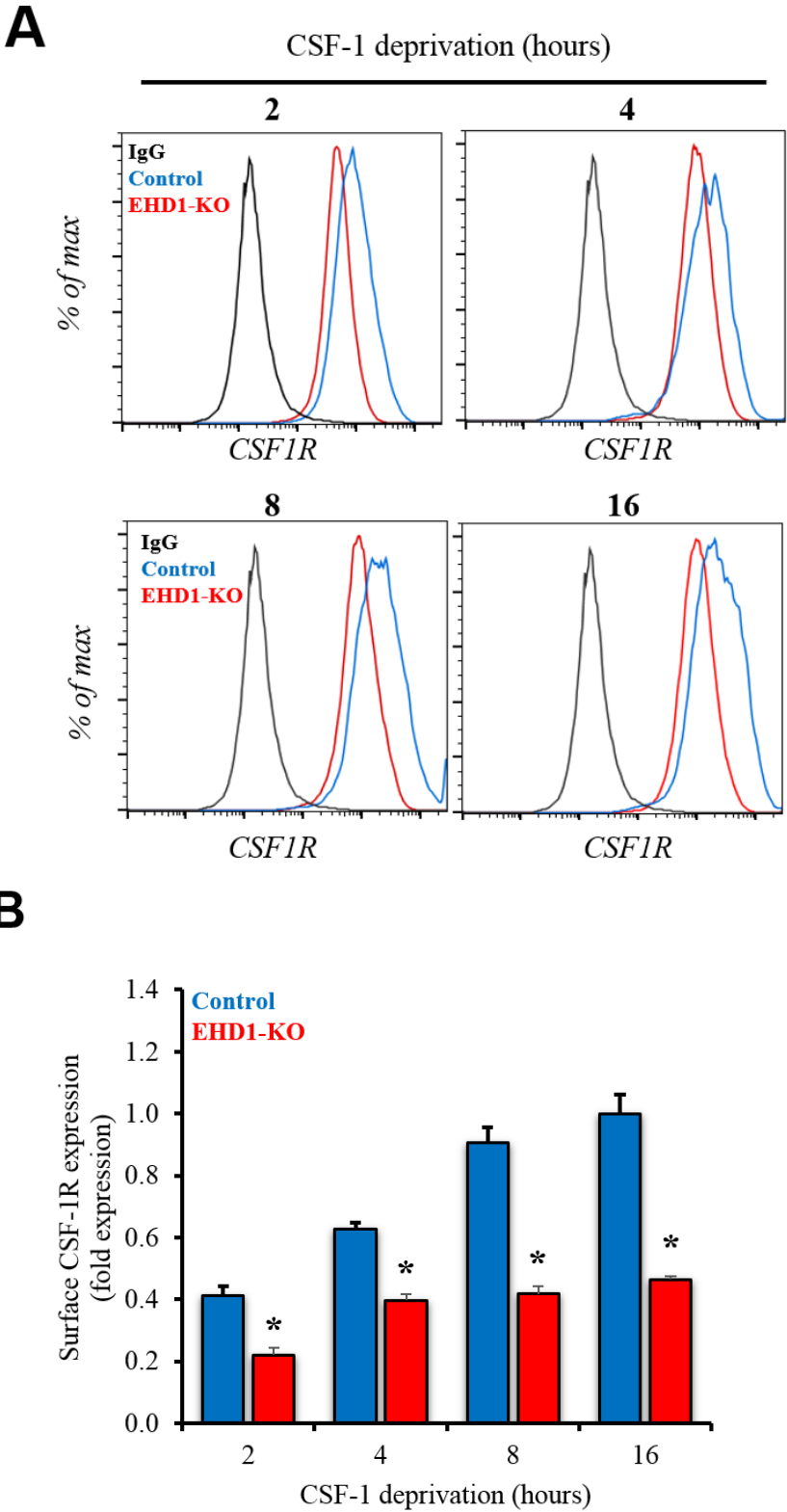


Figure 3.20. EHD1 deletion has no significant effect on activated CSF-1R degradation. BMDMs were prepared as in 3.28A and stimulated with CSF-1 for 0, 2.5, 5, 10 or 30 minutes. Cells were fixed, permeabilized, and stained for total CSF-1R and imaged using immunofluorescence microscopy. (B) Quantification of the data in Figure 3.20A is displayed. Representative data from 3 separate biological replicates are shown (mean \pm SEM; * p <0.05, n.s. = not significant).

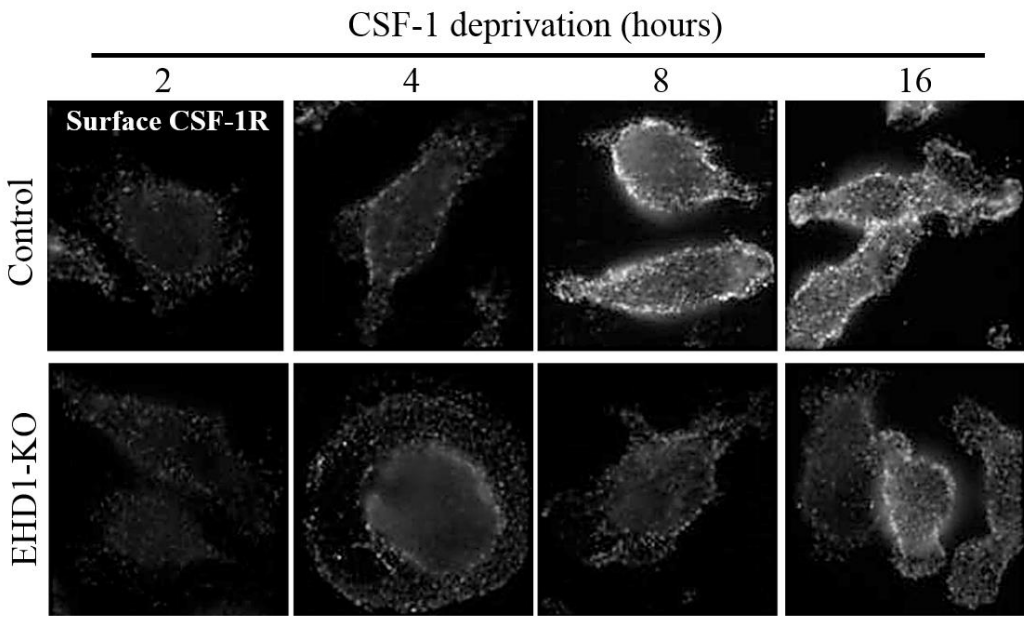
Figure 3.21. EHD1-KO BMDMs have reduced surface CSF-1R expression.



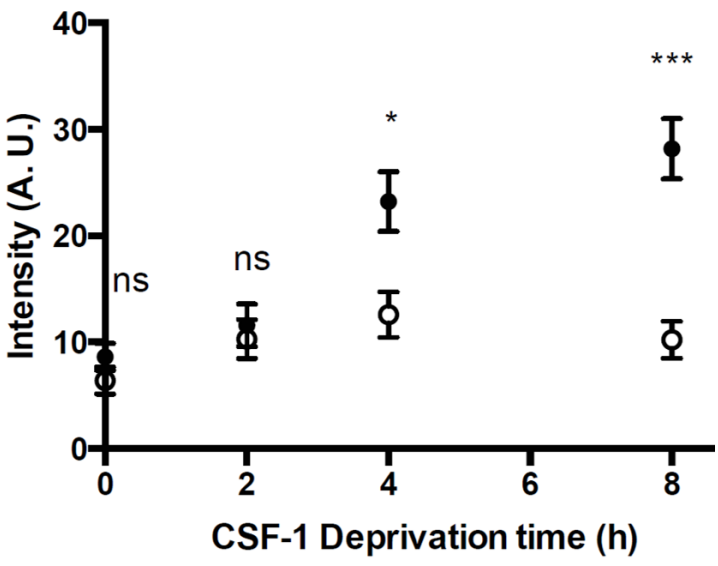
3.21 EHD1-KO BMDMs have reduced surface CSF-1R expression. (A) Live-cell flow cytometry analysis. Ehd1^{fl/fl}; CreERT2 BMDMs were cultured without (Control) or with (EHD1-KO) TAM were switched from CSF1-containing to CSF1-free medium for 2, 4, 8, or 16 hours and live cells were stained with anti-CSF-1R antibody followed by flow cytometry analysis. Grey histograms are IgG control. (B) Quantification of CSF-1R surface expression from Figure 3.21A is shown. Data are presented as the fold change of MFIs, with control BMDMs deprived of CSF-1 for 16 hours set to 1. Representative data from 3 separate biological replicates are shown (mean \pm SD; * $p < 0.05$).

Figure 3.22. EHD1 deletion in BMDMs results in reduced surface CSF-1R expression.

A



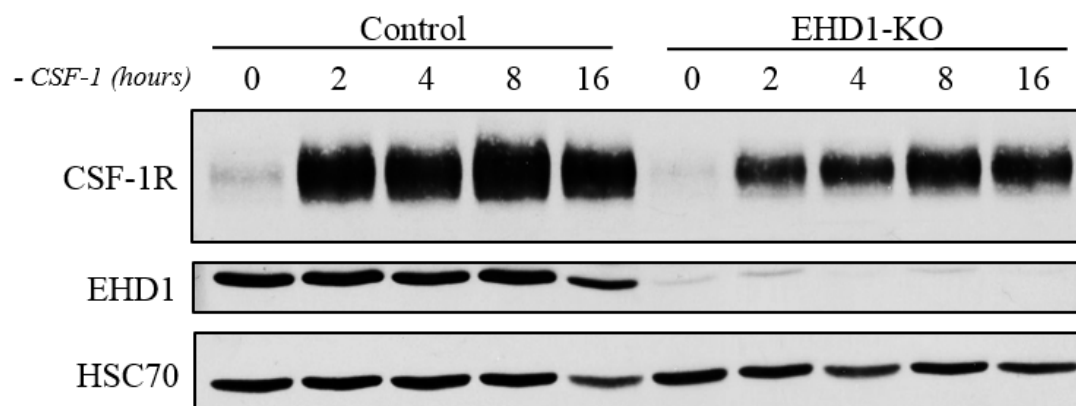
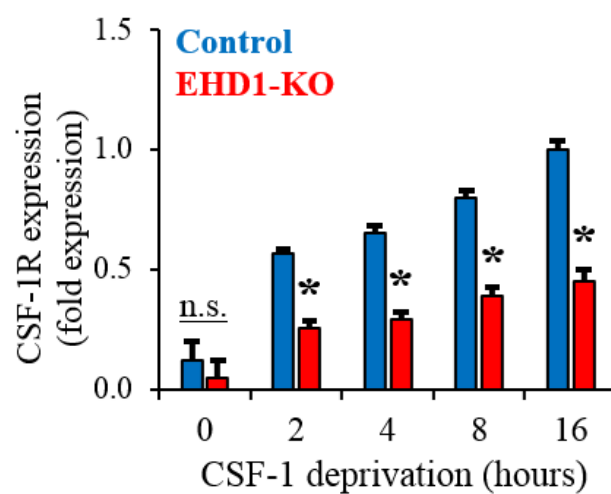
B



3.22 EHD1 deletion in BMDMs results in reduced surface CSF-1R

expression. (A) Immunofluorescence analysis of surface CSF-1R. Ehd1^{fl/fl}; CreERT2 BMDMs were cultured as in Figure 3.21 but on coverslips, fixed with 2% PFA for 5 minutes and stained with anti-CSF-1R antibody followed by imaging to visualize surface CSF-1R accumulation over time. (B) Quantification of data from Figure 3.22A. Representative data from 3 separate biological replicates are shown (mean \pm SEM; * p <0.05, *** p <0.001, n.s. = not significant).

Figure 3.23. EHD1 deletion in BMDMs leads to a reduction in total CSF-1R, demonstrated by immunoblotting.

A**B**

3.23 EHD1 deletion in BMDMs leads to a decrease in total CSF-1,

demonstrated using immunoblotting. (A) *Ehd1^{fl/fl}; Cre^{ERT2}* BMDMs cultured without (Control) or with (EHD1-KO) TAM were switched from CSF1-containing to CSF1-free medium for 2, 4, 8 or 16 hours, and 40 µg aliquots of lysate protein were analyzed by immunoblotting with anti-CSF-1R (upper), anti-EHD1 (to show EHD1 deletion) and anti-HSC70 (loading control). (B) Quantification of CSF-1R signals from data in Figure 3.23A. The CSF-1R band pixels were quantified from scanned blots using ImageJ software, normalized based on HSC70 and expressed as a fold change by setting total CSF-1R from control BMDMs deprived of CSF-1 for 16 hours to 1. Representative data from 3 separate biological replicates are shown (mean ± SEM; * $p < 0.05$, n.s. = not significant).

Figure 3.24. EHD1-KO BMDMs have reduced total CSF-1R using IF.

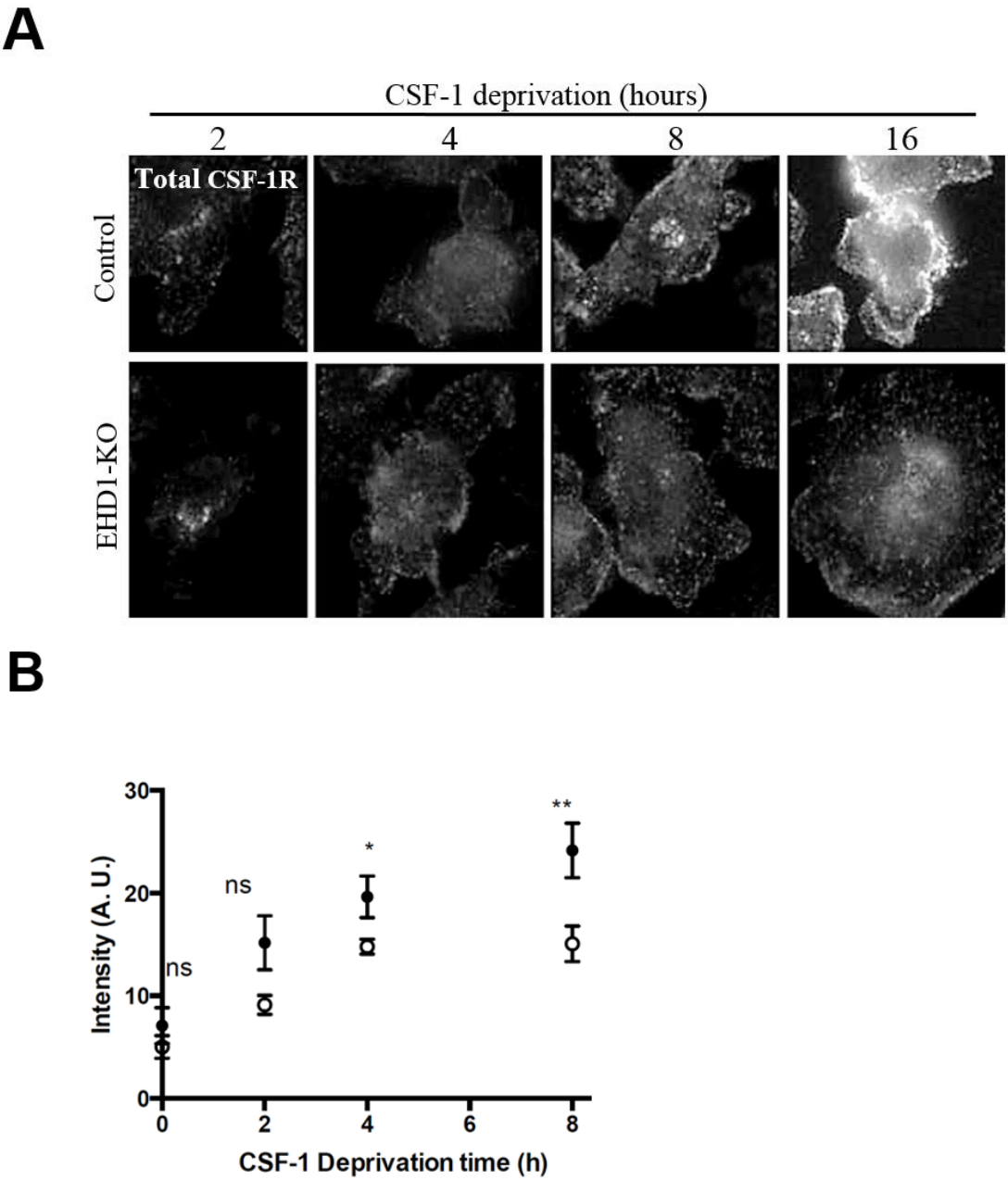


Figure 3.24. EHD1-KO BMDMs have reduced total CSF-1R using IF. (A)

Analysis of total CSF-1R using immunofluorescence microscopy. BMDMs cultured as in A but on coverslips were fixed, permeabilized, and stained for with anti-CSF-1R antibody to visualize total CSF-1R. (B) Quantification of data from Figure 3.24A. Representative data from 3 separate biological replicates are shown (mean \pm SD; * p <0.05, ** p <0.01, n.s. = not significant).

Figure 3.25. EHD1 deletion does not affect CSF-1R synthesis.

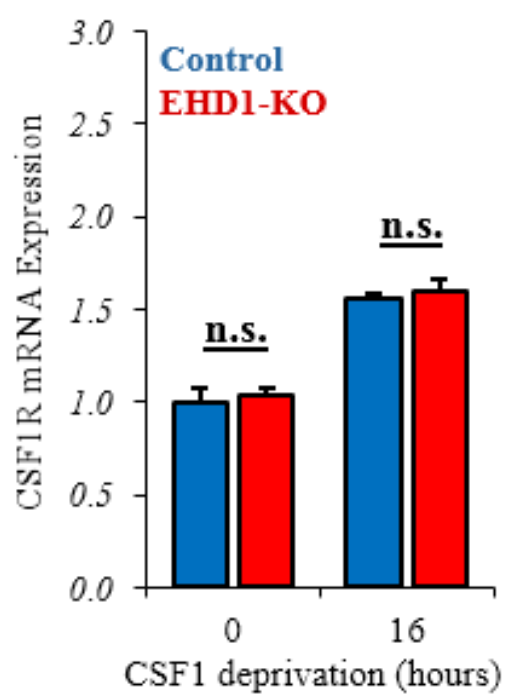


Figure 3.25. EHD1 deletion does not affect CSF-1R synthesis. EHD1 deletion does not affect CSF-1R mRNA expression. RNA was isolated from *Ehd1^{fl/fl}; Cre^{ERT2}* BMDMs cultured without (Control) or with (EHD1-KO) TAM were grown under steady state conditions (with CSF-1) and without CSF-1 for 16 hours, harvested, and quantitative qRT-PCR was performed. Data were normalized to GAPDH and expressed as a fold change relative to CSF-1R mRNA expression of control BMDMs at steady state. Representative data from 3 separate biological replicates are shown (mean \pm SEM; n.s. = not significant).

.

Figure 3.26. EHD1-KO deletion reduces transport of newly synthesized CSF-1R to the cell surface.

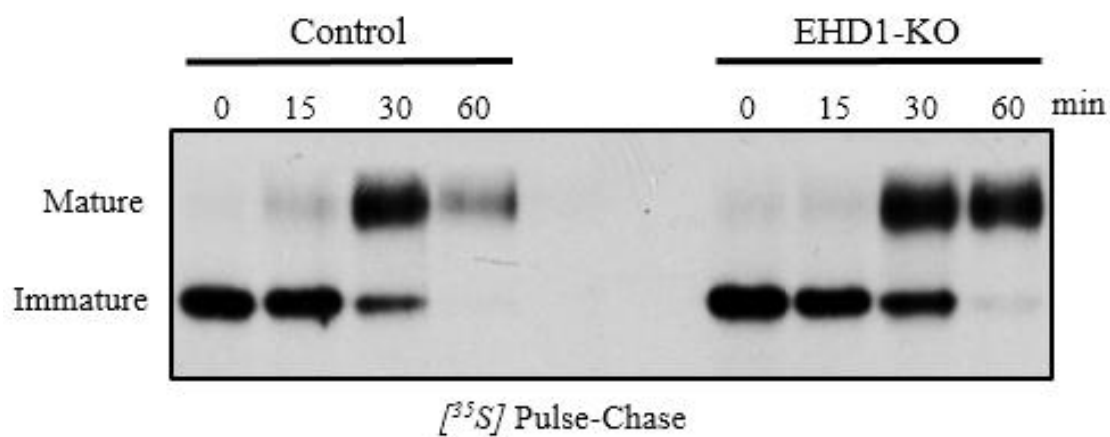


Figure 3.26. EHD1-KO reduces transport of newly synthesized CSF-1R to the cell surface. Metabolic pulse-labelling to show unaltered translation and maturation with a block of surface transport of newly synthesized CSF-1R in EHD1-KO BMDMs. *Ehd1^{fl/fl}; Cre^{ERT2}* BMDMs cultured without (Control) or with (EHD1-KO) TAM were metabolically pulse-labeled with [³⁵S] for 15 min and subjected to chase in unlabeled methionine/cysteine-enriched medium in the presence of CSF-1 for the indicated times followed by cell lysis. 40 µg aliquots of sample lysates were subjected to anti-CSF-1R immunoprecipitation followed by autoradiography. Lower band: immature/non-glycosylated CSF-1R; upper band: mature/fully glycosylated CSF-1R. Note comparable lower band signals at time 0 and similar rates of conversion to the upper band; however, the mature upper band signals are lost in control BMDMs but remain intact in EHD1-KO BMDMs. Representative data from 3 separate biological replicates are shown.

Figure 3.27. CSF-1R co-localizes to a EHD1+/GM130+ compartment.

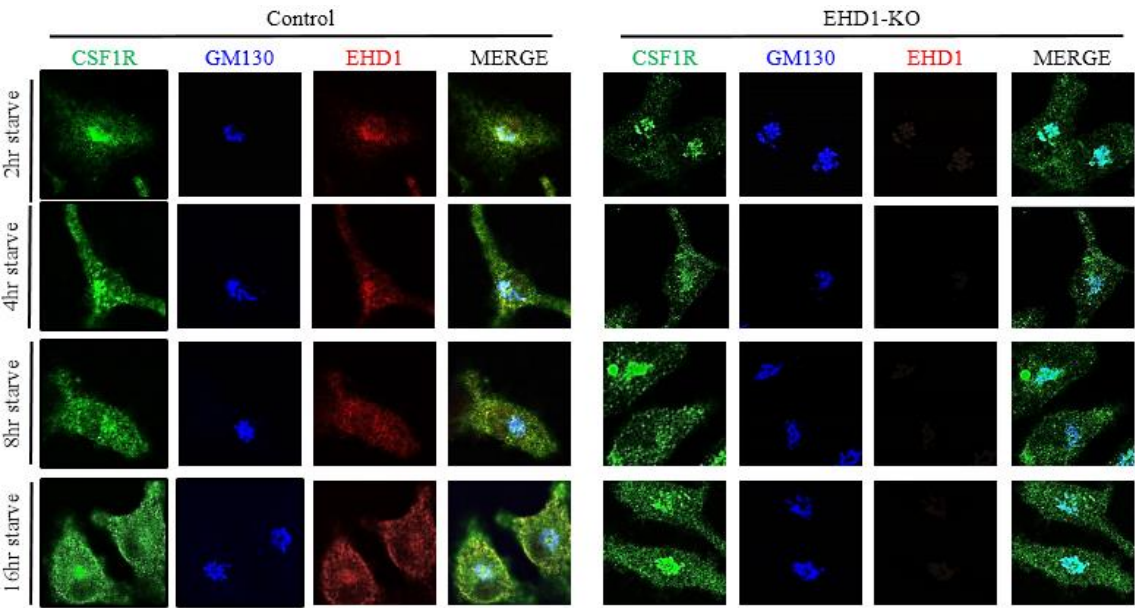


Figure 3.27 CSF-1R co-localizes to a EHD1⁺/GM130⁺ compartment.

Confocal immunofluorescence. Co-localization of EHD1 with CSF-1R at the Golgi apparatus. *Ehd1^{fl/fl}; Cre^{ERT2}* BMDMs cultured without (Control) or with (EHD1-KO) TAM were switched from CSF1-containing medium to CSF1-free medium for 2, 4, 8 or 16 hours and subsequently fixed, permeabilized and stained for CSF-1R (green), EHD1 (Red) and GM130-Golgi marker (Blue) and analyzed by confocal microscopy. Representative data from 3 separate biological replicates are shown.

Figure 3.28. EHD1-KO BMDMs have increased CSF-1R lysosomal degradation.

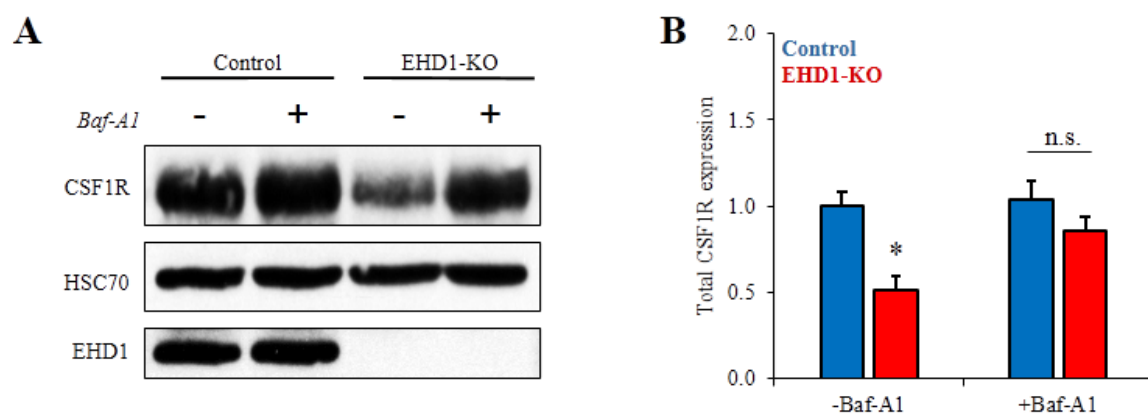


Figure 3.28. EHD1-KO BMDMs have increased CSF-1R lysosomal

degradation. (A) Western blot analysis to show recovery of total CSF-1R levels in EHD1-KO BMDMs upon inhibition of lysosomal degradation. *Ehd1^{fl/fl}; Cre^{ERT2}* BMDMs cultured without (Control) or with (EHD1-KO) TAM were switched from CSF1-containing medium to CSF1-free medium for 4 hours in the absence (-Baf-A1) or presence (+Baf-A1) of lysosomal inhibitor: Baf-A1, 100 nM. 40 µg aliquots of sample protein lysates were immunoblotted for total CSF-1R (Top), HSC70 (central; loading control) and EHD1 (bottom; to show EHD1 deletion). (B) Quantification of total CSF-1R signals from Figure 3.29A. Data were normalized to HSC70 signals and expressed as a fold change relative to values for the control BMDM population without Baf-A1 treatment. Representative data from 3 separate biological replicates are shown (mean ± SEM; * $p < 0.05$, n.s. = not significant).

Figure 3.29. EHD1-KO BMDMs shunt CSF-1R to the lysosome.

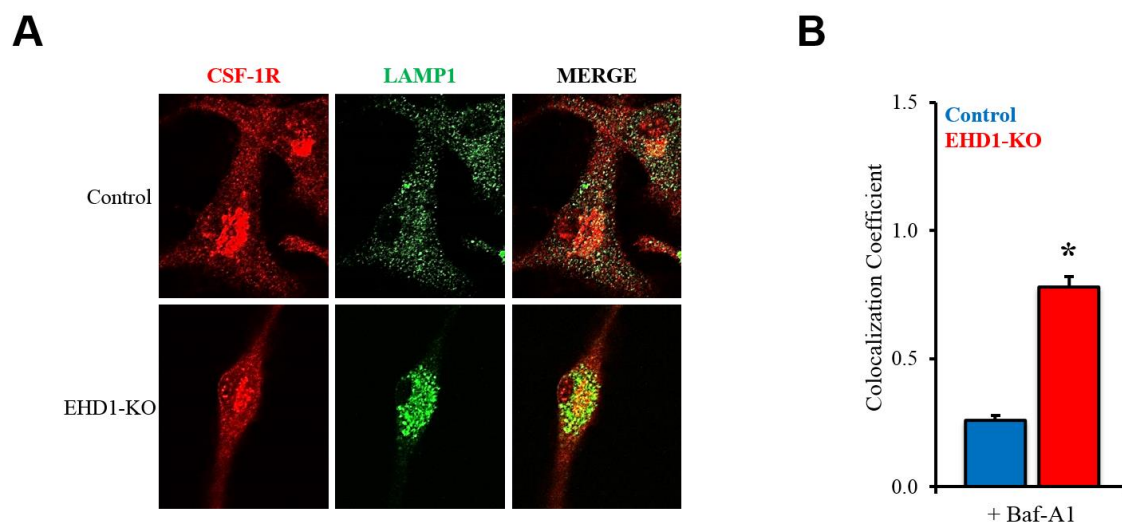


Figure 3.29. EHD1-KO BMDMs shunt CSF-1R to the lysosome. (A)

Representative confocal immunofluorescence image showing co-localization of CSF-1R in LAMP1+ lysosomes of EHD1-KO BMDMs upon lysosome inhibition via Baf-A1. *Ehd1^{fl/fl}; Cre^{ERT2}* BMDMs cultured without (Control) or with (EHD1-KO) TAM were switched from CSF1-containing to CSF1-free medium for 4 hours in the presence of 100 nM Baf-A1. Cells were fixed, permeabilized, and stained for analysis utilizing immunofluorescence: CSF-1R (red) and LAMP1 (green); merged pictures on right show co-localization (yellow). (B) Quantification of CSF-1R and LAMP1 co-localization from Figure 3.29A. Co-localization of CSF-1R and LAMP1 fluorescence signals was assessed in 50 cells each in 3 independent experiments to determine the co-localization coefficient \pm SEM (n = 150). Representative data from 3 separate biological replicates are shown (mean \pm SEM; * $p < 0.05$).

CHAPTER 4: DISCUSSION & CONCLUSION

The material covered in the following chapter is the topic of the following published article:

Luke R. Cypher, Timothy Alan Bielecki, Oluwadamilola Adepegba, Lu Huang, An Wei, Fany Iseka, Haitao Luan, Eric Tom, Matthew D. Storck, Adam D. Hoppe, Vimla Band, Hamid Band. CSF-1 receptor signalling is governed by pre-requisite EHD1 mediated receptor display on the macrophage cell surface.

(Accepted for Publication: *Cellular Signalling*, Available online 17 May 2016)

Discussion

The CSF-1R is essential for the development and diverse functions of the monocyte-macrophage lineage, which includes specialized tissue-specific cells such as microglia in the central nervous system (CNS) (67). Abnormal CSF1R-dependent macrophage functions resulting from aberrant CSF-1R dependent signaling contribute to a variety of human diseases (7, 15, 68, 69). A pre-requisite for all CSF1R-mediated macrophage functions is the delivery and display of the receptor at the cell surface. This requirement of macrophage cell surface presentation of CSF-1R is due to the initial activation step of ligand (CSF-1) stabilization of the dimerized form of the receptor tyrosine kinase (17). Without this key initial step, CSF-1R signaling cannot occur and macrophage biology will be compromised. Mechanisms that govern the post-synthesis maturation and traffic of CSF-1R to the macrophage cell surface are therefore biologically pivotal. Furthermore, understanding these mechanisms will likely lead to the development of effective therapies and treatments of devastating human conditions aimed at targeting the inhibition of CSF-1R signaling.

In this dissertation, I have used primary bone marrow-derived macrophages (BMDMs) from constitutive and inducible knockout mouse models to provide evidence that EHD1, a member of the EHD protein family of endocytic recycling regulators, serves a novel and critical role in ensuring Golgi-to-cell surface traffic of CSF-1R. I show that this novel gate-keeper function of EHD1 helps direct the post-synthesis traffic itinerary of CSF-1R away from an alternate fate of delivery to lysosomes where it is degraded. My experiments demonstrate

that EHD1-dependent cell surface transport of CSF-1R ensures subsequent ligand-induced CSF-1R signaling and macrophage functional activation. EHD1, a member of the EHD family of endocytic recycling regulators, has only previously been shown to function in receptor recycling and retrograde traffic from the early endosome to the Golgi. I report in this dissertation a new critical function for EHD1 in the presentation of CSF-1R upon the macrophage cell surface. This novel gate-keeper function of EHD1 helps direct the post-synthesis traffic itinerary of CSF-1R away from an alternate fate of delivery to lysosomes where it is degraded. My data demonstrate that EHD1 functions in the cell surface transport of CSF-1R—ensuring subsequent ligand-induced cellular activation. Furthermore, a novel function for EHD1 as a positive regulator of basal post-synthetic CSF-1R traffic to the cell surface has been revealed. Previously known only to function in recycling of internalized receptors back to the cell surface (41–47) these findings define a new role for a member of the entire EHD protein family,.

To investigate the role of EHD1 in the context of CSF-1R signaling in macrophages, I chose the physiologically relevant model (due to CSF-1R dependence *in vitro*) of primary bone-marrow derived macrophages (BMDMs) from constitutive *Ehd1*-null mice as well as a novel inducible EHD1 deletion mouse model only available in our laboratory. We engineered constitutive and inducible EHD1-deletion mouse models. The inducible deletion has been engineered such that the incorporation of a tamoxifen-inducible *Cre*^{ERT2} allele allows inducible deletion of *Ehd1*^{fl/fl} under controlled conditions of TAM treatment.

Using the BMDMs from our laboratories' constitutive EHD1 deletion mouse model, the initial analysis showed that BMDMs only express EHD1 and EHD4 and not significant levels of EHD2 or EHD3. Furthermore, BMDMs derived from constitutive Ehd1-null as compared to EHD1-WT mice were found to have a significant impairment of CSF-1R surface expression, CSF-1 induced CSF-1R signaling, and subsequent downstream CSF1-mediated macrophage functional effects.

Due to the noticeable decrease in total levels of CSF-1R apparent on initial Western blots (Figure 3.7) after starvation of CSF-1 in EHD1-null BMDMs, I suspected the decreases in macrophage signaling and function might simply be due to less CSF-1R available to bind CSF-1 on the macrophage cell surface. All receptor tyrosine kinases (RTK) signaling begins with proper delivery and display of the receptor at the cell surface. If an RTK is not oriented properly at the cell surface, the receptor cannot bind ligand, be activated, signal, and produce downstream effects (20).

A potential effect on macrophage development in constitutive Ehd1-null mice due to defective cytokine signals and niche elements cannot be ruled out. Due to initial results using EHD1-null BMDMs from constitutively EHD1-deleted mice, I utilized EHD1-KO BMDMs to assure the effects observed were not due to abnormalities in bone marrow development. I conducted a series of experiments with inducible EHD1-KO compared to Control BMDMs to assess macrophage surface and total CSF-1R protein levels under conditions of CSF-1 removal from the culture media (CSF-1 deprivation). Analysis of surface and total levels of

CSF-1R protein under conditions of CSF-1 deprivation was performed using a combination of flow cytometry (Figures 3.8 and 3.21), Western blotting (Figure 3.23), metabolic pulse-chase (Figure 3.26), and immunofluorescence imaging of non-permeabilized (Figure 3.22) or permeabilized BMDMs (Figures 3.24 and 3.27). This combination of experiments demonstrated an overall reduction in CSF-1R levels when EHD1 was deleted and a clear impairment in the ability of newly synthesized CSF-1R to be transported to the cell surface.

There are two possible mechanisms behind the change in macrophage biology I had observed (decreased total CSF-1R). When a cell has less total protein, either less of the protein is being made by the cell or the cell is degrading the protein at a higher rate. I excluded the possibility that the EHD1-KO BMDMs were making less of CSF-1R by conducting qRT-PCR and metabolic pulse-chase labeling of newly synthesized CSF-1R with [³⁵S] (Figures 3.25 and 3.26).

Previous studies have also shown that reduced surface expression of CSF-1R can result from defective glycosylation. Reduced surface CSF-1R expression resulting from defects in glycosylation of the receptor is seen upon expression of the HIV protein NEF, which inhibits glycosylation through incompletely understood mechanisms involving NEF activation of the SRC-family tyrosine kinase HCK as well as through HCK-independent mechanisms (70, 71). Naturally occurring loss-of-function mutations of CSF-1R have been identified in patients with hereditary diffuse leukoencephalopathy with spheroids (HDLS), and most of these mutations result in reduced CSF-1R protein expression (12). In both of the cases above, CSF-1R glycosylation in the Golgi is defective. In

contrast, metabolic pulse-chase studies showed that immature CSF-1R was fully converted into a mature form (fully glycosylated; higher molecular weight) in EHD1-KO BMDMs with essentially the same kinetics as in control cells (Figure 3.26). CSF-1R mRNA expression is under the regulation of several transcription factors (19). However, transcriptional expression was unchanged. Similarly, a potential block in CSF-1R translational and subsequent maturation of the receptor (glycosylation) was excluded via metabolic pulse-chase analysis (Figure 3.26). Thus, decreased CSF-1R production was ruled out as a potential mechanism for decreased CSF-1R signaling and macrophage function when EHD1 is absent from the cell.

These findings clearly pointed to the possibility that post-synthetic transport of CSF-1R after its Golgi processing was defective in EHD1-KO BMDMs. Consistent with this idea, I observed that CSF-1R co-localizes with a cohort of CSF-1 in the Golgi compartment stained for GM130 (Golgi marker) (Figure 3.27). Our metabolic pulse-chase studies carried out in the presence of CSF-1 exposed the newly synthesized CSF-1R to its ligand, which promotes its rapid degradation (71). While this was clearly seen in control BMDMs, the mature band of CSF-1R remained intact for the duration of the experiment (Figure 3.26), supporting the conclusion that this cohort of CSF-1R did not reach the cell surface, consistent with our flow cytometry (Figure 3.8 and 3.21) and confocal imaging (Figure 3.22) analyses. When combined with the reduction in total CSF-1R levels in EHD1-KO BMDMs, these results led to the idea that lack of EHD1 allows CSF-1R traffic from the Golgi to a compartment where it is degraded.

Since other RTKs are degraded in lysosomes (20, 25) and a variety of receptors are known to traffic from the Golgi to the lysosome directly (72, 73), I considered the possibility that CSF-1R is alternatively sorted into the lysosome in EHD1-KO BMDMs where it is degraded. Our Western blotting analyses demonstrating that CSF-1R protein accumulates in EHD1-KO BMDMs when in the presence of Baf-A1 (Figure 3.28), together with confocal imaging of Baf-A1 treated BMDMs (Figure 3.29), support this mechanism. It is of obvious interest to assess if the EHD1-dependent CSF-1R traffic pathway I describe is also important for other RTKs or represents a more restricted adaptation for CSF-1R. How the balance of these pathway operates and whether it is tunable during development, differentiation or functional responses of macrophage-lineage or other cells will be of considerable interest, especially in the context of human diseases in which inhibition of CSF-1R signaling would likely be desired (7, 13, 16, 74).

Although a novel role for EHD1 has been revealed *in vitro*, it will undoubtedly be necessary further to investigate the physiological requirement of EHD1 for CSF1R-dependent generation of macrophage lineage cells *in vivo*. The question of whether or not EHD1 is essential to generate CSF1R signaling *in vivo* to help maintain monocyte-macrophage lineage under homeostasis and to help switch to monocyte-skewed hematopoiesis during immunological stress will need to be answered. *In vivo* analyses of tissue macrophages using an HSC-intrinsic inducible EHD1 deletion (chimeric mice utilizing *Ehd1^{fl/fl}; Cre^{ERT2}* bone marrow) mouse model would be one way to answer these lingering questions directly. The

impact of EHD1 deletion *in vivo* on CSF-1R signaling needs to be verified to determine if the findings presented in this dissertation point to a physiologically relevant pathway of biological macrophage regulation. Using a chimeric approach with utilizing *Ehd1^{fl/fl}; Cre^{ERT2}* bone marrow would allow selective EHD1 deletion in hematopoietic lineages alone using a chimeric approach (Sieweke & Allen, 2013). Using tamoxifen treatment of live mice, the analysis could be done of peripheral blood (blood cell analyzer and blood smears) and spleens (FACS and immunohistochemistry) to changes in the development and function of the monocyte-macrophage lineage.

A CSF-1R specific inducible system could also be of great value when assessing the role of EHD1 in CSF-1R signaling *in vivo*. Tamoxifen-inducible deletion via a CSF-1R specific deletion is currently available through Jackson Laboratories. However, the background of the CSF-1R inducible Cre mouse is FVB. Since *Ehd1^{fl/fl}* mice are predominantly C57BL/6 background (Bhattacharyya et al., 2016; Rainey et al., 2010), the appropriate backcrosses would take an inconvenient amount of time. In contrast, the bone marrow chimeric model proposed previously could be carried out with existing mouse models.

Targeting of CSF-1R signaling as a treatment of disease has made its way into clinical trials and has thus far been conducted regarding either inhibiting the receptor after activation or blocking receptor activation by using via an antibody that binds CSF-1R and inhibits CSF-1 binding (68). The decreased surface expression resulting from EHD1 deletion suggested a new target enabling the result of blocking CSF-1R signaling. Further studies will be conducted in order to

elucidate the mechanism of EHD1 further in the transport of CSF-1R to the macrophage cell surface due to the number of cells in the human body which express EHD1. Due to potential off-target effects, EHD1 alone is not a viable target of CSF-1R signaling inhibition. However, the possibility of blocking CSF-1R transport to the macrophage cell surface is an attractive possible target. This project encourages the pursuit of further studies aimed at understanding of the mechanisms governing receptor tyrosine kinase presentation.

Conclusion

In conclusion, my findings show that exit of fully glycosylated, mature, CSF-1R from the Golgi is a regulated process under the control of two competing sorting procedures: a dominant EHD1-dependent pathway to facilitate its traffic to the cell surface and an alternate pathway to lysosomes for degradation. My findings support the conclusion that EHD1-dependent CSF1R transport, from the Golgi to the cell surface, are of key significance in determining the ultimate level of CSF-1R signaling (Figures 3.7 and 3.18) and downstream biological responses (Figures 3.3-3.6; 3.13-3.17). Collectively, the data from this study reveals a novel function for EHD1 in the exit of unstimulated CSF-1R from the Golgi apparatus to the macrophage cell surface for physiological activation of the receptor (Figure 4.1).

The stage has been set for more in-depth studies of EHD proteins in other macrophage functions such as antigen presentation through MHC class I and MHC class II, processing of pathogens/antigens, and macrophage-assisted

pathologies. These findings will also serve as a basis for future studies aimed at uncovering the importance of the EHD proteins in trafficking of receptors on the cell surface in normal immune physiology and disease.

CHAPTER 4: FIGURES

Figure 4.1. Working model of the novel EHD1 function in CSF-1R delivery and display on the macrophage cell surface.

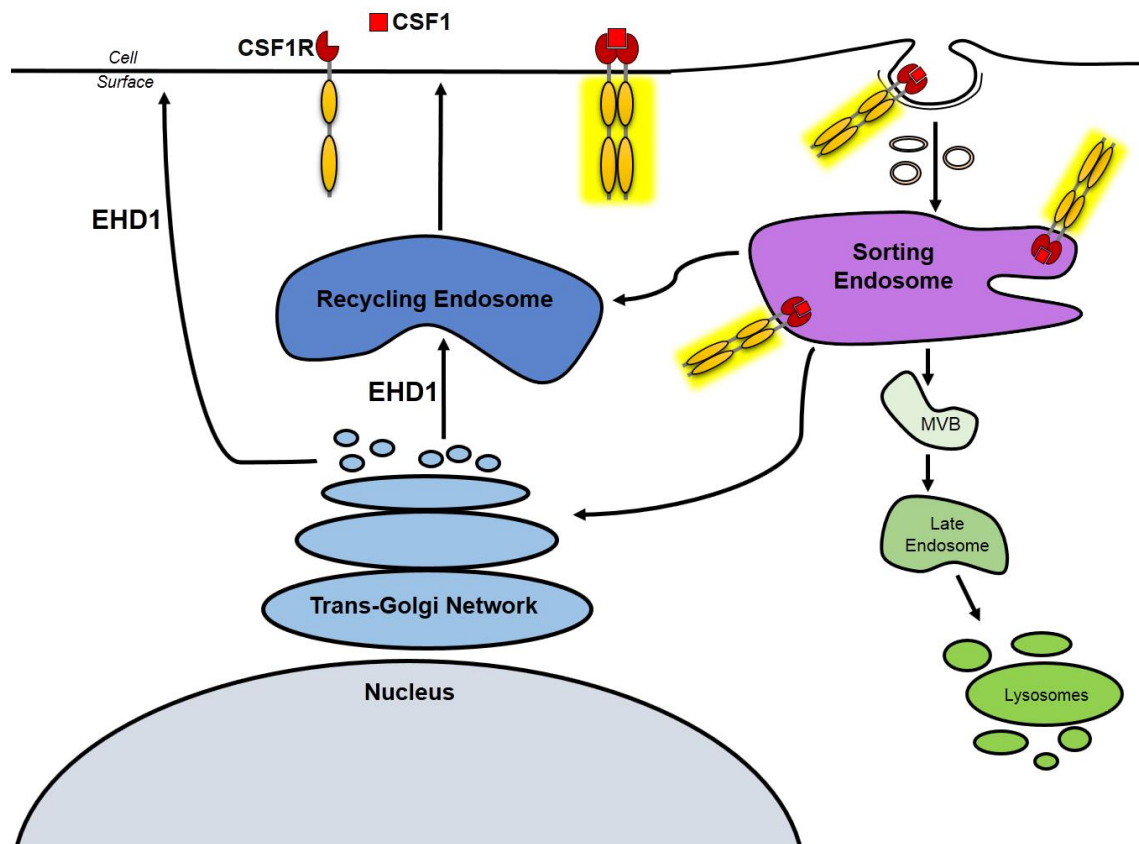


Figure 4.1. Working model of the EHD1 function in CSF-1R delivery and display on the macrophage cell surface. EHD1-dependent post-Golgi sorting of newly synthesized CSF-1R in BMDMs directs the receptor towards the cell surface and away from the lysosome. In EHD1-expressing BMDMs, the surface delivery dominates. In the absence of EHD1, the lysosomal delivery is dominant, resulting in lower surface CSF-1R and reduced CSF1R-dependent cellular activation together with increased CSF-1R delivery to the lysosome for degradation.

BIBLIOGRAPHY

1. Shima, M., Teitelbaum, S. L., Holers, V. M., Ruzicka, C., Osmack, P., and Ross, F. P. (1995) Macrophage-colony-stimulating factor regulates expression of the integrins alpha 4 beta 1 and alpha 5 beta 1 by murine bone marrow macrophages. *Proc. Natl. Acad. Sci. U. S. A.* **92**, 5179–83
2. Rieger, M. A, Hoppe, P. S., Smejkal, B. M., Eitelhuber, A. C., and Schroeder, T. (2009) Lineage Choice. *Science*. **325**, 217–218
3. Weidenbusch, M., and Anders, H. J. (2012) Tissue microenvironments define and get reinforced by macrophage phenotypes in homeostasis or during inflammation, repair and fibrosis. *J. Innate Immun.* **4**, 463–477
4. Mosser, D. M., and Zhang, X. (2008) Activation of murine macrophages. *Curr. Protoc. Immunol.* **Chapter 14**, Unit 14.2
5. Shi, C., and Pamer, E. G. (2011) Monocyte recruitment during infection and inflammation. *Nat. Rev. Immunol.* **11**, 762–74
6. Stein, M., Keshav, S., Harris, N., and Gordon, S. (1992) Interleukin 4 potently enhances murine macrophage mannose receptor activity: a marker of alternative immunologic macrophage activation. *J. Exp. Med.* **176**, 287–292
7. Chitu, V., and Stanley, E. R. (2006) Colony-stimulating factor-1 in immunity and inflammation. *Curr. Opin. Immunol.* **18**, 39–48
8. Hamilton, J. A. (2008) Colony-stimulating factors in inflammation and autoimmunity. *Nat. Immunol.* **23**, 533–544
9. Pollard, J. W. (2009) Trophic macrophages in development and disease.

Nat. Rev. Immunol. **9**, 259–70

10. Toh, M. L., Bonnefoy, J. Y., Accart, N., Cochin, S., Pohle, S., Haegel, H., De Meyer, M., Zemmour, C., Preville, X., Guillen, C., Thioudellet, C., Ancian, P., Lux, A., Sehnert, B., Nimmerjahn, F., Voll, R. E., and Schett, G. (2014) Bone- and cartilage-protective effects of a monoclonal antibody against colony-stimulating factor 1 receptor in experimental arthritis. *Arthritis Rheumatol.* **66**, 2989–3000
11. Bogie, J. F. J., Stinissen, P., and Hendriks, J. J. A. (2014) Macrophage subsets and microglia in multiple sclerosis. *Acta Neuropathol.* **128**, 191–213
12. Sundal, C., Fujioka, S., Van Gerpen, J. A., Wider, C., Nicholson, A. M., Baker, M., Shuster, E. A., Aasly, J., Spina, S., Ghetti, B., Roeber, S., Garbern, J., Tselis, A., Swerdlow, R. H., Miller, B. B., Borjesson-Hanson, A., Uitti, R. J., Ross, O. A., Stoessl, A. J., Rademakers, R., Josephs, K. A., Dickson, D. W., Broderick, D., and Wszolek, Z. K. (2013) Parkinsonian features in hereditary diffuse leukoencephalopathy with spheroids (HDLS) and CSF1R mutations. *Park. Relat. Disord.* **19**, 869–877
13. Aikawa, Y., Katsumoto, T., Zhang, P., Shima, H., Shino, M., Terui, K., Ito, E., Ohno, H., Stanley, E. R., Singh, H., Tenen, D. G., and Kitabayashi, I. (2010) PU.1-mediated upregulation of CSF1R is crucial for leukemia stem cell potential induced by MOZ-TIF2. *Nat. Med.* **16**, 580–585, 1p following 585
14. Qian, B.-Z., Li, J., Zhang, H., Kitamura, T., Zhang, J., Campion, L. R.,

- Kaiser, E. A., Snyder, L. A., and Pollard, J. W. (2011) CCL2 recruits inflammatory monocytes to facilitate breast-tumour metastasis. *Nature*. **475**, 222–5
15. Laoui, D., van Overmeire, E., de Baetselier, P., van Ginderachter, J. A., and Raes, G. (2014) Functional relationship between tumor-associated macrophages and macrophage colony-stimulating factor as contributors to cancer progression. *Front. Immunol.* **5**, 1–15
 16. Hernandez, L., Smirnova, T., Kedrin, D., Wyckoff, J., Zhu, L., Stanley, E. R., Cox, D., Müller, W. J., Pollard, J. W., Rooijen, N. Van, and Segall, J. E. (2009) The EGF/CSF-1 paracrine invasion loop can be triggered by heregulin β 1 and CXCL12. *Cancer Res.* **69**, 3221–3227
 17. Pixley, F. J., and Stanley, E. R. (2004) CSF-1 regulation of the wandering macrophage: Complexity in action. *Trends Cell Biol.* **14**, 628–638
 18. Huynh, J., Kwa, M. Q., Cook, A. D., Hamilton, J. A., and Scholz, G. M. (2012) CSF-1 receptor signalling from endosomes mediates the sustained activation of Erk1/2 and Akt in macrophages. *Cell. Signal.* **24**, 1753–1761
 19. Friedman, a D. (2007) Transcriptional control of granulocyte and monocyte development. *Oncogene.* **26**, 6816–6828
 20. Goh, L. L. K., and Sorkin, A. (2013) Endocytosis of receptor tyrosine kinases. *Cold Spring Harb. Perspect.* **5**, a017459
 21. Wei, S., Nandi, S., Chitu, V., Yeung, Y.-G. Y.-G., Yu, W., Huang, M., Williams, L. T. T., Lin, H., and Stanley, E. R. R. (2010) Functional overlap but differential expression of CSF-1 and IL-34 in their CSF-1 receptor-

- mediated regulation of myeloid cells. *J. Leukoc. Biol.* **88**, 495–505
22. Liu, H., Leo, C., Chen, X., Wong, B. R., Williams, L. T., Lin, H., and He, X. (2012) The mechanism of shared but distinct CSF-1R signaling by the non-homologous cytokines IL-34 and CSF-1. *Biochim. Biophys. Acta - Proteins Proteomics.* **1824**, 938–945
 23. Li, W., and Stanley, E. R. (1991) Role of dimerization and modification of the CSF-1 receptor in its activation and internalization during the CSF-1 response. *EMBO J.* **10**, 277–88
 24. Mohapatra, B., Ahmad, G., Nadeau, S., Zutshi, N., An, W., Scheffe, S., Dong, L., Feng, D., Goetz, B., Arya, P., Bailey, T. a., Palermo, N., Borgstahl, G. E. O., Natarajan, A., Raja, S. M., Naramura, M., Band, V., and Band, H. (2013) Protein tyrosine kinase regulation by ubiquitination: Critical roles of Cbl-family ubiquitin ligases. *Biochim. Biophys. Acta.* **1833**, 122–139
 25. Lee, P. S. W., Wang, Y., Dominguez, M. G., Yeung, Y. G., Murphy, M. A., Bowtell, D. D. L., and Stanley, E. R. (1999) The Cbl protooncoprotein stimulates CSF-1 receptor multiubiquitination and endocytosis, and attenuates macrophage proliferation. *EMBO J.* **18**, 3616–3628
 26. Wang, Y., Yeung, Y. G., and Stanley, E. R. (1999) CSF-1 stimulated multiubiquitination of the CSF-1 receptor and of Cbl follows their tyrosine phosphorylation and association with other signaling proteins. *J. Cell. Biochem.* **72**, 119–134
 27. Roepstorff, K., Grandal, M. V., Henriksen, L., Knudsen, S. L. J., Lerdrup,

- M., Grøvdal, L., Willumsen, B. M., and Van Deurs, B. (2009) Differential effects of EGFR ligands on endocytic sorting of the receptor. *Traffic*. **10**, 1115–1127
28. Jopling, H. M., Howell, G. J., Gamper, N., and Ponnambalam, S. (2011) The VEGFR2 receptor tyrosine kinase undergoes constitutive endosome-to-plasma membrane recycling. *Biochem. Biophys. Res. Commun.* **410**, 170–176
 29. Guilbert, L. J., and Stanley, E. R. (1986) The interaction of ¹²⁵I-colony-stimulating factor-1 with bone marrow-derived macrophages. *J. Biol. Chem.* **261**, 4024–4032
 30. Naslavsky, N., and Caplan, S. (2010) EHD proteins: key conductors of endocytic transport. *Trends Cell Biol.* **21**, 122–131
 31. George, M., Rainey, M. A., Naramura, M., Ying, G., Harms, D. W., Vitaterna, M. H., Doglio, L., Crawford, S. E., Hess, R. A., Band, V., and Band, H. (2010) Ehd4 is required to attain normal prepubertal testis size but dispensable for fertility in male mice. *Genesis*. **48**, 328–342
 32. Arya, P., Rainey, M. A., Bhattacharyya, S., Mohapatra, B. C., George, M., Kuracha, M. R., Storck, M. D., Band, V., Govindarajan, V., and Band, H. (2015) The endocytic recycling regulatory protein EHD1 Is required for ocular lens development. *Dev. Biol.* **408**, 1–15
 33. Bhattacharyya, S., Rainey, M. A., Arya, P., Dutta, S., George, M., Storck, M. D., McComb, R. D., Muirhead, D., Todd, G. L., Gould, K., Datta, K., Waes, J. G., Band, V., and Band, H. (2016) Endocytic recycling protein

- EHD1 regulates primary cilia morphogenesis and SHH signaling during neural tube development. *Sci. Rep.* **6**, 20727
34. Posey, A. D., Pytel, P., Gardikiotes, K., Demonbreun, A. R., Rainey, M., George, M., Band, H., and McNally, E. M. (2011) Endocytic recycling proteins EHD1 and EHD2 interact with Fer-1-like-5 (Fer1L5) and mediate myoblast fusion. *J. Biol. Chem.* **286**, 7379–7388
 35. Posey, A. D., Swanson, K. E., Alvarez, M. G., Krishnan, S., Earley, J. U., Band, H., Pytel, P., McNally, E. M., and Demonbreun, A. R. (2014) EHD1 mediates vesicle trafficking required for normal muscle growth and transverse tubule development. *Dev. Biol.* **387**, 179–190
 36. Rainey, M. A., George, M., Ying, G., Akakura, R., Burgess, D. J., Siefker, E., Bargar, T., Doglio, L., Crawford, S. E., Todd, G. L., Govindarajan, V., Hess, R. A., Band, V., Naramura, M., and Band, H. (2010) The endocytic recycling regulator EHD1 is essential for spermatogenesis and male fertility in mice. *BMC Dev. Biol.* **10**, 37
 37. George, M., Rainey, M. A., Naramura, M., Foster, K. W., Holzapfel, M. S., Willoughby, L. L., Ying, G., Goswami, R. M., Gurumurthy, C. B., Band, V., Satchell, S. C., and Band, H. (2011) Renal thrombotic microangiopathy in mice with combined deletion of endocytic recycling regulators EHD3 and EHD4. *PLoS One.* **6**, e17838
 38. Curran, J., Makara, M. A., Little, S. C., Musa, H., Liu, B., Wu, X., Polina, I., Alecusan, J. S., Wright, P., Li, J., Billman, G. E., Boyden, P. A., Gyorke, S., Band, H., Hund, T. J., and Mohler, P. J. (2014) EHD3-dependent

endosome pathway regulates cardiac membrane excitability and physiology. *Circ. Res.* **115**, 68–78

39. Gudmundsson, H., Curran, J., Kashef, F., Snyder, J. S., Smith, S. A., Vargas-Pinto, P., Bonilla, I. M., Weiss, R. M., Anderson, M. E., Binkley, P., Felder, R. B., Carnes, C. A., Band, H., Hund, T. J., and Mohler, P. J. (2012) Differential regulation of EHD3 in human and mammalian heart failure. *J. Mol. Cell. Cardiol.* **52**, 1183–1190
40. Curran, J., Musa, H., Kline, C. F., Makara, M. A., Little, S. C., Higgins, J. D., Hund, T. J., Band, H., and Mohler, P. J. (2015) Eps15 homology domain-containing protein 3 regulates cardiac T-type Ca^{2+} channel targeting and function in the atria. *J. Biol. Chem.* **290**, 12210–12221
41. Rapaport, D., Auerbach, W., Naslavsky, N., Pasmanik-Chor, M., Galperin, E., Fein, A., Caplan, S., Joyner, A. L., and Horowitz, M. (2006) Recycling to the plasma membrane is delayed in EHD1 knockout mice. *Traffic*. **7**, 52–60
42. Caplan, S., Naslavsky, N., Hartnell, L. M., Lodge, R., Polishchuk, R. S., Donaldson, J. G., and Bonifacino, J. S. (2002) A tubular EHD1-containing compartment involved in the recycling of major histocompatibility complex class I molecules to the plasma membrane. *EMBO J.* **21**, 2557–2567
43. Jović, M., Naslavsky, N., Rapaport, D., Horowitz, M., and Caplan, S. (2007) EHD1 regulates beta1 integrin endosomal transport: effects on focal adhesions, cell spreading and migration. *J. Cell Sci.* **120**, 802–814
44. Sengupta, S., George, M., Miller, K. K., Naik, K., Chou, J., Cheatham, M. A., Dallos, P., Naramura, M., Band, H., and Zheng, J. (2009) EHD4 and

- CDH23 are interacting partners in cochlear hair cells. *J. Biol. Chem.* **284**, 20121–20129
45. Yap, C. C. C., Lasiecka, Z. M., Caplan, S., and Winckler, B. (2010) Alterations of EHD1/EHD4 protein levels interfere with L1/NgCAM endocytosis in neurons and disrupt axonal targeting. *J. Neurosci.* **30**, 6646–6657
 46. Buggia-Prevot, V., Fernandez, C. G., Udayar, V., Vetrivel, K. S., Elie, A., Roseman, J., Sasse, V. A., Lefkow, M., Meckler, X., Bhattacharyya, S., George, M., Kar, S., Bindokas, V. P., Parent, A. T., Rajendran, L., Band, H., Vassar, R., and Thinakaran, G. (2013) A Function for EHD Family Proteins in Unidirectional Retrograde Dendritic Transport of BACE1 and Alzheimer's Disease A β Production. *Cell Rep.* **5**, 1552–1563
 47. Koles, K., Messelaar, E. M., Feiger, Z., Yu, C. J., Andrew, C., and Rodal, A (2015) The EHD protein Past1 controls postsynaptic membrane elaboration and synaptic function. *Mol. Biol. Cell.* **26**, 1–31
 48. Shao, Y., Akmentin, W., Toledo-Aral, J. J., Rosenbaum, J., Valdez, G., Cabot, J. B., Hilbush, B. S., and Halegoua, S. (2002) Pincher, a pinocytic chaperone for nerve growth factor/TrkA signaling endosomes. *J. Cell Biol.* **157**, 679–691
 49. Basha, G., Omilusik, K., Chavez-Steenbock, A., Reinicke, A. T., Lack, N., Choi, K. B., and Jefferies, W. A (2012) A CD74-dependent MHC class I endolysosomal cross-presentation pathway. *Nat. Immunol.* **13**, 237–245
 50. Guermonprez, P., Saveanu, L., Kleijmeer, M., Davoust, J., Van Endert, P.,

- and Amigorena, S. (2003) ER-phagosome fusion defines an MHC class I cross-presentation compartment in dendritic cells. *Nature*. **425**, 397–402
51. Lozano, M. L., Rivera, J., Sánchez-Guiu, I., and Vicente, V. (2014) Towards the targeted management of Chediak-Higashi syndrome. *Orphanet J. Rare Dis.* **9**, 132
 52. Sieni, E., Cetica, V., Hackmann, Y., Coniglio, M. L., Da Ros, M., Ciambotti, B., Pende, D., Griffiths, G., and Arico, M. (2014) Familial hemophagocytic lymphohistiocytosis: When rare diseases shed light on immune system functioning. *Front. Immunol.* **5**, 1–19
 53. Fejer, G., Sharma, S., and Gyory, I. (2015) Self-renewing macrophages - A new line of enquiries in mononuclear phagocytes. *Immunobiology*. **220**, 169–174
 54. Jenkins, S. J., and Hume, D. A. (2014) Homeostasis in the mononuclear phagocyte system. *Trends Immunol.* **35**, 358–367
 55. Schmittgen, T. D., and Livak, K. J. (2008) Analyzing real-time PCR data by the comparative CT method. *Nat. Protoc.* **3**, 1101–1108
 56. Bailey, T. A., Luan, H., Tom, E., Bielecki, T. A., Mohapatra, B., Ahmad, G., George, M., Kelly, D. L., Natarajan, A., Raja, S. M., Band, V., and Band, H. (2014) A kinase inhibitor screen reveals protein kinase C-dependent endocytic recycling of ErbB2 in breast cancer cells. *J. Biol. Chem.* **289**, 30443–30458
 57. Lou, J., Low-Nam, S. T., Kerkvliet, J. G., and Hoppe, A. D. (2014) Delivery of CSF-1R to the lumen of macropinosomes promotes its destruction in

- macrophages. *J. Cell Sci.* **127**, 5228–5239
58. Weischenfeldt, J., and Porse, B. (2008) Bone marrow-derived macrophages (BMM): Isolation and applications. *Cold Spring Harb. Protoc.* **3**, pdb.prot5080–pdb.prot5080
 59. Tushinski, R. J., Oliver, I. T., Guilbert, L. J., Tynan, P. W., Warner, J. R., and Stanley, E. R. (1982) Survival of mononuclear phagocytes depends on a lineage-specific growth factor that the differentiated cells selectively destroy. *Cell.* **28**, 71–81
 60. Simoncic, P. D., Bourdeau, A., Lee-Loy, A., Rohrschneider, L. R., Tremblay, M. L., Stanley, E. R., and McGlade, C. J. (2006) T-cell protein tyrosine phosphatase (Tcptp) is a negative regulator of colony-stimulating factor 1 signaling and macrophage differentiation. *Mol. Cell. Biol.* **26**, 4149–60
 61. Stanley, E. R. (1976) Factors regulating macrophage production and growth: identity of colony- stimulating factor and macrophage growth factor. *J. Exp. Med.* **143**, 631–647
 62. Yeung, Y. G., and Stanley, E. R. (2003) Proteomic Approaches to the Analysis of Early Events in Colony-stimulating Factor-1 Signal Transduction. *Mol. Cell Proteomics.* **2**, 1143–1155
 63. Yanagita, M., Higashi, A., Ikawa, T., Muramatsu, M., Economides, A. N., and Kawamoto, H. (2009) Response to Comment on “Direct Hematological Toxicity and Illegitimate Chromosomal Recombination Caused by the Systemic Activation of CreERT2.” *J. Immunol.* **183**, 2891–2892

64. Pixley, F. J. (2012) Macrophage migration and its regulation by CSF-1. *Int. J. Cell Biol.* **2012**, 501962
65. Wimmer, R., and Baccarini, M. (2010) Partner exchange: Protein-protein interactions in the Raf pathway. *Trends Biochem. Sci.* **35**, 660–668
66. Liao, R. S., Ma, S., Miao, L., Li, R., Yin, Y., and Raj, G. V. (2013) Androgen receptor-mediated non-genomic regulation of prostate cancer cell proliferation. *Transl. Androl. Urol.* **2**, 187–196
67. Hume, D. A. (2008) Differentiation and heterogeneity in the mononuclear phagocyte system. *Mucosal Immunol.* **1**, 432–441
68. Hume, D. A., and MacDonald, K. P. A. (2012) Therapeutic applications of macrophage colony-stimulating factor-1 (CSF-1) and antagonists of CSF-1 receptor (CSF-1R) signaling. *Blood.* **119**, 1810–1820
69. Jeffery, J. J., Lux, K., Vogel, J. S., Herrera, W. D., Greco, S., Woo, H.-H., Abushahin, N., Pagel, M. D., and Chambers, S. K. (2014) Autocrine inhibition of the c-fms proto-oncogene reduces breast cancer bone metastasis assessed with in vivo dual-modality imaging. *Exp. Biol. Med.* **239**, 404–413
70. Hassan, R., Suzu, S., Hiyoshi, M., Takahashi-Makise, N., Ueno, T., Agatsuma, T., Akari, H., Komano, J., Takebe, Y., Motoyoshi, K., and Okada, S. (2009) Dys-regulated activation of a Src tyrosine kinase Hck at the Golgi disturbs N-glycosylation of a cytokine receptor Fms. *J. Cell. Physiol.* **221**, 458–468
71. Hiyoshi, M., Suzu, S., Yoshidomi, Y., Hassan, R., Harada, H., Sakashita,

- N., Akari, H., Motoyoshi, K., and Okada, S. (2008) Interaction between Hck and HIV-1 Nef negatively regulates cell surface expression of M-CSF receptor. *Blood*. **111**, 243–250
72. Gomez, T. S., Gorman, J. A., Artal-Martinez de Narvajas, A., Koenig, A. O., and Billadeau, D. D. (2012) Trafficking defects in WASH-knockout fibroblasts originate from collapsed endosomal and lysosomal networks. *Mol. Biol. Cell*. **23**, 3215–3228
73. Tu, C., Ortega-Cava, C. F., Chen, G., Fernandes, N. D., Cavallo-Medved, D., Sloane, B. F., Band, V., and Band, H. (2008) Lysosomal cathepsin B participates in the podosome-mediated extracellular matrix degradation and invasion via secreted lysosomes in v-Src fibroblasts. *Cancer Res*. **68**, 9147–9156
74. Strachan, D. C., Ruffell, B., Oei, Y., Bissell, M. J., Coussens, L. M., Pryer, N., and Daniel, D. (2013) CSF1R inhibition delays cervical and mammary tumor growth in murine models by attenuating the turnover of tumor-associated macrophages and enhancing infiltration by CD8(+) T cells. *Oncoimmunology*. **2**, e26968